2012

Characterization of Pharmaceutical Materials by Thermal and Analytical Methods

Manik Pavan Kumar Maheswaram
Cleveland State University

CHARACTERIZATION OF PHARMACEUTICAL MATERIALS BY THERMAL AND ANALYTICAL METHODS

MANIK PAVAN KUMAR MAHESWARAM

Master of Science in Chemistry

Cleveland State University

May 2012

Submitted in partial fulfillment of requirements for the degree of

DOCTOR OF PHILOSOPHY IN BIOANALYTICAL CHEMISTRY

at the

CLEVELAND STATE UNIVERSITY

May, 2012

This thesis has been approved for the

Department of Chemistry and the

College of Graduate Studies by

_____Date: _____

Dr. Alan Riga, Department of Chemistry, Cleveland State University

Primary Research Advisor

_____Date: _____

Dr. Mekki Bayachou, Department of Chemistry, Cleveland State University

Dissertation Committee Chairperson

_____Date: _____

Dr. John Turner, Department of Chemistry, Cleveland State University

Advisory Committee Member

_____Date: _____

Dr. Bin Su, Department of Chemistry, Cleveland State University

Advisory Committee Member

_____Date: _____

Dr. Tobili Sam-Yellowe, Department of BGES, Cleveland State University

External Advisory Committee Member

DEDICATION

This thesis dissertation is dedicated to my parents **M. Rukmaiah, M. Sujatha**, and my brothers **M. Manik Prabhu** and **M. Manik Pradeep Kumar**; my sister-in-law **M. Swetha** and my nephew **M. Sathvik;** my loving friends for their endless love, support and encouragement they provided me throughout the years.

Also, this thesis is dedicated to my "Guru"- Dr. Alan Riga for his outstanding pedagogy.

ACKNOWLEDGEMENTS

First and foremost, I would like to express my deep and sincere gratitude to Dr. Alan T. Riga, my advisor, for his valuable advice, immense support and encouragement in the journey of my academic and scientific research. I wish to thank him for introducing me to the field of Thermal Analysis. Dr. Alan Riga was very patient helpful and has always been there when I needed some encouragement with my work or just as a friend to talk to. There is so much that I have learned from him during the years that we have worked together. Writing this thesis would not have been possible without his interest and guidance.

This thesis was carried out in the Department of Chemistry, Cleveland State University Cleveland, Ohio. Part of the work was done in the College of Pharmacy Practice, University of Toledo, Ohio and The Department of Macromolecular Science and Engineering, Case Western Reserve University, Cleveland, Ohio.

I would like to thank all the people who have been involved in this research, during the years 2008 – 2012.

I am especially thankful to Dr. Kenneth. S. Alexander for his positive attitude and kind support with my work. I also express my gratitude for giving me the opportunity to use the facilities at The College of Pharmacy Practice, University of Toledo, OH and his friendly advice during the years.

Secondly, I would further like to thank Dr. Mekki Bayachou, Dr. John Turner, Dr. Bin Su and Dr. Tobili-Sam-Yellowe for their invaluable time and support and for being part of my dissertation committee.

Finally, I would like to thank Dr. Indika Perera for his advice, immense support and encouragement during the completion of my doctoral studies. Without him Riga Research Team is incomplete.

I would like to bestow this thesis in particular to my family and friends and my Riga Research team members especially Indika, M. Ellen Matthews, Hareesha, Dhruthiman, Shravan, Lakshmi, Jeff Fruscella, and Rajgopal. I thank Robert Cannon for helping me out with PXRD studies.

To all my friends, thank you for your understanding and encouragement in my many, many moments of crisis. Your friendship makes my life a wonderful experience. I cannot list all the names here, but you are always on my mind.

Thank you, God, for always being there for me.

CHARACTERIZATION OF PHARMACEUTICAL MATERIALS BY THERMAL AND ANALYTICAL METHODS

MANIK PAVAN KUMAR MAHESWARAM

ABSTRACT

Morphological and thermodynamic transitions in drugs as well as their amorphous and crystalline content in the solid state have been distinguished by Thermal Analytical techniques, which include dielectric analysis (DEA), differential scanning calorimetry (DSC), and macro-photo-micrography. These techniques were used to establish a structure vs. property relationship with the United States Pharmacopeia (USP) standard set of active pharmaceutical ingredients (API). DEA measures and differentiates the crystalline solid (low; 10^{-2} pS cm^{-1}) and amorphous liquid (high; 10^{6} pS cm^{-1}) API electrical ionic conductivity. DEA ionic conductivity cycle establishes the quantitative amorphous/ crystalline content in the solid state at frequencies of 0.1 - 1.00 Hz and to greater than 30^{o} C below the melting transition as the peak melting temperature. This describes the "activation energy method". An Arrhenius plot, log ionic conductivity vs. reciprocal temperature (K^{-1}), of the pre-melt DEA transition yields frequency dependent activation energy (Ea, J mol^{-1}) for the complex charging in the solid state. The amorphous content is inversely proportional to the Ea. Where, Ea for the crystalline form is higher and lower for the amorphous form with a standard deviation of ± 2%. An alternate technique has been established for the drugs of interest based on an obvious amorphous and crystalline state identified by macro-photomicrography and compared to the conductivity variations. This second "empirical method" correlates well with the "activation energy" method. A comparison of overall average amorphous content by the

empirical method had a linear relationship with the activation energy method with a correlation coefficient of $R^2 = 0.925$.

Additionally, new test protocols have been developed which describe the temperature and material characterization calibration of thermal analyzers with pharmaceuticals. These test protocols can be blended into a universal standard protocol for DSC, DEA and thermomechanical analysis (TMA). While calibrating DSC, a thermodynamic transition i.e. a change in heat flow, is marked by absorption (or release) of energy by the calibrants; for DEA, at the melt transition temperature, an abrupt change in DEA permittivity is observed; for TMA, at the transition temperature of the test specimen, there is a change in dimensional stability and a measured change in the coefficient of thermal expansion or contraction/softening is recorded. These test protocols were accomplished based on "The ASTM standard test methods for temperature calibration of thermal analytical methods". The R^2 correlation value of the calibrants for known standard literature transition temperatures vs. DSC melting peak temperatures, DEA Permittivity melting temperatures and TMA extrapolated onset-melting temperatures was 0.999.

Next, drug salts were investigated by DEA in order to evaluate ionic conductivity in pharmaceuticals. The ionic conductivity varied by several orders of magnitude in the amorphous form of the drug salt. The drug salts have an enhanced DEA ionic conductivity due to their ionic mobility of the salt component in the liquid phase. The primary aim of this study is to investigate the thermal and electrical behavior of pharmaceutical hydrochlorides using DEA and DSC techniques. From these analyses we can predict the quality, stability and behavior of a drug salt. This study also provides a

comprehensive characterization of ionic conductivity and molecular mobility (related to tan delta in DEA) properties in pharmaceutical salts through the measurement of the characteristic activation energies Ea (k) and Ea (τ) as well as polarization times (τ). The typical ionic conductivity of a melted drug, i.e. the amorphous phase, is 10^5 pS $cm^{-1}$and for the salt it is higher than 10^6 pS cm^{-1}. It is our opinion that a quality and a stable drug salt form will have a high ionic conductivity of $>10^5$ pS cm^{-1}. The DEA properties described here can be further developed to estimate the storage stability or shelf life of the drug salts by activation energies and polarization times. Salts with advantageous properties are typically patentable as new chemical entities. Electro synthesis is suggested for future drug development with the high ionic conductivity of the salts, $>10^5$ pS cm^{-1} to aid reaction kinetics to form new complexes or modified salts.

The dielectric science developed to understand the crystalline and amorphous components in pharmaceuticals would be validated by calorimetry, X-ray diffraction and scanning electron microscopy. It has been established that the crystalline and amorphous content measured by the DEA activation energy method is related to the DSC melting, glass-transition profile as well as the crystal structure by X-ray diffraction and scanning electron microscopic images.

TABLE OF CONTENTS

LIST OF TABLES

Chapter III

LIST OF FIGURES

ABBREVIATIONS

APIs – Active Pharmaceutical Ingredients

DSC - Differential Scanning Calorimetry

DEA – Dielectric Analysis

TMA – Thermomechanical Analysis

TG – Thermogravimetry

Ea (k) – Activation Energy (J mol^{-1})

Ea (δ) – Activation Energy (J mol^{-1})

T_m - Melting Temperature

T_{mp} - Peak Melting Temperature

ΔH_f- Heat of Fusion

T_g -Glass transition

T_c- Crystallization Temperature

T_{cp} - Crystallization peak temperature

ΔH_c - Heat of Crystallization

MW – Molecular Weight

PXRD – Powder X-ray Diffraction

SEM – Scanning Electron Microscope

IDA – Interdigitated electrode array

τ (Tau) -– Polarization time (millisecond)

fc – Tan delta critical peak frequency (Hz)

(ε″/ ε′) – Tan delta (δ)

ε″ – Ionic conductivity (Loss factor)

ε' – Permittivity

pS cm^{-1} – pico Siemens per centimeter

W g^{-1} – Heat Flow

ASTM – American Society for Testing Materials

OBJECTIVES

The main objective of this thesis was to characterize the selected model drugs as APIs using Differential Scanning Calorimetry (DSC) and Dielectric Analysis (DEA). Then develop a structure versus property relationship. The latter process guided the research to acquire a novel and efficient thermal analytical method for accurate and precise quantification of crystalline and amorphous content in pharmaceutical solids using a combined DSC and DEA Method. The electrical properties of the drugs and nylon 6 polymers were studied using Dielectric Analysis. The physical properties of the pharmaceutical solids were studied by employing DSC and TMA. Employing Scanning Electron Microscopy (SEM), Powder X-ray diffraction (PXRD), and Macro-photomicrography the structural attributes of the solids (drugs) were studied. The initial phase of this thesis was to characterize and develop new unique calibration procedures for the pharmaceutical industry based on physical properties of pure APIs and Excipients. This study describes the temperature and material characterization calibration of differential scanning calorimeters, dielectric analyzers and thermomechanical analyzer with pharmaceuticals over the temperature range of 25^{o} C to 250^{o} C. The theory of dielectric behavior of complex chemicals, pharmaceuticals, and polymers was also studied based on the multiple relaxation times, Cole-Cole plot of a Debye curve (for single relaxation time) and The Polaron theory or the "hopping model for conduction" and many alternative theories. These theories are used to describe the transfer of charge between various specific localized sites within a material under the influence of an electric field. This research was under taken as the basis for the later part of this study, where the drugs and an excipient were carefully evaluated by these techniques (DEA,

DSC and TMA) and the data interpreted was compared and ranked. Excipients are the inactive pharmaceuticals that are used to make up a medication. The DEA technique is a relative newcomer to thermal analysis in pharmaceutical field and it added a significant amount of new characterization data. DEA uniquely measures the electrical properties of the organic chemicals, drugs and excipients; polymers studied and revealed new physical-chemical properties, e.g., example, electrical ionic conductivity is a function of temperature and time.

In the next phase of my study, pharmaceutical solids (drugs) and nylon 6 polymers were characterized and evaluated further for morphological and thermodynamic transitions by the DSC and DEA instrumental methods. Nylon 6 polymers were used as models (reference polymers) for crystalline and amorphous content. These techniques were used successfully to establish a structure vs. property relationship with the API of drugs. The physical and electrical properties of the drugs were determined and were used to identify and quantify the crystalline and amorphous content in pharmaceutical solids. The major value of this research is to develop a novel analytical protocol utilizing dielectric analysis to define and quantify the crystalline and amorphous content in pharmaceutical solids. These inventive techniques will give pharmaceutical scientists new insights in how to understand the nature and behavior of the drug in the solid state as this information is of the utmost importance in pre-formulation studies of drug development.

Next, I studied the thermal and electrical behavior of hydrochloride salts of drug substances using thermo-analytical methods. This analysis provides a perspective on the use of the data from these techniques for predicting the quality, stability and behavior of

these materials. This study is also aimed at providing a comprehensive characterization of ionic conductivity and molecular mobility, related to tan delta as the (loss factor/ permittivity) in DEA, properties in pharmaceutical salts i.e., crystalline and amorphous forms through the measurement of the characteristic activation energies Ea (k) and Ea (τ) as well as polarization times (τ).

Finally, this portion of the thesis is to validate the DEA characteristic properties of an amorphous and crystalline material by: DSC, SEM, Macro-photography and PXRD. Quinapril.HCl (Q.HCl) and Clopidogrel Hydrogen Sulfate (CHS) were selected and prepared as model samples for amorphous characterization. These materials were prepared by the solvent evaporation method. The DEA confirmation for Q.HCl and CHS is based on an overlay of their DEA amorphous form 2^{nd} run to another amorphous sample prepared outside by the solvent evaporation method. The overlay was perfect in the physical layout of both since they both attained the same ionic conductivity level. Additionally, another amorphous entity (quench cooled) compared favorably with the DEA amorphous form.

PROTOCOL

Characterization of Pharmaceutical Materials and Polymers by Thermal - Analytical Techniques

Overview

a. Nature of the test: diverse structure property tests for evaluating drugs (APIs), excipients and Polymers

b. Characterizations of Crystalline/Amorphous content in pure pharmaceutical drugs, hydrochloride salts of drug substances and polymers.

Scope

- Purpose of the techniques: Quantitative and Qualitative (DEA, DSC, TMA, PXRD, SEM and Macro photomicrography).
- Define physical and chemical properties to be evaluated in this study.
- State limitations of each method

Terminology

- Define all significant terms
- Define all abbreviations

Summary of Methods

- Brief outline of each test method or protocol
- Brief statement of the test method principle and instrumentation

Significance in Use

- Relevance in meaning of each test method
- Practical Advantages and disadvantages of each test method
- Pre-formulation studies and drug design and development

- Stability of drugs in different forms (crystalline and amorphous forms)
- Development and research of new formulations

Methods

- Differential Scanning Calorimetry
- Dielectric Analysis
- Thermomechanical Analysis
- SEM
- PXRD
- Macro-photomicrography

Hazards

- Warnings: Care should be taken in handling specific drugs and salts, e.g., Quinine, Should be sampled in dark, light sensitive.

Calibration

- Detailed instructions for calibrations: Follow instructions of the instrument manufacturer.
- Standardization and use of reference materials

Procedure

- Sequenced detailed directions
- Describe successive steps for all the procedures

Interpretation of results

- Directions for evaluating the results
- List of all the tables and figures and equations
- Specify significant figures

Research report

- Detailed information required in reporting the results
- Significance of the multiple evaluations
- Correlating the results
- Determine average, standard deviation, % relative error as well as accuracy and repeatability when studying statistical analysis.

References

- References to publications supporting or providing needed information
- Keywords: identify words, terms or phrases that best represent the technical information reported

Conclusions

- Summarize all collected data
- Compare data from different methods
- Site all relevant information

CHAPTER I

INTRODUCTION

The chemical structure of a drug in a solution and its interaction with its receptor determines its activity in the patient [1]. However, in order to deliver the active drug molecule and excipients to the body in a physically stable state, i.e. typically as an oral solid dosage form, it is necessary to formulate it as a drug product. Therefore, the efficacy and safety of a drug product largely depends on the solid-state properties that include physicochemical and material properties.

1.1 Solid Forms

Presently majority of the solid drugs and dosage forms are prepared from crystalline active pharmaceutical ingredients (APIs). Solid materials can exist as either crystalline or amorphous forms. The crystalline form is characterized by a regular ordered crystal lattice structure, where there is no long-range order in amorphous form, as in liquids [2]. Between amorphous and crystalline forms there can be states of partial order, as in liquid crystals (see Figure 1.1.).

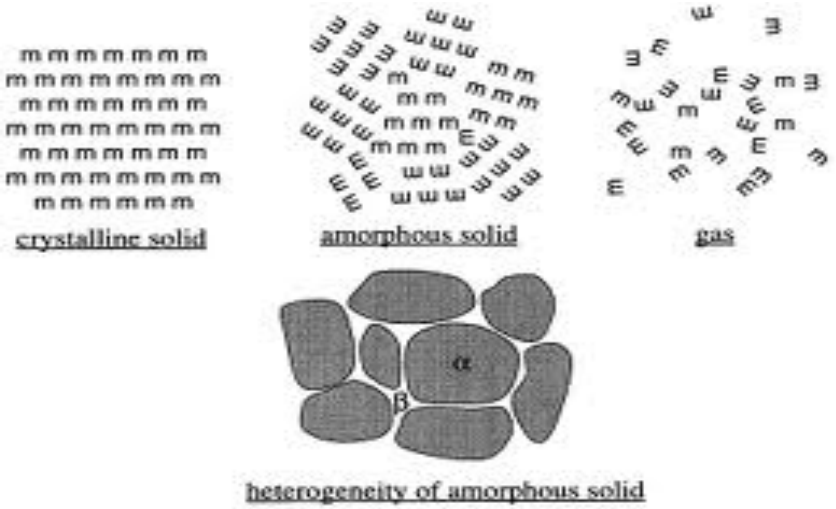

Figure 1.1. Schematic representation of structure of a crystalline and amorphous solid [3]

Mostly, organic molecules prefer to exist in crystalline solid form. Crystalline material is thermodynamically more stable than isolable amorphous material [2]. The practical significance of this amorphous property is that there is energetic pressure for an amorphous solid to recrystallize, so while selecting an amorphous form of a drug for development must be made with this in mind.

In addition, to variations in the relative amount of molecular order in solids, there can also be variations in the nature of the order. The classification of an organic molecular solid and its sub classification of crystalline solid are shown in (Figure 1.2.). The crystalline solids are divided in to polymorphs and hydrates. Different polymorphs have the same molecular structure but the molecules are arranged differently in the crystal lattice. The crystal lattice structures of solvates, hydrates and co-crystals are similar and are made up of more than one type of molecule. A crystal is composed of the API and a guest molecule in the pharmaceutical environment; solvates contain a solvent molecule, under ambient conditions organic compounds incorporate water or solvents

into their crystal lattice and in co-crystals the guest molecule included in the crystal structure [2, 4].

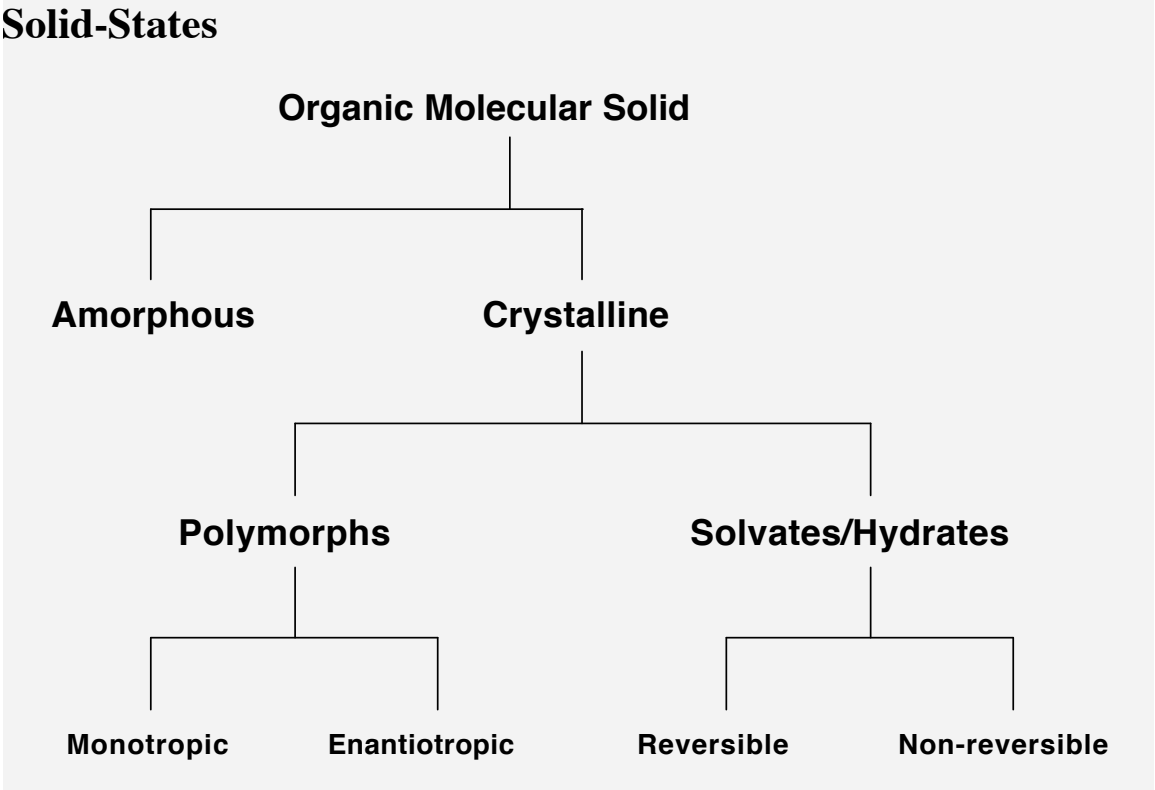

Figure 1.2. The classification of an organic molecular solid

The solid-state forms have different physicochemical as well as mechanical properties. They are as follows: Packing properties (density, refractive index, conductivity, hygroscopicity); Thermodynamic properties (Melting/Tg, enthalpy, entropy, heat capacity, thermodynamic activity, solubility); spectroscopic properties (Electronic, vibrational, rotational and nuclear spin); Kinetic properties (Dissolution rate, physical and chemical stability; Surface properties (Surface energy, habit); Mechanical properties (Hardness, tensile strength, compressibility, flow ability [5].

1.1.1 Amorphous state. During recent years the pharmaceutical scientists have studied the amorphous state in detail and there are a few drug products that have reached the market [6]. There is a growing interest in the amorphous state in the field of

pharmaceutics. For example, asthma medicine Accolate® (Zafirlukast) [7, 8]; antibiotic Zinnat ® / Ceftin® (cefuroxime axetil) [9, 10], and ACE-inhibitor Accupro® / Accupril® (Quinapril.HCl) [11, 12]. However, amorphous solids have poor stability, because of its high chemical reactivity, both during manufacturing and storage often hinders the development of amorphous drug formulations.

The significance of amorphous solids in pharmaceutical environment lies in their useful properties, instability and common occurrence relative to corresponding crystals. Due to the existence of polymorphism in the crystalline state, many scientists have raised the question of occurrence of different solid-state forms in the amorphous state. This phenomenon is called Polymorphism. A first order phase transition has to separate two amorphous phases in order for the polymorphism to exist [13-16]. Polymorphism was first found to exist in water and in some inorganic materials [17, 18]. There are some evidences that small organic materials also exist as polymorphs [13-16].

Based on the molecular packing, intermolecular bonding network, or amorphous material having local domains of different densities several theoretical models of amorphous materials have been proposed in the literature during recent years [19]. The potential energy differs in these regions with different packing densities. The physical and chemical properties are significantly affected by these differences in local structure of an amorphous material [19]. The heterogeneity nature of the amorphous state combined with structural relaxation could explain some of the differences in the differently prepared amorphous samples of the same drug or API.

1.1.1.1 Preparation of amorphous form. Amorphous material can be prepared during several pharmaceutical-processing steps both unintentionally as well as

intentionally through different pathways (see Figure 1.3.), through a solution, a liquid, a vapor, and a solid state [3, 4, 20].

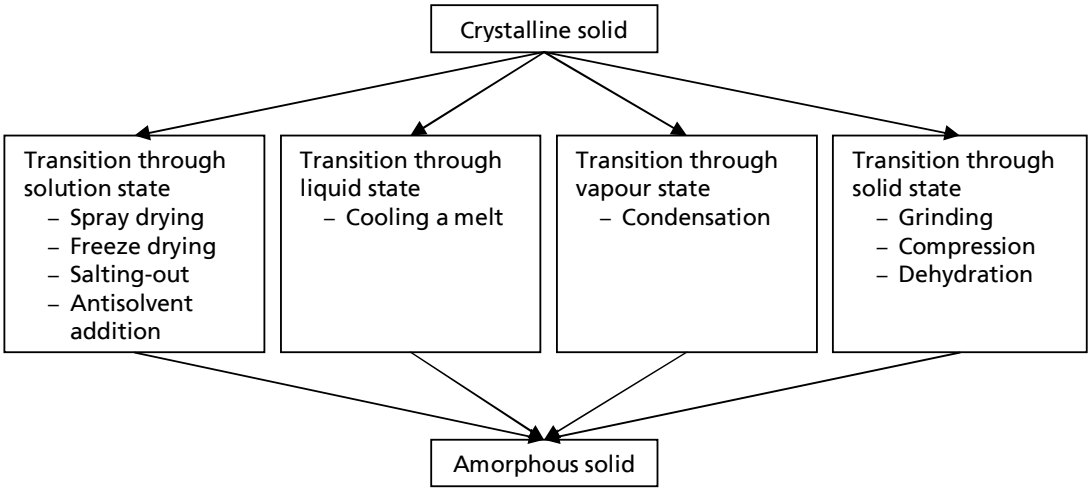

Figure 1.3. Different pathways to prepare amorphous pharmaceutical materials [21]

1.1.1.2 Quantification of amorphous content. The determination of amorphous content or crystalline content is based on the various differences in the physical properties between solids-state forms. There are several methods to quantify crystalline and amorphous content in pharmaceutical solids (See Figure 1.4.).

Method	XRD	DSC	IR	FT Raman	Solid state NMR
Analysis Time (min)	6-60	6-40	10-60	6-120	30-6000
Weight (mg)	200-400	4-10	5-50	2000	600
Limit of Detection	~10%	~5%	~1-2%	<1%	0.5%
Calibration	No	Yes	No	No	No
Destructive	No	Yes	No	No	No
Phased detected Crystalline/ Amorphous	Crystalline	Both	Both	Both	Both
Surface vs. Bulk	No	No	No	No	No
Internal std	Yes/No	No	No	No	No
Drawbacks	Diffraction affected by dimensions of sample	Crystallinity measured at Tm point only	Quantitative subtraction of Matrix req.	Complem entary quantifica tion tech to IR	Applicable only to Carbon containing Compounds

Figure 1.4. Comprehensive Characterization of Various Quantification Techniques [22]

1.2 References

1. C.R. Gardner, C.T. Walsh, Ö. Almarsson, 2004. Drugs as materials: valuing physical form in drug discovery. Nat. Rev. Drug Discov., 3, 926-934.
2. Ohannesisan L, Streeter AJ. "Handbook of Pharmaceutical Analysis", Marcel Dekker Inc., NY 2002, pages 1-581.
3. L. Yu, 2001. Amorphous pharmaceutical solids: preparation, characterization and stabilization. Adv. Drug Deliv. Rev., 48, 27-42.
4. Y. Cui, 2007. A material science perspective of pharmaceutical solids. Int. J. Pharm., 339, 3-18.

5. D.J.W. Grant, Theory and Origin of Polymorphism, in: H.G. Brittain (Ed.), Polymorphism in Pharmaceutical Solids, Marcel Dekker, New York, USA, 1999, pp. 1-33.

6. B.C. Hancock, 2002. Disordered drug delivery: destiny, dynamics and the Deborah number. J. Pharm. Pharmacol., 54, 737-746.

7. S.J. Corvari, J.R. Creekmore, PCT appl. WO9932082: Pharmaceutical compositions, 1999.

8. Accolate, 2008. http://www.astrazeneca-us.com/pi/accolate.pdf.

9. H.A. Crisp, J.C. Clayton, L.G. Elliott, E.M. Wilson, PCT appl. DE3327449: Amorphous cefuroxime axetil for improved bioavailability from the gastrointestinal tract, 1984.

10. Zinnat (Ceftin), 2008. http://us.gsk.com/products/assets/us_ceftintablets.pdf

11. S.M. Jennings, PCT appl. US2004192613: Preparation of quinapril hydrochloride, 2004.

12. Accupro (Accupril), 2008. http://www.pfizer.com/files/products/uspi_accupril.pdf

13. B.C. Hancock, E.Y. Shalaev, S.L. Shamblin, 2002. Polyamorphism: a pharmaceutical science perspective. J. Pharm. Pharmacol., 54, 1151-1152.

14. P.H. Poole, T. Grande, C.A. Angell, P.F. McMillan, 1997. Polymorphic phase transitions in liquids and glasses. Science, 17 322-323.

15. B. Rodríguez-Spong, C.P. Price, A. Jayasankar, A.J. Matzger, N. Rodríguez-Hornedo, 2004. General principles of pharmaceutical solid

polymorphism: a supramolecular perspective. Adv. Drug Deliv. Rev., 56, 241-274.

16. O. Mishima, L.D. Calvert, E. Whalley, 1984. 'Melting ice' I at 77 K and 10 kbar: a new method of making amorphous solids. Nature, 310, 393-395.

17. M. Grimsditch, 1984. Polyamorphism in amorphous silicon dioxide. Phys. Rev. Lett., 52, 2379-2381.

18. K.H. Smith, E. Shero, A. Chizmeshya, G.H. Wolf, 1995. The equation of state of polyamorphic germania glass: a two-domain description of the viscoelastic response. J. Chem. Phys, 102, 6851-6857.

19. S. Bates, G. Zografi, D. Engers, K. Morris, K. Crowley, A. Newman, 2006. Analysis of amorphous and nanocrystalline solids from their X-ray diffraction patterns. Pharm. Res., 23, 2333-2349.

20. B.C. Hancock, G. Zografi, 1997. Characteristics and significance of the amorphous state in pharmaceutical systems. J. Pharm. Sci., 86, 1-12.

21. Savolainen M., 2008. New Insights into the Amorphous State and Related Solid-State Transformations. Dissertationes bioscientiarum molecularium Universitatis Helsingiensis in Viikki, 26/2008, 49 pp.

22. Shah B, Kaumanu VK, Bansal AK. Analytical techniques for quantification of amorphous/crystalline phases in pharmaceutical solids. J Pharm Sci. 2006;95: 1641–65.

CHAPTER II

INSTRUMENTS AND METHODS

Thermal analysis is the term used to describe the analytical techniques that measure the physical and chemical properties of the sample as function of temperature or time. Some of the most important thermal analysis includes Differential Thermal Analysis (DTA), Differential Scanning Calorimetry (DSC), Thermogravimetry (TG), Thermomechanical Analysis (TMA), Dynamic Mechanical Thermal Analysis (DMA), and Dielectric Thermal Analysis (DEA).

2.1 Theory of Dielectric Analysis (DEA) Operation

2.1.1 Instrument. The DEA technique is relative newcomer to the thermal analysis field. It can be used to determine the dielectric properties of a material i.e., mobility of an ions and dipoles of a material as a function of time, temperature, and frequency. Dielectric instrument (Figure 2.1. Dielectric Analyzer TA 2970) measures two fundamental electrical characteristics of a material.

- Capacitive (insulating) nature, which represents its ability to store electric charge
- Conductive nature, which represents its ability to transfer electric charge

These electrical properties are important in themselves but have even more significance when they are correlated to activity on a molecular level [1-3]. This correlation allows you to probe the physical and chemical structure, process behavior, and molecular mobility (relaxations) of pharmaceutical materials, chemicals, polymers and composites [3-5].

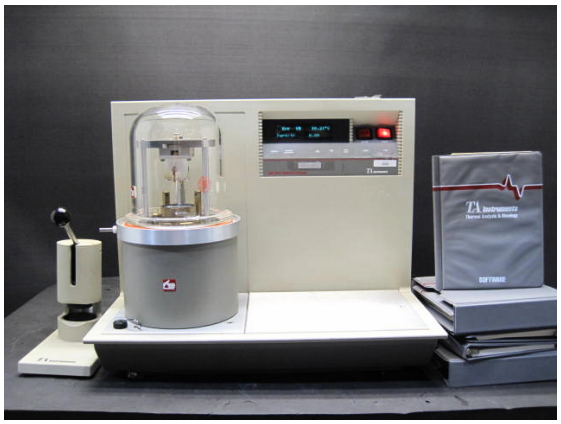

Figure 2.1. Dielectric Analyzer TA 2970 Instrument

Some uses of dielectric analysis are as follows:

- Surface properties versus bulk properties
- Frequency dependence of thermal transitions
- Frequency-dependent transitions at a constant temperature
- Influence of Crystallinity or amorphicity
- Activation energies for transitions
- Storage stability information
- Identification of multiple phases
- Change in properties due to exposure to a given environment (oxidation, thermal breakdown) [3,4]

2.1.2 Principle. In dielectric analysis, a sample is placed on a single surface gold ceramic inter-digitated electrode (see Figure 2.2.) when an alternating (sinusoidal voltage) electric field is applied. This voltage polarizes the sample, causing an oscillation of the molecules at the same frequency as the electric field but has a phase angle (or phase shift) δ. This phase angle shift is measured by comparing the applied voltage to the measured current (see Figure 2.3.) [4, 5]. The measured induced current is separated into capacitive (ε′) and conductive (ε″) components via the relationships shown in (Figure 2.4.). The ratio of ε″/ε′ is known as the loss tangent (tanδ).

Capacitance (C) and conductance (*1/R*) are calculated using the following equations:

$$\text{C (farads)} = \frac{I_{measured}}{V_{applied}} \text{ x } \frac{Sin\ \delta}{2\pi f} \quad (1)$$

$$1/R \text{ (mhos)} = \frac{I_{measured}}{V_{applied}} \text{ x } cos\ \delta \quad (2)$$

Where:

R = resistance (ohms)

I = measured current (amps). V = applied voltage (volts)

f = applied frequency (Hz)

δ = Phase angle shift

ω = Angular frequency, $2\pi f$ (rad/sec) [4, 5]

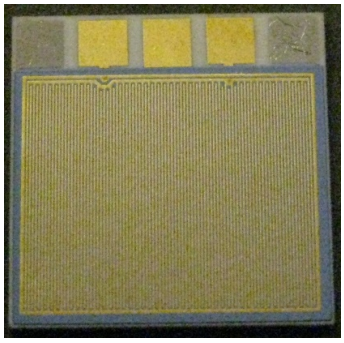

Figure 2.2. Single surface gold ceramic

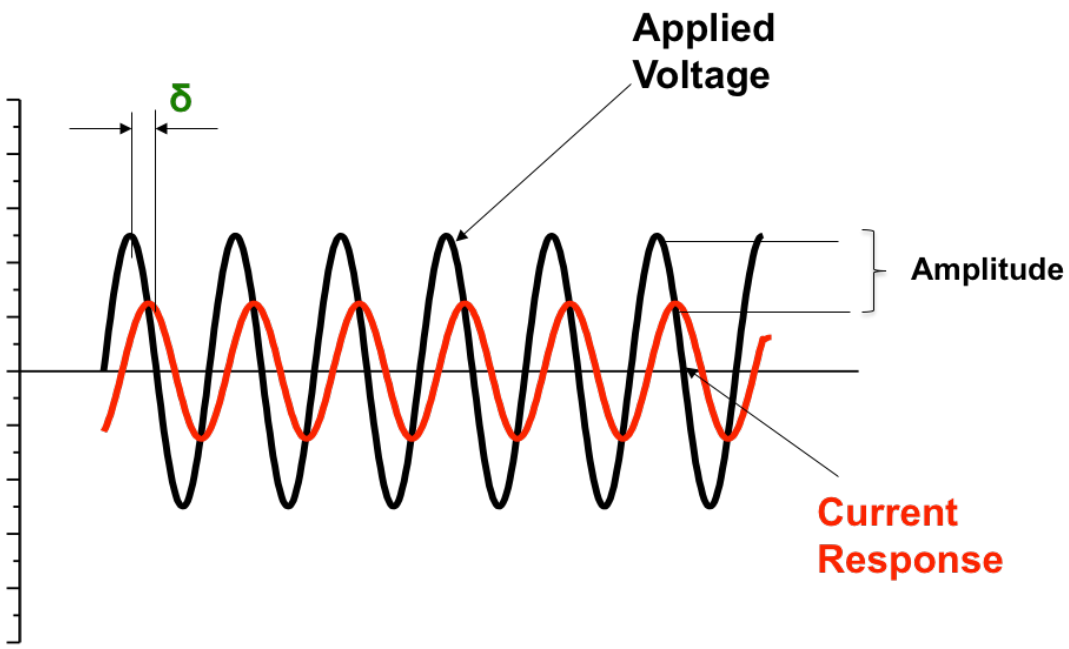

Figure 2.3. Applied Voltage/ Current Response

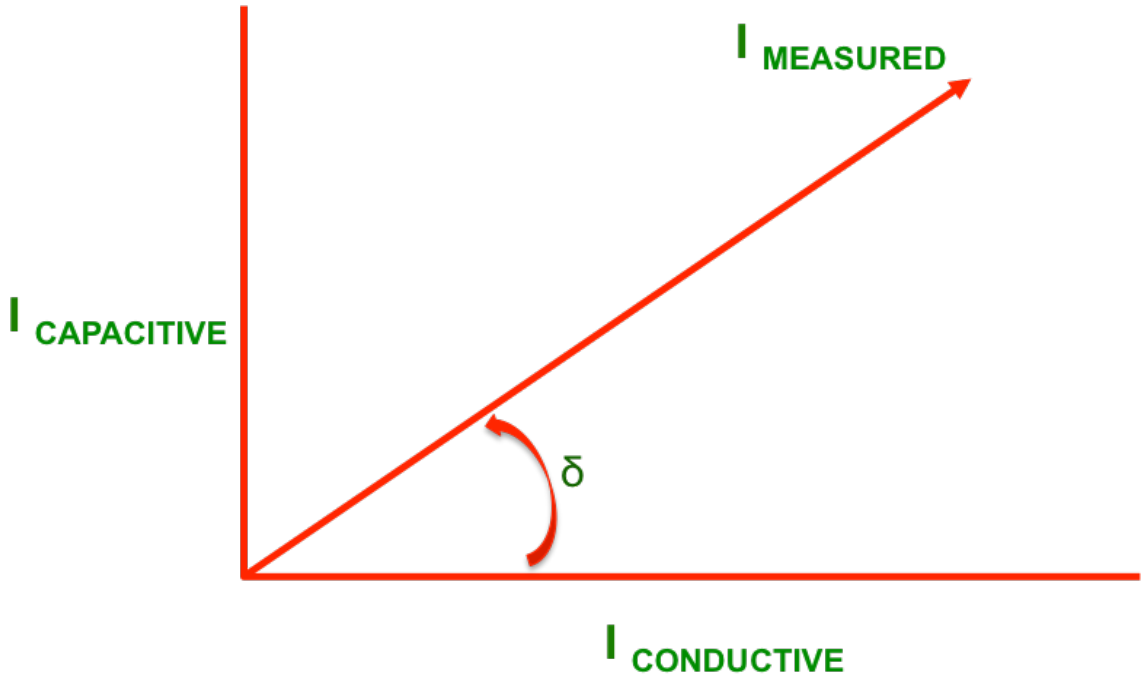

Figure 2.4. Calculations of Capacitive and Conductive Components

The current can be measured by using the current to charge a load capacitor and then measure the voltage across the capacitor [4, 5].

Measurements of capacitance and conductance of material are used to calculate the following variables over wide range of frequencies, which provide valuable information about molecular motion [5, 6]:

- Permittivity (ε′, real part), which is proportional to capacitance and measures the alignment of dipoles (molecular groups) in the electric field.
- Loss factor (ε″, imaginary part) is proportional to conductance or ion conductivity and represents the energy required aligning dipoles and moving molecular groups or ions.
- Complex dielectric constant (ε*) consists of both the "real" (permittivity) and the "imaginary" (loss factor) parts: ε* = ε′- iε″

A chemical bond that has an unbalanced distribution of charge in a molecule is a *dipole*. One part is partially positive and the other is partially negative in a dipole. In the absence of an applied electric field permanent dipoles exist, due to the differences in the electro-negativity of the bonded atoms (e.g., carbonyl group, cyano group). An applied electric field creates induced dipoles, which causes redistribution of electrons shared between the bonded atoms with similar electro-negativity. The orientation process requires a characteristic time, called the dipole or molecular relaxation time and denoted byτ_d[5, 6].

For Single surface and parallel plate electrodes, ε′and ε″can be calculated as follows:

$$\varepsilon' = \frac{Cd}{A\,\varepsilon_o} \tag{3}$$

$$\varepsilon'' = \frac{d}{RA2\pi f\varepsilon_o} \tag{4}$$

Where:

C = capacitance (farads)

A = electrode plate area

d= plate spacing

R = resistance (ohms) [conductance = 1/R]

f = frequency (Hz)

ε_o= absolute permittivity of free space (equal to 8.85 x 10^{-12} F m^{-1})

Debye developed an orientation mechanism assuming a single dipole or a single molecular relaxation time (τ_d) for all the molecules [7]. The classic Debye equations for $\varepsilon'$and $\varepsilon''$are as follows:

$$\varepsilon' = \varepsilon_u + \frac{(\varepsilon_r - \varepsilon_u)}{1+(2\pi f \tau_d)^2} \quad (5)$$

Where: ε_u = unrelaxed permittivity due to induced dipoles. ε_r = relaxed permittivity. $\frac{(\varepsilon_r - \varepsilon_u)}{1+(2\pi f \tau_d)^2}$= Permittivity due to alignment of dipoles

$$\varepsilon'' = \varepsilon_u + \frac{(\varepsilon_r - \varepsilon_u)2\pi f \tau_d}{1+(2\pi f \tau_d)^2} \quad (6)$$

to account for conductivity, can be written as:

$$\varepsilon'' = \frac{(\varepsilon_r - \varepsilon_u)2\pi f \tau_d}{1+(2\pi f \tau_d)^2} + \frac{\sigma}{2\pi f \varepsilon_0} \quad (7)$$

Where:

$\frac{(\varepsilon_r - \varepsilon_u)2\pi f \tau_d}{1+(2\pi f \tau_d)^2}$ = Dipole loss factor term

$\frac{\sigma}{2\pi f \varepsilon_0}$ = Ionic conduction term

σ = Ionic conductivity (mhos cm^{-1})

Both loss factor and permittivity are frequency and temperature dependent.

Permittivity has low values for pharmaceutical materials, chemicals and polymers when measurements are performed at low temperature, below thermal transitions, because molecules are frozen in place and the dipoles cannot move to orient and align themselves in the direction of the electric field. When dipoles are excited by moderate frequencies, they have enough time to become oriented, and their permittivity is high while loss factor is low. But when the frequency becomes so high that the dipoles can no longer follow the field, the dielectric constant falls steeply and material shows dispersion. This phenomenon is also followed by a sharp increase in dipole loss, resulting in a peak in loss factor. It consists of two contributions: energy losses due to the orientation of molecular dipoles, and conduction of ionic species [5, 6, 8 & 9].

The magnitude of the conductivity term relative to the dipole term can be adjusted by changing the frequency as the frequency is in the denominator of the ionic conduction term. At high frequency, the dipole loss factor term is dominant; at low frequency, the ionic conduction term is dominant. Ionic conduction is not significant until the pharmaceutical material and polymer becomes fluid (e.g., above Tg or melting point). Therefore, ε'' represents the energy to align dipoles or move ions below and through Tg [5]

Above Tg, ε'' can be used to calculate the bulk ionic conductivity as follows:

$$\sigma = \varepsilon'' 2\pi f \varepsilon_o \quad (8)$$

Bulk ionic conductivity can be used to follow the physical transitions in the material that takes place during change in degree of alignment of dipoles and ion mobility. Ionic conductivity is related to viscosity, because fluidity is identified by the ease with which

charged ions usually present as impurities or polar constituents in drugs can migrate through the samples [5].

The frequency dependence of ε' andε'', can be illustrated by a preferred method - Argand diagram (Known as Cole-Cole plot) [10]. Where ε'' is plotted vs. ε' taking ω as a parameter. When the ionic conductivity (σ) is zero, the Argand diagram corresponds to a Debye model is a perfect semicircle with intercepts $\varepsilon_u$and ε_r on the X-axis and with a maximum value of $(\varepsilon_u - \varepsilon_r)/2$, shown in (Figure 2.5.). The dielectric behavior of complex chemicals or polymers quite often can be characterized by a distribution of relaxation times rather than by a single relaxation time, leading to departure from a perfect semicircular arc, or appearance of more than one arc of relaxation times. As σ increases, the Argand diagram exhibits a vertical line with an intercept ε_u at the ε' axis. This is due to conduction and interfacial (Maxwell-Wagner) polarization resulted from accumulation of charges at the electrode interfaces [5, 6 & 9].

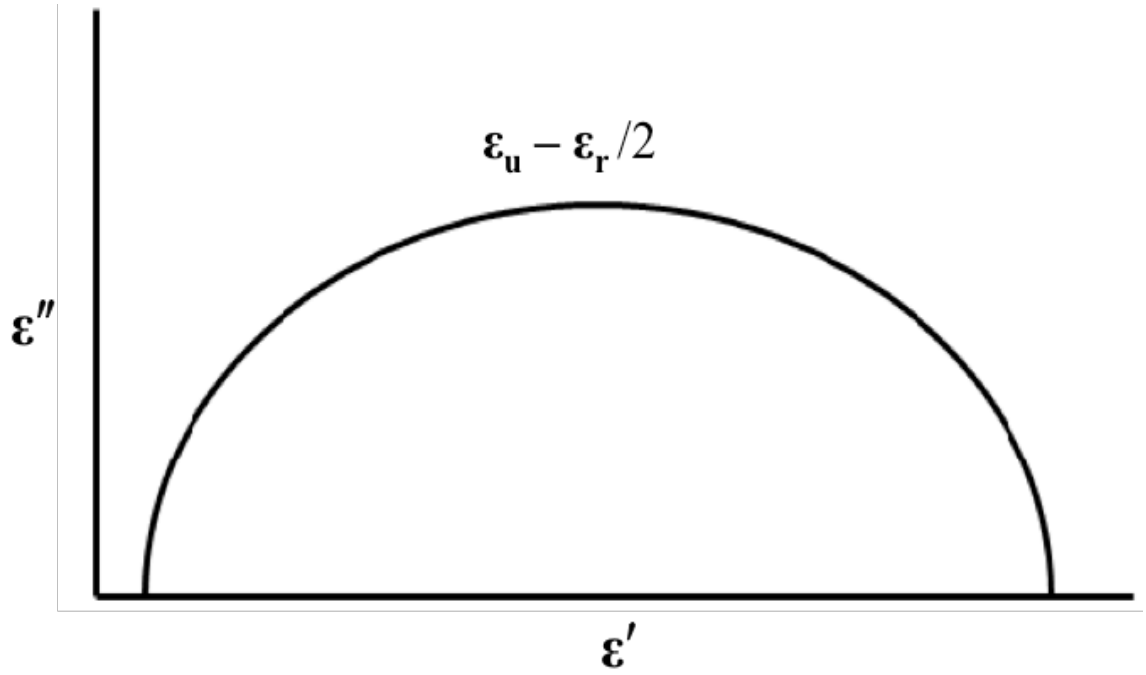

Figure 2.5. Cole-Cole plots corresponding to the Debye curve

Practically, the observed Argand diagrams deviate from the ideal ones, due to various reasons: ionic conductivity, electrode polarization, the existence of more than one dipole relaxation time for most materials, thus originating a distribution of relaxation times, causing some differences between calculated and observed results.

One of the principal difficulties associated with studying the dielectric behavior of solid samples is lack of generally agreed interpretive model. Several empirical corrections modify the Debye model, among these, those proposed by Cole–Cole [11], Davidson–Cole [12] and Havriliak–Negami [13-14]. The Debye model is, in practice, if ever applicable to solid systems, is based on the assumption of non- interacting dipoles. Cole and Cole noted that these general features of peak in dielectric loss and dispersion in the real part of the susceptibility are commonly observed and suggested that the discrepancy from the Debye model was due to the existence of more than one, almost overlapping dipole relaxation times. When one considers the physical basis of this distribution, it is because of inhomogeneities in the solid structure such as crystal defects or, a distribution of orientations of the molecules within that structure.

Hill and Jonscher [15] criticized this approach on the basis that the widths of the relaxation peaks observed in practice are so great that the distribution of relaxation times would have to be extremely wide. An alternative and equivalent approach is to consider the dielectric behavior to be a function of the probability of charge hopping between specific sites in a solid or material, where the peak broadening is due to a distribution of probabilities [16-17].

The Polaron theory or the “hopping model for conduction” is used to describe the transfer of charge between various specific localized sites within a material under the

influence of an electric field. According to this theory a corresponding phonon field involving polar modes accompanies the transfer of electronic charge. This composite of the electron and the associated phonon field are treated as a quasiparticle, i.e., the Polaron. A slow moving electron in a dielectric induced crystal interacting with the lattice ions through long-range forces will be surrounded by a field of lattice polarization caused by the moving electron. The charge jumps or hops discontinuously from site to site [18].

2.2 Differential Scanning Calorimetry (DSC)

DSC is by far the most popular thermal analytical technique for the characterization of pharmaceutical solids [1]. DSC monitors the energy required to maintain the sample and a reference at the same temperature as they are heated. The difference in energy is recorded as a function of temperature to give a DSC scan [19]. Heat flow corresponds to transmitted power and is measured in watts (W) or (mW) [20].

2.2.1 Principle. When the sample undergoes a phase transition or transformation, a heat difference occurs between the sample and reference. Therefore, a heat would either flow or get absorbed depending on whether the reaction is endothermic or exothermic. If the sample absorbs energy then the enthalpy change is called endothermic. If the sample liberates energy then enthalpy change is said to be exothermic. By recording the difference in the heat flow between the sample and the reference material DSC measures the energy difference of the sample. The result of a DSC experiment is a curve of heat Flow ($W\ g^{-1}$) vs. temperature (^{o}C) or vs. time (min) [21-23].

DSC measurements provide information on thermal effects, which are characterized by an enthalpy change and by temperature range, such as melting behavior, purity, crystallization, polymorphism, solid-solid transitions and chemical reactions.

Since DSC also measures the specific heat capacity, a change in heat capacity such as that occurs at glass transition can also be determined [20]. DSC is widely used in the pharmaceutical industry to characterize APIs (Active Pharmaceutical Ingredients) and excipients for purity determination, melting points, polymorphism behavior, crystallization, glass transition, crystalline and amorphous contents, and decomposition temperatures and more (see Figure 2.6.) [22].

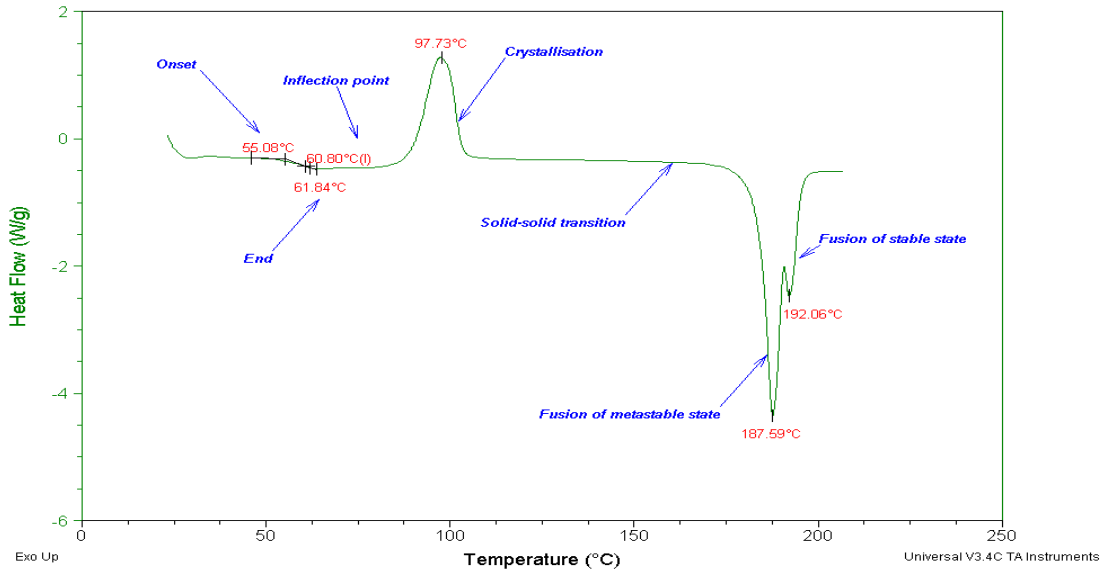

Figure 2.6. DSC profile for the amorphous form of an API

2.2.2 Types of DSC. A DSC is available in two types: Heat-flux DSC and Power-compensation DSC [24]. The principles of both techniques are outlined below.

2.2.2.1 Heat-flux DSC. Heat-flux DSC is rather similar to DTA. The big difference is that DTA does not allow quantitative measurements to be performed, while heat-flux DSC, owing to the well-defined thermal resistances in the cell, is eminently suited to this kind of measurement. (Formerly, heat-flux DSC was called quantitative DTA).

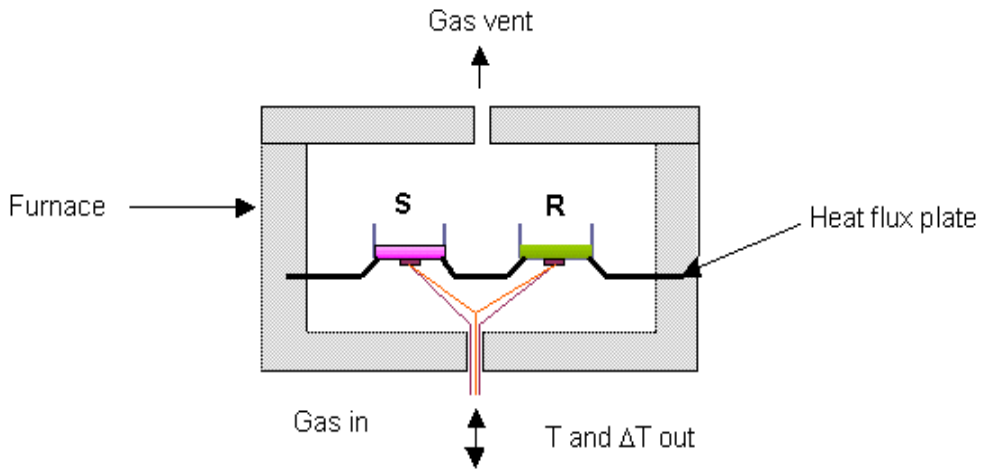

Figure 2.7. Schematic drawing of a heat-flux DSC cell; S: sample, R: reference [25]

Sample and reference substance are place in small crucibles and positioned on heat-flux plate (Figure 2.7.). This plate generates a very controlled heat flow from the furnace wall to the sample and reference of changes in the thermal resistance of the sample is eliminated. In this way, enthalpy changes in the sample can be measured accurately.

2.2.2.2 Power-compensation DSC. Here, in contrast to heat-flux DSC, sample and reference are completely isolated from each other (Figure 2.8.). Both, the sample crucible and the reference crucible have their own heating element and temperature-sensing element. With the aid of a temperature programmer, both sample and reference are heated and always controlled to have the same temperature. As soon as changes in the sample occur, extra (in the case of an endothermic reaction) or less (with an exothermic reaction) heat will be needed to maintain the set-heating rate. With the aid of special electronic circuitry, extra (or less) power is now sent to the sample holder in order to keep the temperature difference zero [26]. In this way, power and consequently heat flow and the enthalpy changes are measured.

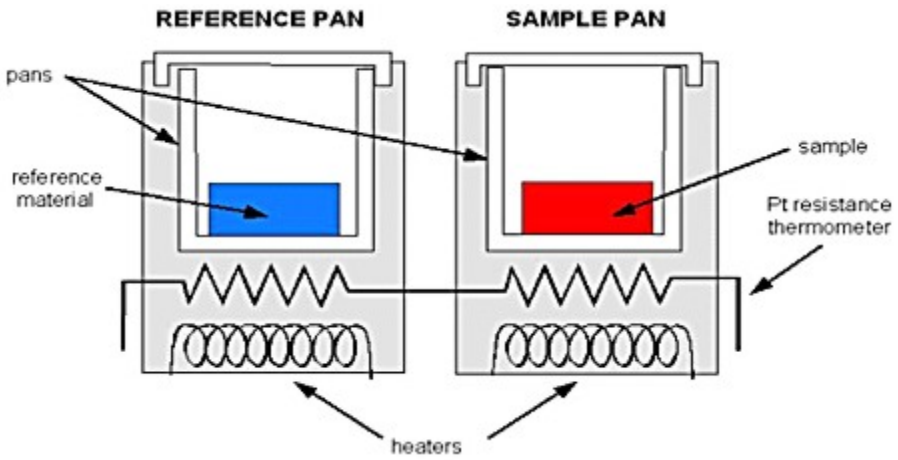

Figure 2.8. Schematic drawing of a power-compensation DSC cell: (Red) sample pan and (Blue) reference pan [27]

Heat-flux and power-compensation DSC instruments in their modern form constitute very sensitive pieces of equipment, having the capacity to measure heat flow of the order of micro Watts. This feature makes the applicability of the technique almost unlimited: every physical change or chemical reaction takes place with a change of the enthalpy and consequently absorption or release heat [28].

A characteristic DSC curve of an amorphous form of an API is shown in Figure. 6. The temperature, is always, plotted on the x-axis and Heat Flow is plotted on y-axis. In this case a change in the specific heat leads to the baseline shift at about 61^{o} C and corresponds to a glass transition. The first peak corresponds to an exothermic crystallization and the second peak to the endothermic melting of the substance (an API). According to the standards of the ICTA (International Confederation for Thermal Analysis), endothermic peak are plotted downward and exothermic peak upward. According to DIN (Deutsche Industrie Norm) standard 51005, endothermic peaks are plotted upward. Normally, every curve carries an indication of its mode or presentation.

2.2.3 Applications. There are a very large number and variety of applications of DTA and DSC. The applications may be divided roughly into two categories [26]:

1. Physical changes and measurements, such as melting, crystalline phase changes, changes in liquid and liquid crystalline states and in polymers, phase diagrams, heat capacity, and glass transitions, thermal conductivity and diffusivity and emissivity.
2. Chemical reactions such as dehydration, decompositions, polymer curing, glass formation and oxidative attack.

The numerous applications for DSC have been clearly cited in a number of reviews and research articles [26-28].

2.3 X-ray Powder Diffractometry (PXRD)

2.3.1 Introduction. Diffraction techniques are perhaps the most definitive method of detecting and quantifying molecular order in any system. An x-ray diffraction study requires a clear understanding of the crystallographic structure, chemical composition, physical properties of solid, metals, films and other polymeric materials present in a given sample. It is a widely used in chemistry, material science, biology, geology and environmental science, forensic science, polymer science and pharmaceutical sciences. Other diffraction techniques that have been used to study order in pharmaceutical systems are as follows: conventional, wide-angle and small-angle diffraction techniques [29-30]. Conventional X-ray powder diffraction, also known as PXRD (see Figure 2.9.) can be used to quantify non-crystalline material and by controlling the temperature and environment it can also be used to follow the kinetic phase transformation. Small-angle X-ray diffraction technique measurements have been used to study the subtle structural changes in polymers. Although, these methods only “observe” molecular order, and the disorder in the system is predicted by the absence of the order [31]. PXRD is a rapid

analytical technique primarily used for phase identification of a crystalline material and can provide information on unit cell dimensions. Crystalline organic solids are made up of molecules that are packed or ordered in a specific arrangement. This molecular arrangement is defined as unit cell, which is the smallest repeating unit of a single crystal [32].

X-Ray difraction (XRD) is most widely used in numerous industries for identification of crystalinity in compound by studying their difraction pattern. Some other specific benefits of XRD are listed below.

- Single phase materials in several samples such as chemicals, ceramics, polymers, etc., are identified.
- Determination of polymorphs.
- Evaluating amorphous and crystalliine content in pharmaceuticals or other chemicals.
- Recognition of multiple phases in samples like rocks, minerals, meltas, etc,.
- Quantitative determination of different phases is possible by advanced technique called PXRD, which different phases by calculating peak ratios.

In order to interpret the data obtained from XRD you need to know a few basic principles like how the X-rays interact with the sample, possible errors and the different source. The mathamatics and physics involved in generating the monochromatic X-rays and X-ray difracttion is not necessary.

2.3.2 Sample preparation. The most critical factor in obtainig a quality analytical data relies on preparation of the specimen. In order to have a ideal sample

preparation you need to have random distribution of crystals which should be less than 10μm. Specimen should be mounted such a way that there should be no crystallite. Considering the above factors sample preparation is considered to be a significant topic.

2.3.3 Generate analytical x-rays. Experimental results are much better as we get closer to the monochromatic beam in our X-ray beam. In X-ray difracttion of most organic and inorganic crystals copper tubes are used. For copper the most stongest radiation (Kα) is 1.54 angstroms. There are low energy and high energy radiations produced by tubes. Kα1, Kα2 and Kβ are the high energy radiations of which we use Kα1 for analytical data. A monochromator or an energy selective detector is used to eliminate Kβ, and Kα2 is electronically removed from X-ray data during processing.

2.3.4 XRD Principle. Sample is exposed to X-rays this interaction leads to secondary wave which is produced by the cones in the sample. According to the mathamatical equation Braggs law the produced secondary wave is related to the interplanar spacing in the crysalline sample.

Braggs Law:

$$n\lambda = 2d \sin\theta \quad (9)$$

Where n is an integer

λ is the wavelenght of X-rays

d is the interplanar spacing generating the diffraction

θ is the diffraction angle

Diffraction maxima are measured along 2θ diffractometer circle for powder samples having infinet amount randomly oriented crystal. According to Braggs law the angle of diffraction is related to the interplanar spacing d, and the intensity of the

diffraction is related to the strenght of those diffractions in the specimen. Electronic detectors are used to measure and record angles and intensities of diffraction. Specialized software is utilized to create plots of 2θ (X axis) vs. intensity (Y axis) for the sample. Units for λ and d are measured in angstroms.

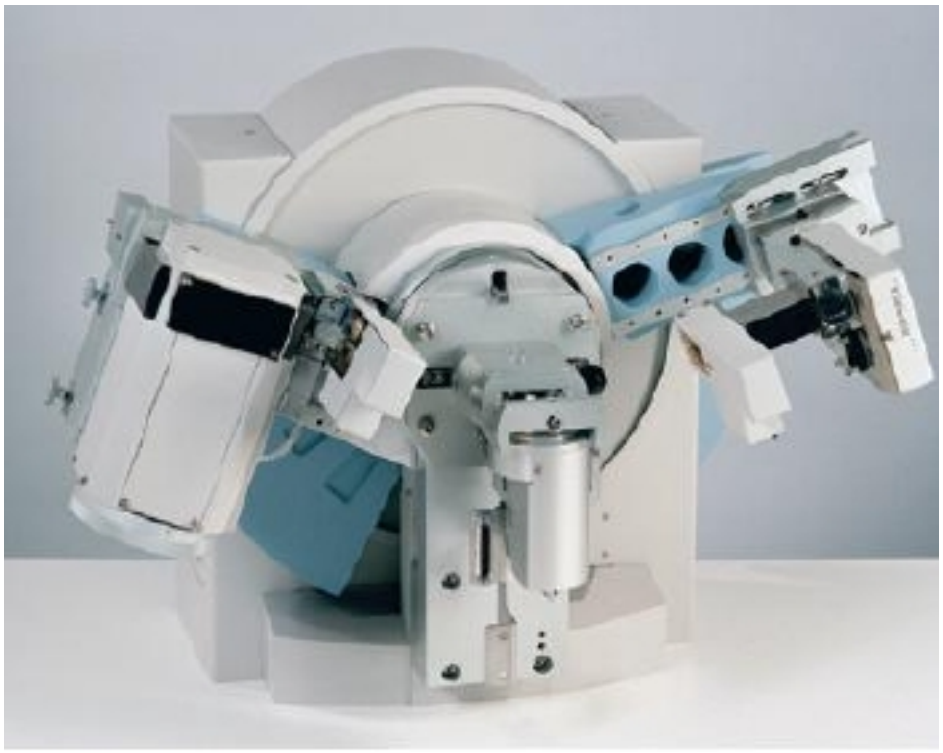

Figure 2.9. Phillips X-ray Diffractometer [29]

2.4 Scanning Electronic Microscopy (SEM)

SEM was first build by Von Ardenne in 1938 later it was developed and described by Zworykin in 1942 [1,2]. A wide range of sample specimens can be analyzed to micro structural scale using SEM. You can have an image 500 times greater than light microscopy using SEM it gives a precise measurement of small objects down to 50nm. An electron beam with high energy is employed to illuminate the specimen and produce image on a fine scale. High-resolution images produced by SEM are used to analyze chemical structure, identify micrographic and crystallographic orientation of many

materials. A back-scattered image from SEM is used to identify phase in a multi-phase analysis.

2.4.1 Instrumentation. Electron Guns: A stable source of electron beam is produced by electron gun. Field emission and thermionic emission are two strategies used to produce these electrons for electron beam. In thermionic electron gun a wire or any compound is heated to very high energies so that the electrons overcome the work function of cathodes and escape in to the source. The cathode filament is placed close to anode disc and maintained at a high negative voltage so that the produced electrons are accelerated easily.

In field emission transport of electrons from the metal surface occurs as a result of delocalization. This transport of electrons by delocalization is known as tunneling effect [6].

2.4.1.1 Electron lenses. Magnets are used to manipulate configuration of electron beam. Condenser and objective lens de-magnify electron image formed at crossover of electron gun. In some cases demagnification is high as 10,000. Usually one or more lenses are utilized in the condenser lens, which determines the current impinging on to the sample while the final spot size is determined by objective lens.

2.4.1.2 Detectors. Types of detectors used in SEM are (1) solid state detectors, (2) specimen current detectors, (3) scintillator photomultiplier detector, and (4) cathode luminescence detector [4].

2.4.1.3 Image processing. There are three basic ways to process image: (1) optical photographic method, which is a traditional method where image is printed using lens available in the photographic enlarger. (2) Electric analog method in which the

electric or analog is manipulated by the detection system in SEM. (3) digital image process this is much advanced technique with better grey definition, sophisticated storage methods and freedom from deterioration.

2.4.2 Sample preparation. Preliminary treatment is required in many samples before mounting. Avoid volatile compounds, as they tend to vaporize. Conducting samples yield better images. Non-conducting samples require conductive coating. To prevent charging under electron beam sputter coating should be done.

2.4.2.1 Sputter coating. Image quality in a non-conductor is affected as they tend to collect electrons from the electron beam and become negative. To prevent this samples are covered with a very thin layer of metals such as gold or silver. This process of coating is carried out in a glass chamber that is evacuated by rotary pump and argon gas is pumped to 0.1 torr pressure. High voltage is applied to electrodes that bombard ions and sputtering of atoms on to the sample. Thickness of the atoms on the sample can be controlled (see Figure 2.10.). To protect fragile material from electron bombardment cold sputtering is available.

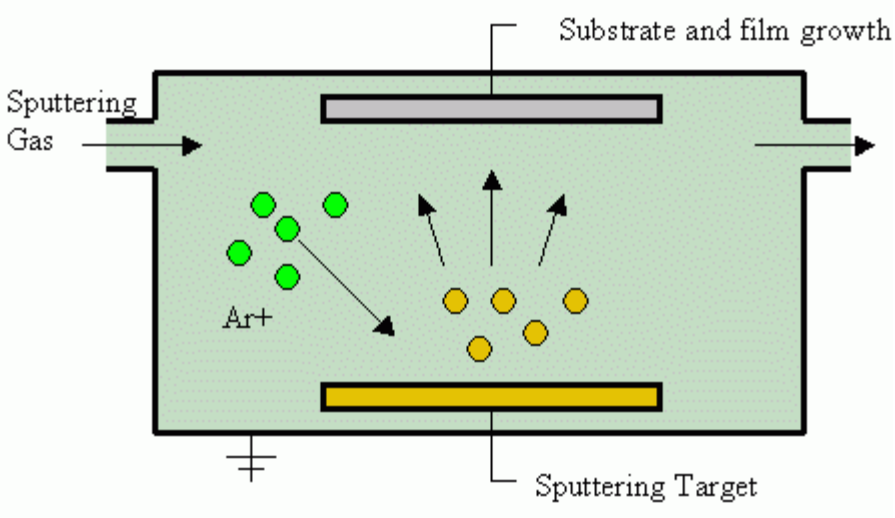

Figure 2.10. Sputter Coater

2.5 Macro-Photomicrography

A Konica-Minolta DG SLR Camera with a 28-80 mm macro lens was used for Macro- photomicrography to characterize the crystalline and amorphous materials on the single surface interdigitated array gold electrodes, and material in the DSC pans. An eyepiece reticule was used to calibrate the Macro-photomicrography system.

2.6 References

1. Brown ME. Principles and practice. Handbook of thermal analysis and Calorimetry, Vol. 1. Amsterdam: Elsevier; 1998.
2. Núńez L, Fraga F, Núńez MR, Castro A, Fraga L. J ApplPolym Sci 1999;74:2997.
3. Guma, N.C., Kale, K. and Morris, K.R., "Investigation of Film Curing Stages by Dielectric Analysis and Physical Characterization", J of Pharm Sci, Vol.86, No.3, 1997, pp.329-334.
4. Suwardie, J. H., "Analysis of Curing Using Simultaneous Dynamic Mechanical and Dielectric Measurements," *Materials Characterization by Dynamic and Modulated Thermal Analytical Techniques, ASTM STP 1402*, A.T. Riga and L. Judovits, Eds., American Society for Testing Materials, West Conshohocken, PA, 2001.
5. DEA 2970 Dielectric Analyzer, Operator's Manual. PN 901201.001 Rev. B 118947 B. Issued August 1989.
6. LisardoNúńez, et al. "Use of the dielectric analysis to complement previous thermoanalytical studies on the system diglycidyl ether of bisphenol A/1,2 diamine cyclohexane," polymer 45 (1167-1175): Elsivier/Polymer; 2004.

7. Debye P. Polar molecules. New York: Chemical Catalog Co; 1929.

8. Seanor, D.A., "Electrical Conduction in Polymers," Electrical Properties of Polymers, D. A. Seanor, Ed., Academic Press, 1982, pp. 16.

9. Hedvig, P. Dielectric Spectroscopy of Polymers, John Wiley, New York, 1977.

10. Hunt BJ, James MI. Polymer characterization. Great Britain: Blackie Academic and Professional; 1993.

11. Cole KS, Cole RH. J Chem Phys 1941; 9:341.

12. Davidson DW, Cole RH. J Phys Chem 1951; 19(12):1484.

13. Havriliak S, Negami S. Polym Sci C 1966; 14:99.

14. Havriliak S, Negami S. Polymer 1967; 8:161.

15. Hill, R.M. and Jonscher, A.K. (1983) Contemp. Phys. 24 75

16. Butcher, P.N and Morys, P. (1973) J. Phy. C 6 2147.

17. Butcher, P.N. and Ries, B. (1980) Phil. Mag. B44 179.

18. Alan T. Riga, PhD Thesis, The Electrochemical and Dissolution Properties of Nickel Oxide and LithiatedNiO, Western Reserve University, pp 32-39; 1967 and J.M. Ziman, "Electrons and Phonons", Theory of Transport Phenomena in Solids, Clarendron, Oxford, England, p308-310, 1963

19. Barnes A.F., Hardy M.J, Lever T.J.; A review of the applications of thermal methods in the pharmaceutical industry; J. Therm. Anal.; 1993, 4:; 499.

20. Widmann G, Dr. Riesen R, Mettler-Toledo Analytical, Dr. Verlag A.H.; "Thermal Analysis, Therms, Methods, Applications", Heidelberg, 1984, 3. Edition, ISBN 3-7785-1050-9.

21. Ford J.L., Timmins P., "Pharmaceutical Thermal Analysis Techniques and Applications", Ellis Horwood, 1989, pp10.

22. Giron. D., "Applications of Thermal Analysis in the Pharmaceutical Industry", J. Pharm & Biomed. Anal. 4, 6, 755-770, 1986.

23. Schawe, L.E.K. "Modulated temperature DSC measurements: the influence of experimental condition", Thermochim. Acta. 1996, 271:127-140

24. Skoog D. A., Holler, F. J., Nieman, T. A. "Principle of Instrumental Analysis", Saunder's College Publishing, 5th edition, USA, 1998, pp 806.

25. http://www.anasys.co.uk/library/dsc1.htm

26. Haines P.J.; Thermal methods of analysis; Blackie academic & professional; 1995; New Zealand.

27. http://www.evitherm.org/default.asp? lan=1&ID=982&Menu1=982

28. Skoog D.A., Leary J.J.; Principles of instrumental analysis; Saunders College Publishing; 4th Edition; 1971; U.S.A.

29. Pikal MJ, Lukes Al, Lang JE, Gaines K. 1978 Quantitative crystallinity determinations for β-lactam antibiotics by solution calorimetry: Correlation with stability. J Pharm Sci 67:767-772.

30. Yoshioka M, Hancock BC, Zografi G. 1994. Crystallization of indomethacin from the amorphous state below and above its glass transition temperature. J Pharm Sci 83: 1700-1705.

31. Hancock BC, Zografi G. 1997. Characteristics and significance of the amorphous state in pharmaceutical systems. J Pharm Sci 86: 1-12.

32. Ohannesisan L, Streeter AJ. "Handbook of Pharmaceutical Analysis", Marcel Dekker Inc., NY 2002, pages 23-27.

CHAPTER III

STANDARD TEMPERATURE CALIBRATION PROTOCOLS AND MATERIAL CHARACTERIZATION WITH PHARMACEUTICALS BY THERMAL ANALYSIS

Manik Pavan Kumar Maheswaram

(Manuscript submitted for publication and is under review)

(Journal of Testing and Evaluation ASTM International)

3.1 Introduction

There are thousands pharmaceutical materials known today [1-3]. There is a need for each material that is synthesized and discovered, to be tested and standardized. Calibration typically uses metals e.g., Indium and Zinc to calibrate the three instruments described in this study [4]. In order to make DSC, DEA and TMA more user friendly in the pharmaceutical community, we have implemented the use of analytical grade APIs and excipients for temperature and material characterization as well as calibration. Calibration is performed by observing the melting transition temperature of standard pharmaceutical materials within the temperature range of interest. DSC is used to determine the glass transition temperature, melting temperature, heat of fusion and heat of crystallization of pure materials. These first and second order thermodynamic

transitions can also be delineated using pure drug samples. DEA is typically used to measure the ionic conductivity and dielectric properties of a broad range of materials [5]. TMA measures the dimensional variability of a solid polymer or material, and can also be used to characterize powdered APIs [6]. To design an efficient procedure for calibration, understanding the thermal analysis of all these instruments is crucial.

3.1.1 Differential Scanning Calorimetry. DSC is a thermal analysis technique used to measure the changes in the heat flow of a sample, which involves exothermic or endothermic processes, as a function of time and temperature. It is widely applicable to a variety of materials such as pharmaceuticals, polymers, ceramics, metals, food and inorganics etc [7-11]. DSC is a well-established tool for pharmaceutical or material analysis, and provides information regarding melting temperatures, heats of fusion and crystallization temperatures, glass transition, drug and excipient interaction, thermal stability of pure materials or APIs. These properties are crucial for pre-formulation and drug dosage design of pharmaceuticals.

The experimental variables considered while performing DSC are the sample size, environment, heating rate and pan type (open pan, closed pan etc.). The performance of DSC is dependent on all these experimental variables [2, 5-7]. The heat of fusion (Jg^{-1}) is associated with the DSC examination of the crystalline API (Run 1). The thermal analysis curve represents a physical chemical property of the sample drug, i.e., melting. Cooling of the active pharmaceutical ingredient sample after melting through the crystallization yields the temperature and heat of crystallization ($J\ g^{-1}$) and is needed to further characterize the APIs.

3.1.2 Dielectric analysis. DEA is a material characterization technique used to measure quantitative thermal and dielectrical information on wide variety of materials, which include solid, liquids, films and polymers [12]. It can be used e.g., to determine the polymer viscosity, thermal transitions of polymers, characterization of food products and pharmaceuticals. As DEA is a thermal analysis tool it compliments DSC by allowing a measurement of molecular motion initiated by the A.C. electric field.

3.1.2.1 Principle of dielectric analysis. An applied sinusoidal voltage on a sample placed on a single surface gold ceramic interdigitated electrode creates an alternating electric field, producing polarization in the sample that oscillates at the same frequency as the electric field. There is a phase angle shift δ measured by comparing the applied voltage to the measured current, which is separated into capacitive (e') and conductive (e'') components [13].

- *Capacitance*- High frequency permittivity (e') or dielectric constant.
- *Electrical conductivity (pS cm^{-1})* - Loss factor (e") x Applied frequency (Hz) x 2π.

From known geometrical constants, such as electrode arrangement and electrode spacing of the IDA electrode, desired electrical properties of the test sample or material can be recorded. Such electrical properties are ionic conductivity, dielectric constant, dielectric loss angle, dissipation factor, dipole relaxation time, permittivity (e'), loss factor (e") and tangent delta (e''/e'). These properties are recorded as a function of time, temperature and frequency during the course of the experiment by varying and measuring these independent parameters [14-15].

- *Permittivity (e')* is a measure of the alignment of molecular groups (dipoles) in the electric field.
- *Loss factor (e'')* is a measure of the energy required to move the molecular groups or ions and is proportional to ionic conductivity.
- *Tan delta* is the ratio of the loss factor divided by the permittivity; Tan delta = e''/e'.

3.1.3 Thermomechanical Analysis. TMA is a thermal analysis technique used to measure changes in the physical dimensions (length or volume) of a sample as a function of temperature and time under a non-oscillatory load [6]. This technique is widely applicable to a variety of materials such as pharmaceuticals, polymers, ceramics and metals etc. TMA has been used in pharmaceutical analysis [17-19]. The variables considered while performing the thermal mechanical analysis are; applied load, gas environment, temperature range and heating rate as well as TMA probe type. The tests are run in a heating mode at a desired heating rate and temperature range of interest. Probe displacement profiles are subsequently analyzed in terms of coefficient of thermal expansion, softening and melting temperatures, and glass transition temperatures. Information obtained based on the different TMA probe types are shown in (Table 1), and recorded as a function of temperature.

Table 1

Types of TMA Probes and Resulting Measured Properties

TMA Probe Type	Information Obtained
Flat probe/ Light load	Coefficient of Thermal Expansion and T_g
Dilatometer	Coefficient of Thermal Expansion and T_g
Penetration probe/Significant load	Softening/ T_g, Melting and creep modulus
Tension accessory	Tg, melting and cure behavior
Parallel plates	Melting, Viscosity and Gelation
Flexure accessory	Softening/ T_g and Melting

**Tg =Glass transition temperature*

The focus of this study is to extend the selection of calibration materials from metals to pharmaceuticals i.e., APIs for the three instruments described in this study. Primarily by introducing a modified ASTM standard where the temperature is calibrated with a current NIST (National Institute of standards and Technology) standard material in addition to the use of APIs. Our overall focus is to calibrate the temperature axis of DSC, DEA and TMA with the melting temperatures of APIs and excipients. These test protocols permit inter-laboratory and intra-laboratory comparison and correlation of instrumental temperature scale data within the pharmaceutical community, and would be more relevant to quality control scientists in the pharmaceutical industry.

3. 2 Experimental

3.2.1 Materials. The following analytical grade >99.9 % pure APIs and an excipient (Vanillin), within the temperature range of interest, were used in this test

development as listed in Table 2 with Chemical Abstract Service (CAS) registry numbers. The ASTM E928-08 "Standard Test Method for Purity by Differential Scanning Calorimetry" was employed to verify the purity of the test specimen used in this study [20].

Table 2

Calibration Materials and Their Transition Temperatures

Calibration Materials*	**Literature Transition Temperatures/ °C (Solid - Liquid)**	**Chemical Abstract Service registry numbers**
Acetophenetidin	132 – 138	62-44-2 [21]
Acetanilide	113 – 116	103-84-4 [22]
Vanillin	81 – 83	122-33-5 [23]
Sulfa pyridine	191 – 193	144-83-2 [24]

**Available from Sigma- Aldrich®*

3.2.2 Instruments. The TAI DSC 2920 was used to measure the heat flow properties of calibration materials as a function of time and temperature. The test specimens of desired temperature range from 25 to 250 °C were heated at a rate of 5 °C min^{-1} with nitrogen gas purge of 50 mL min^{-1}. Open or closed pans were used in this study.

The TAI Dielectric Analyzer 2970 was used for dielectric analysis of the calibration materials (test specimen), possessing dielectric properties that undergo solid-liquid or solid-solid transition, over a wide range of frequencies from 0.1 to 1000 Hz and temperatures from 25 to 250 °C. The test specimen was ramped at a rate of 5 °C min^{-1},

nitrogen gas purge at a flow rate of 50 mL min^{-1} and liquid nitrogen cooling when necessary. The single surface gold ceramic interdigitated (IDA) electrodes were utilized. The TAI TMA 2940 was used to measure the dimensional change (μm) of the calibration materials as a function of temperature. The test specimens, packed into a DSC aluminum pan were studied over a desired temperature range from 25 to 250 °C and heated at a rate of 5 °C min^{-1} with a nitrogen gas purge of 50 $mLmin^{-1}$. Sample height was typically of 0.9 to 1.3 mm was used in the study.

3.2.3 Hazards. This test protocol involves the use of hazardous materials, operations and instruments. It is the responsibility of the user to take care and establish appropriate safety practice and to determine the applicability of regulatory limitations prior to use, adaptation of ASTM method E1363 [6].

3.2.4 Sampling. Calibration materials are analyzed by all the three instruments on "as received" basis. Since sample size is very small, care should be taken, so that the test specimens are homogeneous and representative of the sample. While performing DEA, the test specimen must cover the entire surface of the IDA electrode. The thickness of the test specimen should be at least 1.5 times of the IDA electrode spacing. For DSC and TMA sampling is done by packing the test specimen in a standard aluminum pan.

3.3 Calibration

Temperature signal from the instrument must be calibrated accurately over the desired temperature range, to obtain consistent results from different experimental conditions. Therefore, calibration is a basic process for any instrument in order to obtain accurate results. Calibrate the permittivity and temperature sensors of the DEA instrument using the procedure described by the manufacturer in the operator's manual.

This test protocol was performed and developed by using Standard Test Method for temperature calibration of DSC, DEA and TMA, ASTM method E967 [4], E 2038 [5] and E 1363 [6], respectively.

3.3.1 Experimental procedures for DSC, DEA and TMA.

- Select the calibration material of known transition temperature listed in table 2.
- For DSC, weigh 10 mg of test material into a clean, dry aluminum pan. The sample size for DEA is 20 to 40 mg. Care should be taken, so that the test specimen covers the entire surface of the IDA electrode. Sample height of 0.9 to 1.3 mm was used for TMA analysis.
- Load the test material into the instrument chamber e.g., (DSC, DEA and TMA), and purge the instrument with dry nitrogen gas (99.99% purity purge gas) at constant flow rate of 50 ml min^{-1} throughout the experiment.
- Set the initial temperature of the instrument to a value about 30°C below the estimated transition temperature of the test material, and allow it to equilibrate for 5 min at that temperature.
- Initiate a temperature program at a constant heating rate of $3^{o}Cmin^{-1}$ to a temperature 20°C above the estimated melt transition temperature of the test material.
- **Note:** When a DSC is used, run a Heat-Cool-Heat cycle for each test material. Cool the test material at $3°Cmin^{-1}$ through the crystallization exotherm until the baseline is re-established below the crystallization temperature.

- **Note:** when a DEA is used, initiate the measurement of permittivity at a test frequency of 1,000 Hz and a set of frequencies (1, 10, 100, 1000 Hz). Record permittivity and log Permittivity, on a linear scale, as a function of temperature
- Record the accompanying thermal curve by using the instrument software.
- Repeat the procedure described above for other calibration materials chosen.

3.4 Results and Discussion

3.4.1 For DSC. At a thermodynamic transition temperature, i.e. change in heat flow is marked by absorption (or release) of energy by the calibrants resulting in an endothermic (or exothermic) peak in the heating (or cooling) curve is recorded.

- From the resultant DSC thermal curve, measure the temperatures for the desired points on the curve: Tm, Tmp, Tc, Tcp, Heat of fusion (Jg^{-1}) and Heat of crystallization (Jg^{-1}) for a pure calibration material.

Tm = Extrapolated onset melt temperature

Tmp = Melting peak temperature

Tc = Extrapolated crystallization temperature

Tcp = Crystallization peak temperature

ΔH_f = Heat of fusion

ΔH_c = Heat of crystallization

The DSC thermal curves of Acetanilide (see Figure 3.1.), Acetophenetidin (see Figure 3.2.) and Vanillin (see Figure 3.3.) are described respectively. These heat-cool-heat plots show changes in the heat flow ($W\ g^{-1}$) with respect to time and temperature.

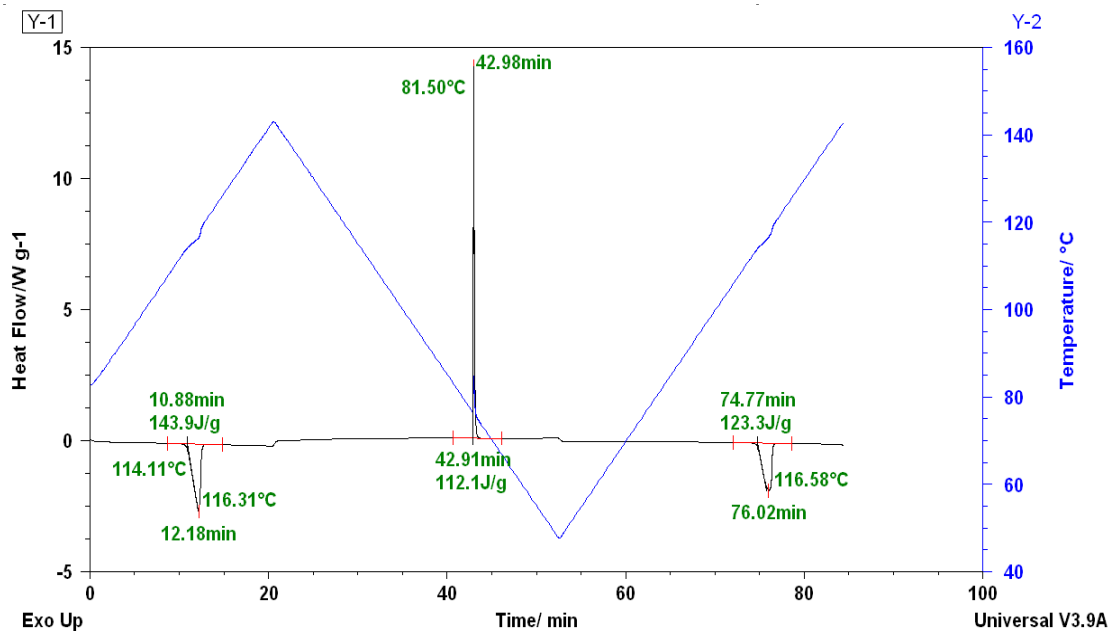

Figure 3.1. Acetanilide DSC curve showing Tmp =116.31° C, Tcp = 81.50° C; Heat of Fusion for first endothermic peak ΔH_f = 143.9 Jg^{-1} and ΔH_f = 123.3 Jg^{-1} for second endothermic peak; Heat of Crystallization, ΔH_c= 112.1 Jg^{-1}.

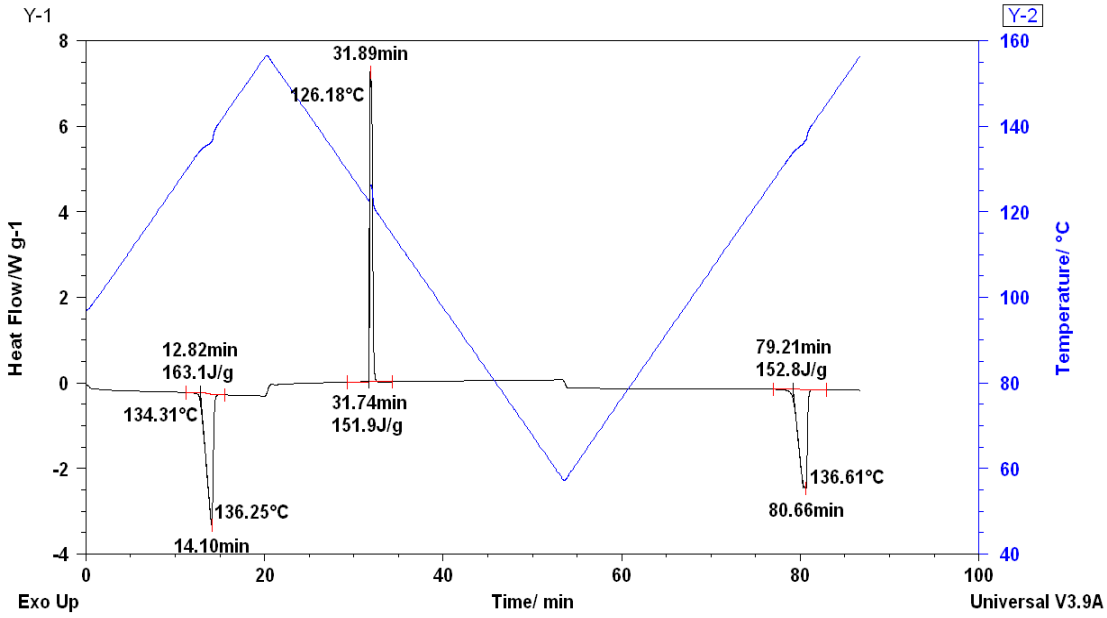

Figure 3.2. Acetophenetidin DSC curve showing Tmp =136.25° C, Tcp =126.18° C; Heat of fusion for first endothermic peak ΔH_f=163.1 Jg^{-1} and ΔH_f = 152.8 Jg^{-1} for second endothermic peak; Heat of crystallization, ΔH_c = 151.9 Jg^{-1}.

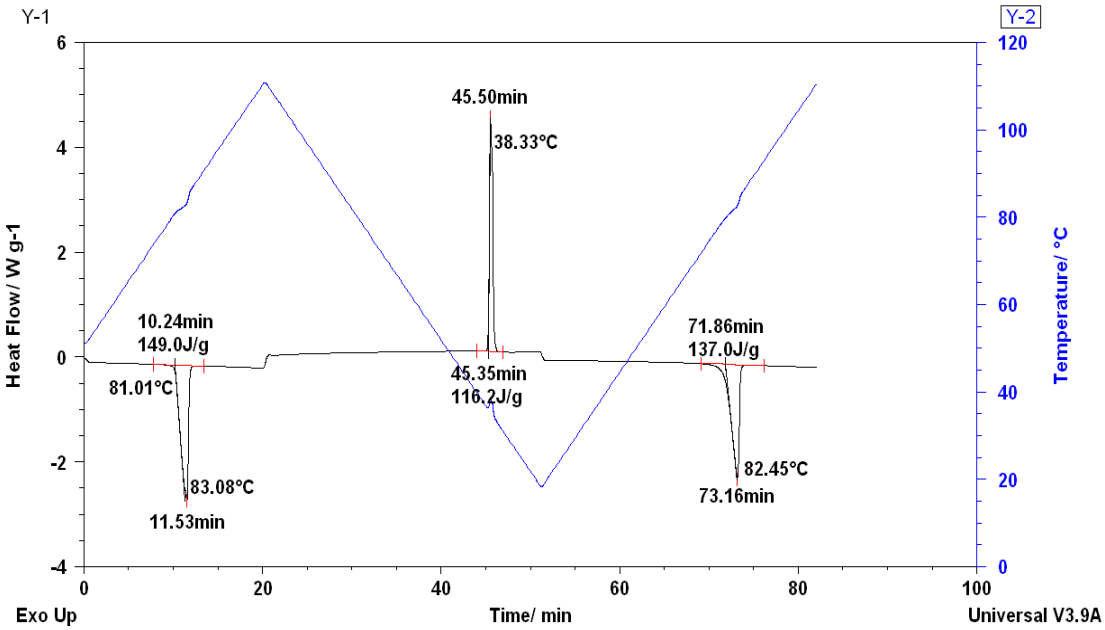

Figure 3.3. Vanillin DSC curve showing Tmp = 83.08° C, Tcp = 38.33° C; Heat of fusion for first endothermic peak ΔH_f = 149.0 Jg^{-1} and ΔH_f = 137.0 Jg^{-1} for second endothermic peak; Heat of crystallization ΔH_c=116.2 Jg^{-1}.

A summary of the DSC melting and crystallization properties of calibration materials is cited in Table 3.

Table 3 describes the Melting peak temperatures (Tmp), Crystallization peak temperatures (Tcp), Heat of fusion (ΔH_f, Jg^{-1}) Heat of crystallization (ΔH_c J g^{-1}) and % Crystallinity of calibration materials evaluated by DSC.

Table 3

DSC Melting and Crystallization Properties of Calibration Materials

Calibration materials	Melting peak Temperatures/ Tmp °C		Cryst peak Temperatures/ Tcp °C	ΔH_f(J g^{-1})		ΔH_c (J g^{-1})	% Crystallinity ($\Delta H_c/\Delta H_f$)*100
	1st Peak	2nd Peak		1st Peak	2nd Peak		
Acetanilide	116.31	116.58	81.50	144	123	112	78
Acetophenetidin	136.25	136.61	126.18	163	153	152	93
Vanillin	83.08	82.45	38.33	149	138	116	78
Sulfapyridine	192	$T_{g=}$(62)	123	174	-	57	33

Note: Tmp = Melting peak temperature. Tcp=Crystallization peak temperature.

3.4.2 For DEA. At the thermodynamic melt transition temperature, an abrupt change in DEA permittivity is observed. The instrument records the temperature observed for this transition.

- From the resultant DEA thermal curve, following parameters are measured to determine the property variation associated with the transition; frequency, permittivity, log permittivity, temperature, derivative of permittivity and log permittivity with respect to temperature.
- Plot the DEA thermal curves of test specimens in the following manner:

a) Plot permittivity vs. temperature and first derivative of the resultant curve

   A single frequency (1000 Hz) and a set of 4 frequencies i.e. (1, 10, 100 and1000 Hz) were used in evaluating each calibration material.

b) Plot log of permittivity vs. temperature and first derivative of the resultant curve

   A single frequency (1000 Hz) and a set of 4 frequencies i.e., (1, 10, 100, and 1000 Hz) were used in evaluating each test material.

c) For both these calibration processes use the first derivative to determine the inflection point of the original thermal curve and this inflection point is used as first onset point. The second point is typically above the known transition temperature on the original thermal curve where the slope is constant.

d) Employ the instrument software to determine the onset temperature and the calibrated temperature.

The DEA curve of acetanilide showing the permittivity transition temperature for a single frequency (1000 Hz) run is described in (Figure 3.4.). Figure 3.5 describes the acetanilide derivative of permittivity transition temperature for a single frequency run when plotted vs. temperature. Figure 3.6 describes the DEA Acetanilide curve showing Log permittivity transition temperature at 10Hz. Figure 3.7 describes the DEA acetanilide curve showing Derivative of log permittivity transition temperature at 1 Hz.

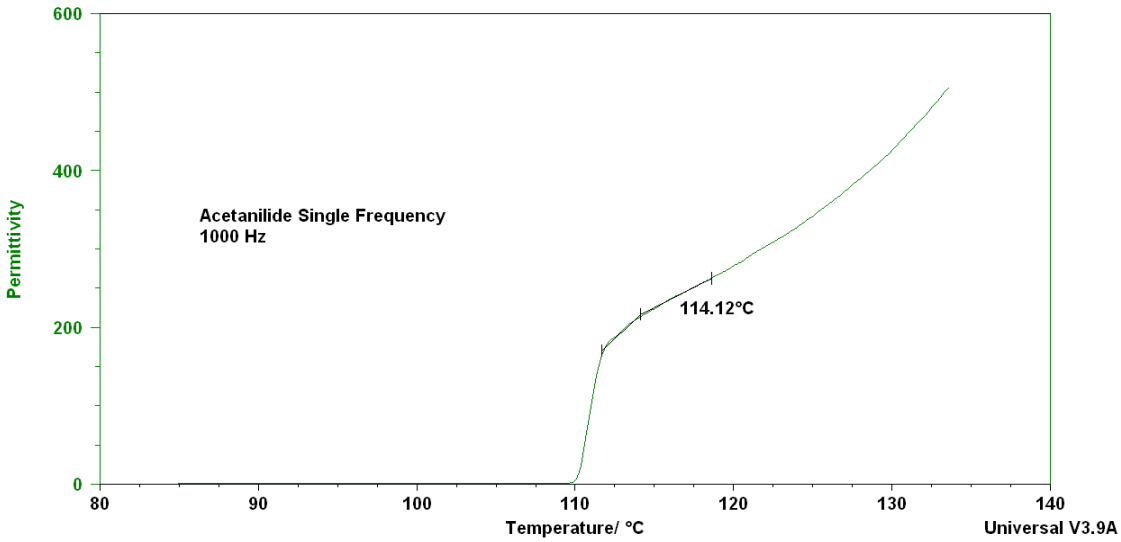

Figure 3.4. DEA curve of Acetanilide showing permittivity transition temperature (114.12 °C) for single frequency (1,000 Hz) run

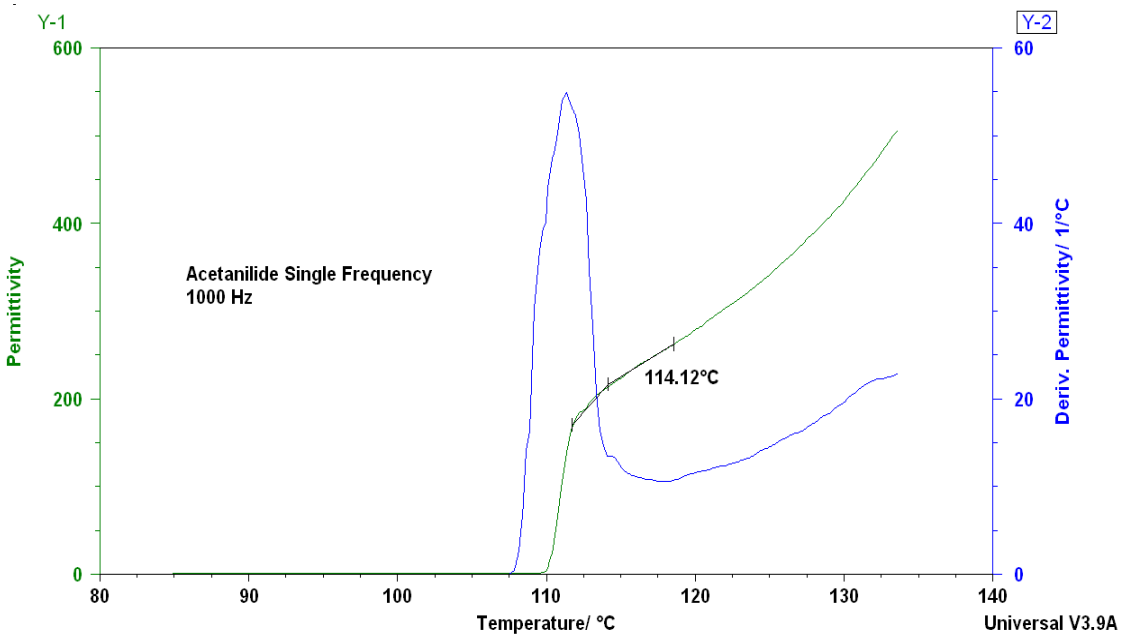

Figure 3.5. DEA curve of Acetanilide showing Permittivity and Derivative of Permittivity transition temperature (114.12 °C) for a single frequency (1000Hz) run

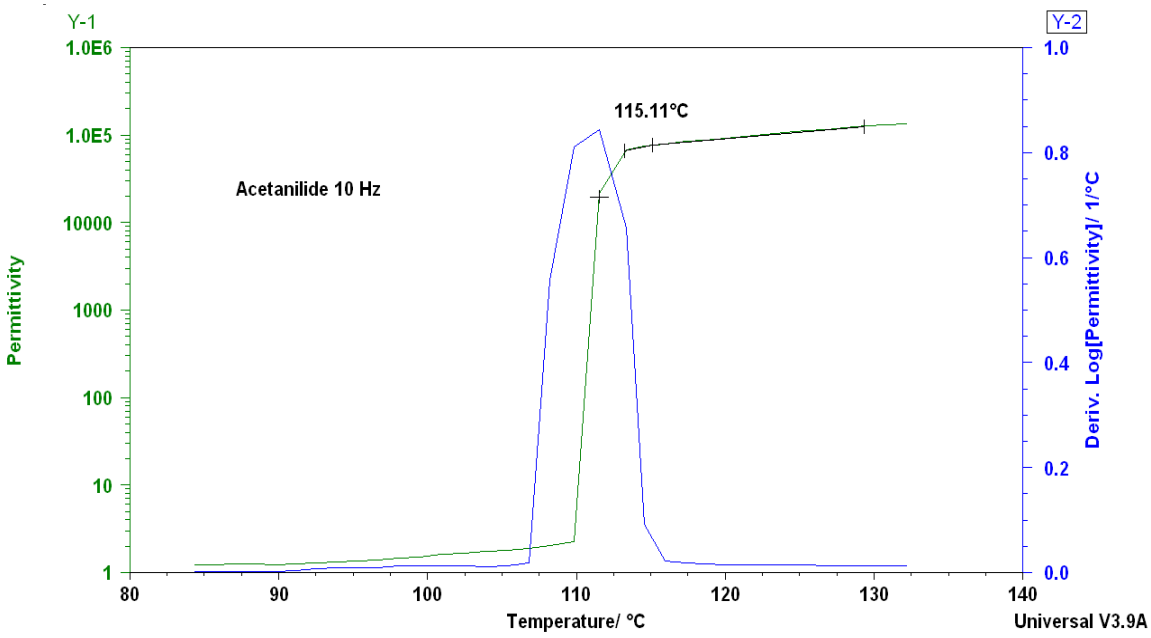

Figure 3.6. DEA curve of Acetanilide showing Log permittivity and Derivative of Log permittivity transition temperature (115.11 °C) at 10 Hz

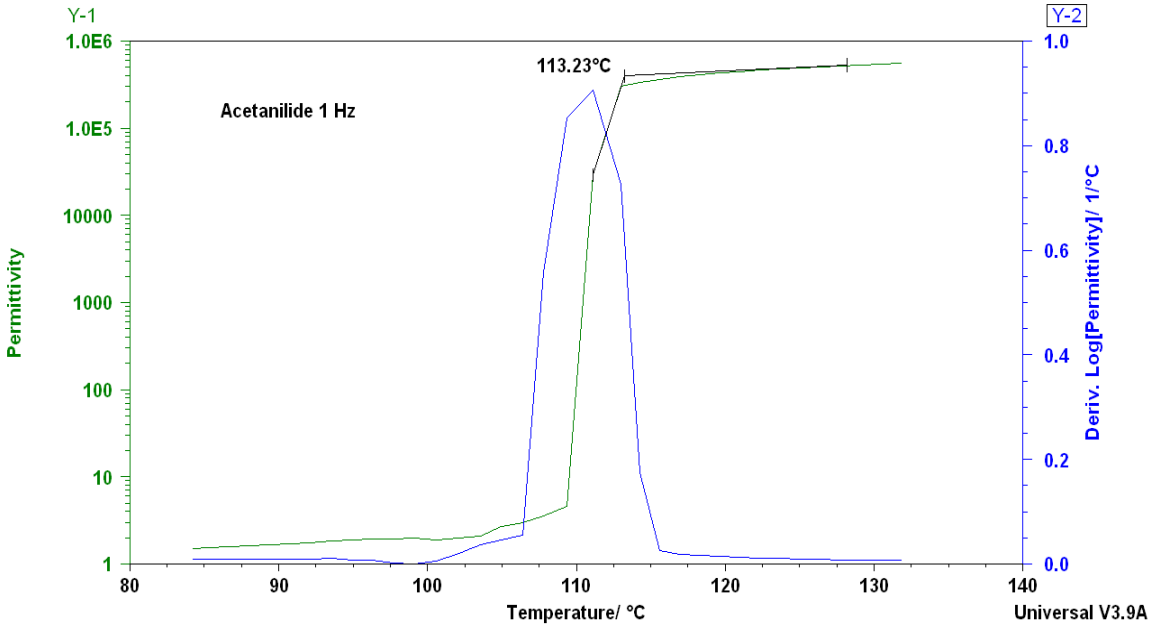

Figure 3.7. DEA curve of Acetanilide showing Log permittivity and Derivative of Log permittivity transition temperature (113.23 °C) at 1 Hz frequency

A summary of frequency used i.e. (single or set of 4 frequencies); permittivity and Log permittivity transition temperatures obtained from the DEA thermal curves of the calibration materials are listed in Table 4: Acetanilide; Table 5: Acetophenetidin; Table 6: Vanillin; and Table 7: Sulfapyridine.

Table 4

DEA Permittivity and Log Permittivity transition temperatures of single (1000 Hz) and set of frequencies (1, 10, 100, 1000 Hz) of Acetanilide Tmp =113-116 °C

Frequency/ Hz	Permittivity Transition Temperatures/ °C	Log Permittivity Transition Temperatures/ °C
1000 Hz	114.2	113.0
1Hz	115.6	113.3
10 Hz	115.1	113.5
100 Hz	113.9	114.0
1000 Hz	114.1	114.0
Average	114.6	113.7
Std Deviation	0.80	0.34
% Relative Error	0.70	0.26

Table 5

DEA Permittivity and Log Permittivity transition temperature of single (1000 Hz) and set of frequencies (1, 10, 100, 1000 Hz) of Acetophenetidin Tmp = 132-138 °C.

Frequency/ Hz	Permittivity Transition Temperatures/ °C	Log Permittivity Transition Temperatures/ °C
1000 Hz	131.0	131.0
1 Hz	132.5	132.3
10 Hz	132.5	132.7
100 Hz	132.6	132.5
1000 Hz	132.7	132.7
Average	132.6	132.6
Std Deviation	0.09	0.23
% Relative Error	0.66	0.17

Table 6

DEA Permittivity and Log Permittivity transition temperature of single (1000 Hz) and set of frequencies (1, 10, 100, 1000 Hz) of Vanillin Tmp = 81- 83 °C

Frequency/ Hz	Permittivity Transition Temperatures/ °C	Log Permittivity Transition Temperatures/ °C
1000 Hz	81.0	80.9
1 Hz	82.3	80.8
10 Hz	82.0	80.9
100 Hz	81.3	80.8
1000 Hz	81.0	80.9
Average	81.5	80.7
Std Deviation	0.90	0.18
% Relative Error	1.09	0.22

Table 7

DEA Permittivity and Log Permittivity transition temperature of single (1000 Hz) and set of frequencies (1, 10, 100, 1000 Hz) of Sulfapyridine Tmp = 191-193° C.

Frequency/ Hz	Permittivity Transition Temperatures/ °C	Log Permittivity Transition Temperatures/ °C
1000 Hz	192.0	191.0
1 Hz	192.7	191.5
10 Hz	192.8	191.0
100 Hz	191.3	190.8
1000 Hz	191.0	191.4
Average	191.9	191.1
Std Deviation	0.9	0.35
% Relative Error	0.47	0.18

3.4.3 For TMA. At the transition temperature of the test specimen, there is a change in dimensional variability and the instrument records a measured change in the coefficient of thermal expansion.

- From the TMA thermal curve recorded, extrapolated onset temperature is measured. This is calculated by extending the pre-transition portion of the curve which to the point of intersection with a line drawn tangent to the steepest portion of the curve which describes the probe displacement [6].

The thermal curves of Acetanilide (see Figure 3.8.) and Acetophenetidin (see Figure 3.9.), and Vanillin (see Figure 3.10.) recorded by the instrument are described showing the extrapolated onset melting temperature.

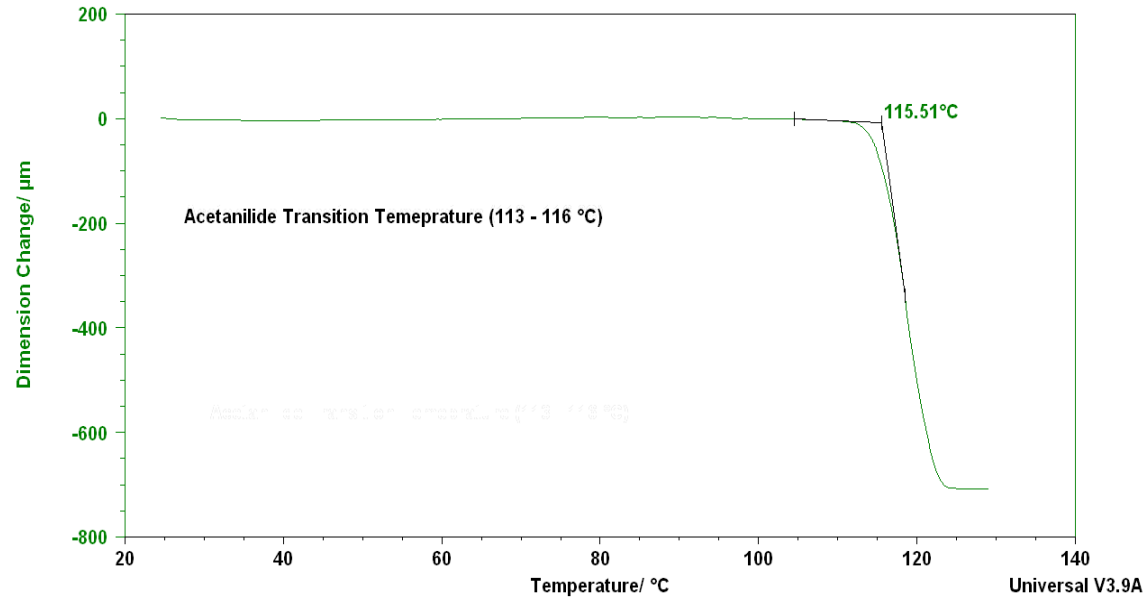

Figure 3.8. TMA of Acetanilide curve showing the extrapolated onset melt temperature (115.51° C).

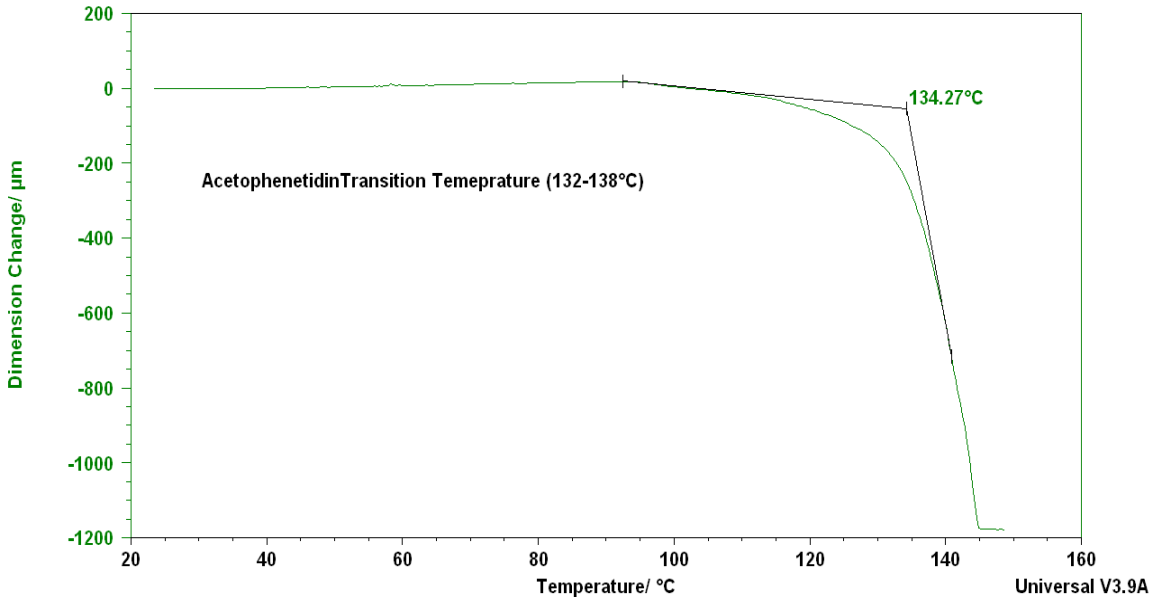

Figure 3.9. TMA of Acetophenetidin curve showing extrapolated onset melt temperature (134.27° C)

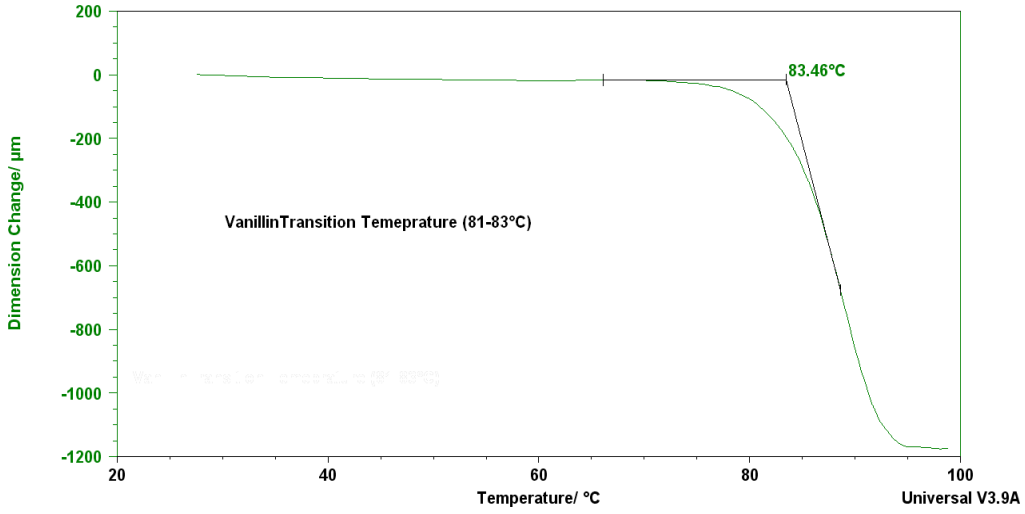

Figure 3.10. TMA of Vanillin curve showing extrapolated onset melt temperature (83.46° C)

A summary of TMA observed extrapolated onset temperatures of calibration materials and literature transition temperatures are cited in Table 8.

Table 8

Summary of TMA extrapolated onset temperatures of calibration materials and literature transition temperatures

Calibration Materials*	TMA Extrapolated Onset Temperatures/ °C	Literature Transition Temperatures/ °C
Acetophenetidin	134.27	132 - 138
Acetanilide	115.51	113 -116
Vanillin	83.46	81-83
Sulfapyridine	192.78	191-193

A summary of DSC, DEA and TMA melting temperatures for the calibrants (API's) studied vs. the standard literature melting temperatures values are given in Table 9.

Table 9

Summary of DSC, DEA and TMA Results

Calibration Materials*	Literature Transition Temperatures / °C	DSC Melting Peak Temperatures/ Tmp °C		DEA Transition Temperatures/ °C		TMA Extrapolated Onset Temp/ °C
		1st Peak	2nd Peak	Permit -tivity	Log Permittivity	
Acetophenetidin	132- 138	136.25	136.61	133.6	132.6	134.27
Acetanilide	113 – 116	116.31	116.58	114.6	113.7	115.51
Sulfapyridine	191 – 193	192	T_g= 62	191.9	191.1	192.78
Vanillin	81 – 83	83.08	82.45	81.5	80.7	84.46

**Available from Sigma Aldrich®, **CAS=Chemistry Abstract Service registry number.*

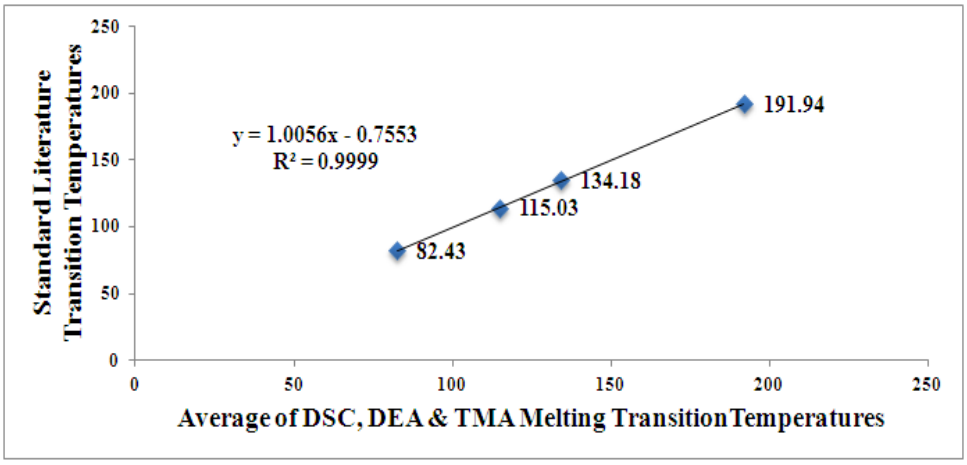

Figure 3.11. A correlation graph of Standard Literature Transition Temperatures vs. Average of DSC, DEA & TMA Melting Transition Temperatures of calibration Materials

3.5 Conclusions

Statistical analysis of the results from the three methods (DSC, DEA and TMA) indicates a high correlation with known literature values. Acetanilide, Acetophenetidin and Sulfapyridine were quality API standards for calibration. Vanillin is a quality excipient calibrant. The three drugs plus the excipient, studied for this standard protocol present outstanding list of viable temperature standards. Their observed melting transition temperature best correlates with the known literature transition temperature values. All, but Sulfapyridine, yielded melting -crystallization - melting properties that enhance the overall characterization of those drugs. The T_g, on the 2^{nd} heat cycle, of Sulfapyridine at 62^oC supplied additional important thermal characterization data. Permittivity is the most appropriate property to calibrate the temperature of DEA as it deals only with dipole variations. The ionic conductivity, though an interesting material property, is a function of multiple properties, that are dipolar and ionic. The R^2 correlation value for known standard literature temperatures vs. DEA permittivity melting temperature for of single (1000 Hz) and set of frequencies (1, 10, 100, 1000 Hz) was 0.99. The R^2 correlation value for known standard literature temperatures vs. TMA extrapolated onset temperatures was 0.999. The R^2 correlation value for known standard literature temperatures value vs. DSC melting peak temperatures was 0.999. The average melting temperature (Tm) for DSC, DEA and TMA correlated with the melting temperatures (Tm) of the known literature values with an R^2 of 0.999. (See Figure 3.11.) It is our quest to infuse these new ASTM type standard test protocols into the pharmaceutical industry for drug pre-formulation and dosage design of pharmaceuticals. These new pharmaceutical based test protocols, permit inter-laboratory comparison and intra-

laboratory correlation of instrumental temperature scale data within the pharmaceutical community, and will be implemented in our chemical pharmaceutical research.

The following ASTM methods were also reviewed in the course of preparing this text:

- E794 Standard Test Method for Melting and Crystallization Temperatures by Thermal Analysis [25].
- E473 Standard Terminology Relating to Thermal Analysis [26].
- E691 Standard Practice for Conducting an Inter-laboratory Study to Determine the Precision of a Test Method [27].
- E1325-02 Standard Terminology Relating to Design of Experiments [28].

3.6 Acknowledgements

We would like to acknowledge the ASTM International for their support and funding this ASTM International Graduate Student Project grant 2010.

3.7 References

1. Ohannesisan L, Streeter AJ. "Handbook of Pharmaceutical Analysis", Marcel Dekker Inc., NY 2002, pages 1-581.
2. Fahlman, Bradley D. "What is Material Chemistry" Materials Chemistry, Springer Netherlands.2nd Edition, 2011, 1-12 pages, Doi: 10.1007/978-94-007-0693-4_1.
3. Hancock BC, Parks M. What is the true solubility advantage for amorphous pharmaceuticals? Pharm Res. 2000; 17(4): 397–404.

4. ASTM Standard E967-08, “Standard Test Method for Temperature Calibration of DSC and DTA”, ASTM International, West Conshohocken, PA, 2008, DOI: 10.1520/E0967-08, www.astm.org.

5. ASTM Standard E2038-08, “Standard Test Method for Temperature Calibration of Dielectric Analyzers”, ASTM International, West Conshohocken, PA, 2008, DOI: 10.1520/E2038-99R08, www.astm.org.

6. ASTM Standard E1363-08, “Standard Test Method for Temperature Calibration of TMA”, ASTM International, West Conshohocken, PA, 2008, DOI: 10.1520/E1363-08, www.astm.org.

7. Wunderlich D, “Learning about Calorimetry”, J. Therm. Anal Calorim. 1997; 49: 7-16.

8. Riga A and Collins R, “Differential Scanning Calorimetry and Differential Thermal Analysis”, “Encyclopedia of Analytical Chemistry”, R. Meyers, Ed., 2006, DOI: 10.1002/9780470027318.a6602.

9. Fischer H, “Calibration of Micro Thermal Analysis of Glass Transition Temperatures and melting points: Repeatability and reproducibility” J. Therm Anal Calorim, Vol. 92 (2008) 2, 625– 30.

10. Verdonck E, Schaap K and Thomas LC, “A Discussion of the Principles and Applications of Modulated Temperature DSC (MTDSC), Int. J. Pharm. 1999; 192: 3-20.

11. Riga AT, Roy S, Alexander KS. A statistical approach for the evaluation of parameter affecting preformulation studies of pharmaceuticals by differential scanning calorimetry. American Pharmaceutical Review. 2003; p. 89–95.

12. Riga A, Judovits L. Materials characterization by dynamic and modulated thermal analytical techniques. San Francisco: ASTM Special Technical Publication; 2001. p. 1402.

13. ASTM Standard E2039-2008, "Standard Test Method for Determining and Reporting Dynamic Dielectric Properties", ASTM International, West Conshohocken, PA, DOI: 10.1520/E2039-2008, www.astm.org.

14. Duncan Q. M. Craig, "Dielectric Analysis of Pharmaceutical Systems, Taylor and Francis Pub. Bristol Pa., 1995; 123-144.

15. Riga A, Alexander KS. Electrical conductivity analysis/dielectric analysis differentiates physical chemical properties of drugs and excipients. Am Pharm Rev. 2005;8(6): 45–51.

16. Neag CM. Thermomechanical analysis in materials science, material characterization by thermomechanical analysis, ASTM STP 1136. In: Riga AT Neag CM, editors. Philadelphia: American Society for Testing and Materials, 1991. p. 3–21.

17. Grady LT, Reamer JT. Testing of heat-sealing by thermal analysis. J Pharm Sci. 1976; 65(4): 628–30.

18. Masilungan FC, Lordi NG. Evaluation of film coating compositions by thermomechanical analysis. I. Penetration mode. Int J Pharm. 1984; 20: 295–305.

19. Badipatla V, Dean Pohlman, Maheswaram MP, et.al. "Evaluating Drug Delivery of Solid Dose Tablets by Isothermal Thermal Mechanical Analysis". J Therm Anal Calorim. 2011. Doi: 10.1007/s10973-011-1477-x.

20. ASTM Standard E928-08, “Standard Test Method for Purity by Differential Scanning Calorimetry”, ASTM International, West Conshohocken, PA, 2008, DOI: 10.1520/E0928-08, www.astm.org.

21. Chemical Abstact Service CAS no. 62-44-2, Acetophenetidin

22. Chemical Abstact Service CAS no. 103-84-4, Acetanilide

23. Chemical Abstact Service CAS no. 122-33-5, Vanillin

24. Chemical Abstact Service CAS no. 144-83-2, Sulfapyridine

25. ASTM Standard E794-06, “Standard Test Method for Melting and Crystallization Temperatures by Thermal Analysis”, ASTM International, West Conshohocken, PA, 2006, DOI: 10.1520/E0794-06, www.astm.org.

26. ASTM Standard E473-11a, “Standard Terminology Relating to Thermal Analysis and Rheology”, ASTM International, West Conshohocken, PA, 2011, DOI: 10.1520/E0473-11A, www.astm.org.

27. ASTM Standard E691-11, “Standard Practice for Conducting an Interlaboratory Study to determine the precision of a test method”, ASTM International, West Conshohocken, PA, 2011, DOI: 10.1520/E0691-11, www.astm.org.

28. ASTM Standard E1325, 02(2008) “Standard Terminology Relating to Design of Experiments”, ASTM International, West Conshohocken, PA, 2008, DOI: 10.1520/E1325-02R08, www.astm.org.

CHAPTER IV

CHARACTERIZATION OF CRYSTALLINE AND AMORPHOUS CONTENT IN PHARMACEUTICAL SOLIDS BY DIELECTRIC THERMAL ANALYSIS

4.1 Introduction

Riga et al. studied the extensive applications of dielectric analysis (DEA) including states of matter as amorphous/crystalline. They characterized drugs, excipients, transdermal patches, carbohydrates, proteins, amino acids, motor oil dispersants and surfactants as well as electro rheological fluids using A.C. electrical properties over a wide range of frequencies [1]. The importance of the amorphous state when studying bioavailability, dissolution, and the development of poorly water-soluble APIs has grown significantly over the recent years [2, 3]. There are two forms of solids: glassy and crystalline forms [4]. Glassy forms or amorphous solid forms generally exist in a variety of industrial fields or products, such as polymers and plastics, textiles, foods and pharmaceuticals, and in the manufacture of semiconductors, ceramics, metals and optical materials [2, 3]. With reference to a crystalline solid, an amorphous solid can be defined as a substance with short-range molecular order; in contrast a crystalline solid has long-range order [2]. For this reason, some amorphous forms are considered as liquids although they can solidify by the removal of thermal energy or a solvent in a way that

avoids crystallization [5]. In pharmaceutical research, the amorphous form of a pharmaceutical solid has been the most important aspect of drug development. The significance of amorphous solids is presently ever-increasing due to their value to the pre-clinical formulation scientists and in general to the pharmaceutical industry due to various advantages [3, 6, 7]: (i) a continuous increase in the development of a number of insoluble APIs; these glassy drug compounds are unique based on their methods of production and screening [8], (ii) The growing attention in regulatory evaluation and distinct economic aspects of pharmaceutical solids development [9], and (iii) The different polymorphs of APIs including the amorphous forms have different interconvertible physical and chemical properties [10] which exhibit different solubility and compressibility characteristics. Processing of an amorphous drug substance is relatively simple, and easy when compared to crystalline drug production [2, 3].

Amorphous forms can be produced by a variety of pharmaceutical techniques, such as granulation, compaction, freeze & spray drying, melt-quench cooling, and solvent evaporation method. These amorphous forms can be used for better solubility, dissolution and bioavailability [6, 11, 12]. The amorphous phase has higher energy with higher chemical reactivity and generally is less stable both physically and chemically than the corresponding crystalline phase. The stability of the amorphous form is the main issue when stored at temperatures close to the glass transition temperature, (T_g). The glass transition temperature is a key characteristic property of amorphous materials. Quantification of the amorphous fraction of an API can be better understood by determining the heat capacity change associated with the T_g [13]. In pharmaceuticals, amorphous solids have several useful properties and are used as both API and excipients

[3]. Some of the useful properties are higher water solubility, higher dissolution rate [14] (i.e. no lattice energy, which is a thermodynamic barrier to dissolution) [15], and better compression characteristics when compared to the crystalline forms [2, 3].

Although the amorphous form has some advantages over its crystalline counterpart, like higher free energy, lattice disorder, higher water solubility, and molecular mobility [6], the amorphous systems have seen limited commercialization due to its thermodynamic instability and higher chemical reactivity [11,12, 16]. The amorphous phase can also occur throughout the particle or solid, in the bulk or at its surface, which can be relatively distinguished by dielectric studies [17]. As the disordered portion is low, it's difficult to detect [11, 12]. But these high-energy reactive portions may cause some significant changes in drug development like: improve product performance, high dissolution rate, decreased chemical stability, solid-solid transitions, and recrystallization during storage [11, 18]. Because of the amorphous phase thermodynamic instability, there can be an irreversible conversion of the metastable form to its stable crystal form during manufacturing or in normal storage. Loss of drug function can occur when the amorphous material transitions to another meta-stable form resulting in, for example, a varying dissolution rate of the original crystalline form [16].

Therefore, one must find a reliable method to monitor and characterize the degree of crystallinity and the amount of disorder in the APIs during their pre-clinical drug development to ensure commercializable formulations [11]. To maximize the efficiency of the amorphous material and prevent transformation of the drug during storage, one needs to understand and characterize the kinetics of the crystallization process, and determine quantitatively the various parameters associated with nucleation

and crystal growth [16]. This need is based on a vigorous test method to monitor the drug throughout its shelf life to assure product safety and quality [18]. Pharmaceutical scientists are making an effort to develop alternative methods that are precise, reliable, and fast, which employ small samples for determining the crystallinity or low levels of amorphicity in the sample [12]. The degree of crystallinity methodology is extensively used to measure the relative crystalline/amorphous content in pharmaceutical materials [19]. Several analytical techniques currently employed in the pharmaceutical industry for quantifying, and/or characterization of crystalline and amorphous forms of pharmaceutical materials include: X-ray diffraction analysis (XRD), dielectric Analysis [20], solid state-NMR [21], FT–Raman [22], FT–IR [23], modulated differential scanning calorimetry [24], thermally stimulated current spectroscopy [11], isothermal microcalorimetry, and solution calorimetry.

Morphological and thermodynamic transitions in drugs as well as their amorphous and crystalline content in the solid state have been initiated by thermal analytical techniques, which include DEA and thermal mechanical analysis [24, 25]. These techniques were used successfully to establish a structure vs. property relationship with the API of drugs [24, 25]. The main focus of this study is to develop a novel analytical protocol utilizing dielectric analysis to define and quantify the crystalline and amorphous content in pharmaceutical solids. These innovative techniques will give pharmaceutical scientists new insights in how to understand the nature and behavior of drugs in the solid state. Pharmaceutical solids studied by these methods have led to a better understanding of the chemistry and molecular mobility that relates to the structure of the drug. This information is of the utmost importance during pre-formulation studies of drug

development. DEA measures the crystalline solid and amorphous liquid API electrical conductivity at temperatures below and above the melting temperature [13-15]. DEA scans the electrical signals over a wide range of frequencies (e.g. 0.10 to 100,000 Hz). The DEA ionic-dielectric conductivity is repeatable and differentiates the solid crystalline drug with a low ionic-dielectric conductivity level ($<10^{-1}$ pS cm^{-1}) and a high ionic dielectric conductivity level associated with the amorphous liquid ($>10^{5}$ pS cm^{-1}). Further, DEA measures changes in phase (solid to liquid) transitions, significant variations in conductivity related to the ionic dielectric behavior of melted drugs and loss of residual solvents as it is subjected to a periodic electric field.

Our new DEA protocols can detect the crystalline and amorphous phase repeatedly and rapidly based on the experimental frequencies, time and temperatures. This A.C. frequency based technique has the ability to differentiate surface vs. bulk amorphicity [25]. Typically surface analysis is best profiled at 0.10-1.0 Hz and bulk analysis is between 1,000 - 10,000 Hz. This methodology is quick and can summarize the relative low levels of non-crystalline and crystalline material, thereby increasing the sensitivity of this technique.

4.1.1 Dielectric Analysis (DEA). Dielectric analysis (DEA) is a material characterization technique that provides scientists with quantitative thermal, rheological and dielectric information on a wide range of materials in their various forms, which include solid, liquids, pastes, films, polymers, and organic additives in lubricating oils [16]. It can be used to determine the flow, thermal transitions, degree and rate of cure in polymers, characterize food products, pharmaceutical materials, and dielectric properties of thermoplastics, composites, as well as adhesives and coatings [1].

As DEA is a thermal analysis tool, it is closely related to DMA (frequency dependent dynamic mechanical analysis), which measures mechanical properties of a material. While DSC measures heat flow through which the heat of fusion and transition temperatures can be determined. DEA compliments DSC by allowing a measurement of molecular motion based on its electrical properties.

The theory of a dielectric or theory of dielectric analysis may be illustrated by the time – dependent electrical response of a sample placed on a single surface gold ceramic inter-digitated electrode when an alternating (sinusoidal voltage) electric field is applied. This process produces polarization within the sample, causing oscillation at the same frequency as the electric field but with a phase angle (or phase shift) δ. This phase angle shift can be measured by comparing the applied voltage to the measured current [1 and 24]. The current is then separated into capacitive (e') and conductive (e'') components.

The two fundamental characteristics of a material measured through dielectrics: as a function of time, temperature, and sampling frequency are:

- Capacitance = High frequency permittivity (e') or dielectric constant.
- Electrical conductivity (pS cm-1) = Loss factor (e") x Applied freq (Hz) x2π

The capacitive nature of the material allows or has an ability to store an electrical charge and this nature dominates the electrical response at low temperatures. The conductive nature of the material has an ability to transfer an electric charge and this factor becomes very important when the solid material is heated above its melting temperature to the liquid state. These electrical properties are significant since they have been related to molecular activity, allowing for probing the chemistry, and molecular

mobility of polymers and pharmaceutical materials. DEA reports three main electrical signals over a wide range of frequencies (e.g. 0.10 to 100,000 Hz):

- *Permittivity* (e') is a measure of the induced dipoles and alignment of molecular groups (dipoles) in the electric field.
- *Loss factor* (e'') is a measure of the energy required to move the molecular groups or ions and is proportional to ion conductivity. Ionic conductivity is associated with the viscosity of the sample because fluidity is identified by the ease with which ionic components can migrate through the sample under the applied electric field.
- *Tan delta* is the ratio of the loss factor divided by the permittivity. Tan delta = e''/e'. Tan delta values are related to molecular mobility, response time to an electric field, and are related to polarization or relaxation of excited molecules or a measure of charge transfer properties [1, 24].

We developed a novel combined DEA-DSC protocol to evaluate amorphous/crystalline content in pharmaceutical solids. The DSC analysis will be used in two different protocols (a) Heat cycle only to measure the temperature range for heating to aid DEA evaluation. (b) Heat and Cool cycle to evaluate % crystalline and % amorphous based on the fusion and crystallization heats.

The focus of these new methods is to determine the relative amounts of amorphous and crystalline content in APIs. Pharmaceutical scientists working on pre-formulation of pharmaceutical drugs as well as those developing quality control of manufactured drugs need new information on the content of amorphous/crystalline matter. This new knowledge is to improve quality and stability of pharmaceuticals for the

consumer. There is a clear rationale for developing these new methods to better understand the effects of the total chemical structure on drug treatment including amorphicity. It is logical that electrical conductivity methods are implemented now since we have discovered significant variations in pharmaceuticals using DEA.

4.2 Methodology

Two novel DEA protocols were developed to determining the amorphous and crystalline content in pharmaceutical drugs. The first method is ***"The Empirical Method".*** It is semi-quantitative method that is based on the observed significant electrical conductivity difference between the amorphous liquid (10^{7} pS cm^{-1}) and crystalline solid (10^{-2} pS cm^{-1}). The second method is the ***"Activation Energy Method"*** and is more quantitative in nature. In this method the Activation Energy, Ea (J mol^{-1}), is calculated from the DEA ionic conductivity. It is based on the fact that the relative Ea for the electrical reactivity (charging or charge transport) in the solid state of the amorphous phase is higher and conversely the Ea is lower (typically 30 -110 $J.mol^{-1}$) and the electrical reactivity of the solid state for crystalline phase is low and conversely the Ea is higher (typically 1,200-2,000 J mol^{-1}).

4.2.1 Empirical method protocol. The empirical method to determine crystalline and amorphous content in pharmaceutical solids is as follows: First, a pure drug (100% crystalline) similar to the drug with unknown content is examined by DEA as a standard. For the pure drug prepared by the pharmaceutical company the % content before the melting temperature is 99.99-100% crystalline and with complete melt it is 100% amorphous in the liquid phase. Then, DEA re-run of the sample is performed to analyze the drug with the unknown amorphous/crystalline content. A combined DEA model plot

for the % content of an unknown drug and the pure drug is shown in the graphical representation (Fig.1**)** as log ionic conductivity vs. temperature. Next, a temperature, Ts, is selected ≤ 30 to 50^{o} C below the melting temperature (T_m) of the drug from the overlayed DSC curve. Then, the linear distance (Δ3) in millimeters of log ionic conductivity on the y- axis is measured from 100% solid crystalline line (point X) to the 100% amorphous line (point Z) at the selected temperature Ts. The 100% amorphous or liquid region is a hypothetical region and the 100% amorphous line is obtained by extrapolating the liquid region log ionic conductivity of the DEA plot. Next, the linear distance (Δ2) in millimeters of log ionic conductivity on the y- axis is measured from the semicrystalline line (point Y) to the 100% amorphous line (point Z)) and (Δ1) in millimeters from 100% solid crystalline line (point X) to semicrystalline line (point Y)) at the temperature Ts are measured. In the semicrystalline region the ratio of amorphous to crystalline content is not known.

The linear log conductivity distance in millimeters is a measure from the crystalline phase to the amorphous phase, which is equated to 100%. The Amorphous and crystalline contents can be calculated from the following equations and Figure 4.11.

% Amorphous = Δ1/Δ3 x 100

% Crystalline = Δ2 /Δ3 x 100

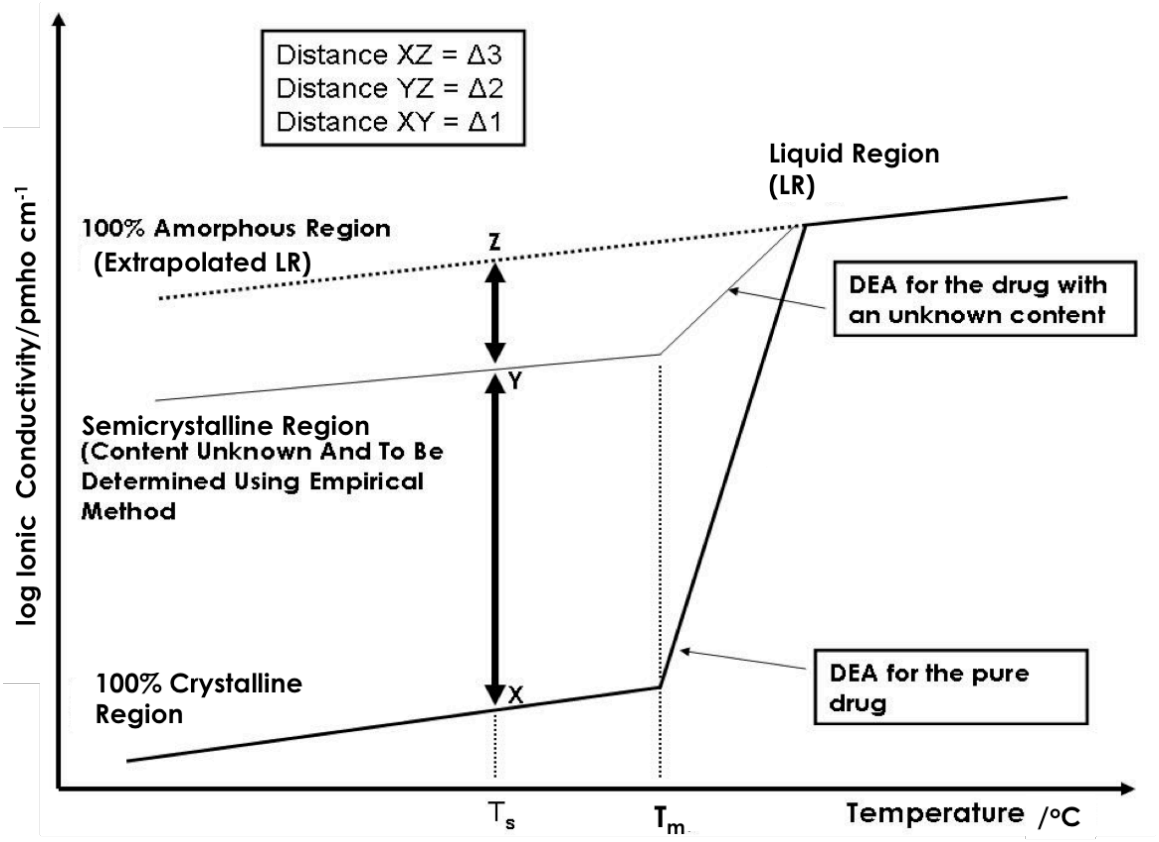

Figure 4.1. Graphical representation of DEA Empirical method

4.2.2 Activation energy method. A second method was developed based on a measurement of a DEA Activation Energy Ea (J mol^{-1}) to determine the amorphous and crystalline content in drugs by dielectric analysis. Sharma and Yashonath [26] investigated ionic transport in a variety of inorganic amorphous glasses (solids). They observed a strong correlation between ionic conductivity and activation energy. Further, they found that higher conductivity is associated with lower activation energies and lower conductivity is associated with higher activation energies. Their results suggest that there is a strong relation between microscopic structure of the amorphous solid, ionic conductivity and activation energy [26].

The Ea (J mol^{-1}) calculation is more quantitative and is based on the relative activation energy for the electrical reactivity (charging or charge transport) in the solid state. The amorphous phase reactivity is higher (ca. 107 pS cm^{-1}) and conversely the Ea is lower (frequency at 1 or 5 Hz typically: 60-200 J mol^{-1}) measured as the slope of the log ionic conductivity vs. reciprocal temperature (K^{-1}) of an Arrhenius plot and as a function of frequency (Hz). The reactivity and conductivity (typically 10^{-2} pS cm^{-1}) of the solid-state crystalline phase is lower and conversely the Ea is higher (typically measured by DEA at a frequency of 1 or 5 Hz: 1,200-2,000 J mol^{-1}), also measured by DEA conductivity vs. reciprocal temperature (K^{-1}) [27 - 29].

4.2.2.1 Activation Energy Ea (J mol-1) Protocol.

1. Record a DEA curve of a pharmaceutical solid sample at a heating rate of 10 $^{o}Cmin^{-1}$ in a nitrogen flow of 60 mL min^{-1}; a sample size of 20 mg. Heat to 20-30^{o} C above the peak melting temperature recorded in the DSC curve.
2. Plot the Ionic conductivity, pmho/cm vs. Temperature at fixed frequencies of 0.10 to 1.0 Hz.
3. Measure the Ionic conductivity responses at < 30^{o} C below the DSC melting point temperature.
4. From the measured responses plot an Arrhenius plot of DEA log ionic conductivity vs. (K^{-1}) x 1000 and perform a linear curve fit to determine the equation of the line. The slope of the linear curve fit is Ea $R^{-1}$and it must be multiplied by 19.14to convert the slope value into Ea (J mol^{-1}). Note: Ea is the activation energy and R is the gas constant of 8.314 J K^{-}

$^{1}mol^{-1}$ and one must include the conversion of natural log (ln) to log base 10, which is 2.303.

Ea (J mol^{-1}) = (slope of the line) x 8.314 x 2.303

5. The Ea (J mol^{-1}) is inversely proportional to the concentration of the amorphous phase in the pharmaceutical sample. Relatively, the lower the Ea corresponds to a higher the ionic conductivity. The 1st DEA run resulting in log conductivity vs. Temperature yielding % crystallinity based on the DSC purity by Heat of Fusion (Jg^{-1}). For an API the % crystallinity is probably 100% for the 1st sampling by DEA. For the 2nd and 3rd runs, samplings of the same API it will be less crystalline and more amorphous, based on a lower Ea (J mol^{-1}) value.

4. 3 Experimental

4.3.1 Drugs. The following drugs were evaluated in this study: Lidocaine (T_m, 68^o C), Lidocaine HCl (T_m, 74-79^o C), Sulfapyridine (T_m, 192^o C), Indomethacin (T_m, 155^o C), and Acetophenetidin (T_m, 135^o C). All the drugs were obtained from Sigma-Aldrich® and meet the USP (United State Pharmacopeias) testing specifications. Quetiapine fumarate (Seroquel®) (T_m, 173^o C), and Procainamide HCl (T_m, 169^o C) were purchased from Haorui Pharma-chem Inc. Edison, NJ.

4.3.2 Experimental procedure. A TAI 2920 DSC (TA Instrument) was used to profile the drug solid-solid transitions, melting, glass transition (T_g), and crystallization properties of the drugs. All the samples were ramped at a rate of 10^{o}C/min in purged nitrogen gas flow at a rate of 60 $mLmin^{-1}$ during heating and cooling cycles. The DSC aluminum pan weighed 13-14 mgs. Samples in the range of 8-10 mg were weighed using

the Mettler AT261 Delta Range® microbalance and loaded into an aluminum pan then closed and crimped. Temperature range was typically from room temperature to 30^{o} C above the peak melting temperature (T_m) for the drugs under study. Heat flow (W g^{-1}) values versus temperature and time were generated using the (TA Thermal Advantage) Universal Analysis 2000 software. The DSC instrument was calibrated using Indium as a standard according to ASTM standard test protocol E967.

A TAI 2970 DEA (TA Instrument) was used to determine the electrical conductivity and Tan delta curve for each drug studied. For each solid powdered drug, a sample of approximately 20 mg was placed on a single surface gold ceramic interdigitated sensor. The samples were ramped from room temperature to 30^{o} C above the melting temperature of the drug at heating rate of 10^{o} C min^{-1}. A purge gas of nitrogen gas flowed at the rate of 60 mL min^{-1}. The gold ceramic interdigitated sensor was calibrated by the fixture supplied by TAI. The DEA instrument was further calibrated according to ASTM E2038 Standard Test Method for Temperature Calibration of Dielectric Analyzers. This standard method was employed for all the drugs studied at 5^{o} C and 10^{o} C min^{-1}. Dielectric analysis was used to evaluate the electrical properties of the drugs. The conductivity measurements were recorded at controlled interval frequencies ranging from 0.10 to 10,000 Hz for all temperatures.

A Konica-Minolta DG SLR Camera with a 28-80 mm macro lens was used for Macro- photomicrography to characterize the crystalline and amorphous materials on the single surface interdigitated array gold electrodes, and samples on the DSC pans. An eyepiece reticule was used to calibrate the Macro-photomicrography system.

4.4 Results and discussions

We tested the applicability of the novel empirical method with several model pharmaceutical APIs. When Lidocaine is heat cycled through the melt and then cooled back to room temperature. The 1st DEA run of Lidocaine reveals the crystalline to amorphous phase transition and change in the ionic dielectric conductivity from $\leq 10^{-2}$ (pS cm^{-1}) for the crystalline phase and 10^5 (pS cm^{-1}) for the amorphous phase. Figure 2 shows the DEA surface analysis profile for Lidocaine at 0.5Hz. Low frequency DEA is confirmed as measurements at the electrode surface e.g. 0.5 Hz. The Lidocaine (Sigma Aldrich®) sample is initially 99.99% crystalline with very low ionic conductivity for the 1st run and upon cooling and reheating a huge increase in ionic conductivity was observed. The 2nd and 3rd runs commensurate with an increasing ionic conductivity value of 10^3 pS cm^{-1} (79% amorphous) and 10^5 pS cm^{-1} (91% amorphous) see Figure 4.2. & 4.3. Figure 4.3 summarizes the % crystalline and % amorphous content in Lidocaine at 0.1, 0.5 and 1.0 Hz by the DEA "Empirical" method. Figure 4.4 summarizes the % crystalline and % amorphous content in Quetiapine Fumarate (Seroquel®) at 0.1, 0.5 and 1.0 Hz by the DEA empirical method. Table 1 shows the list of drugs tested and evaluated for crystalline and amorphous content by the proposed method (Table 1).

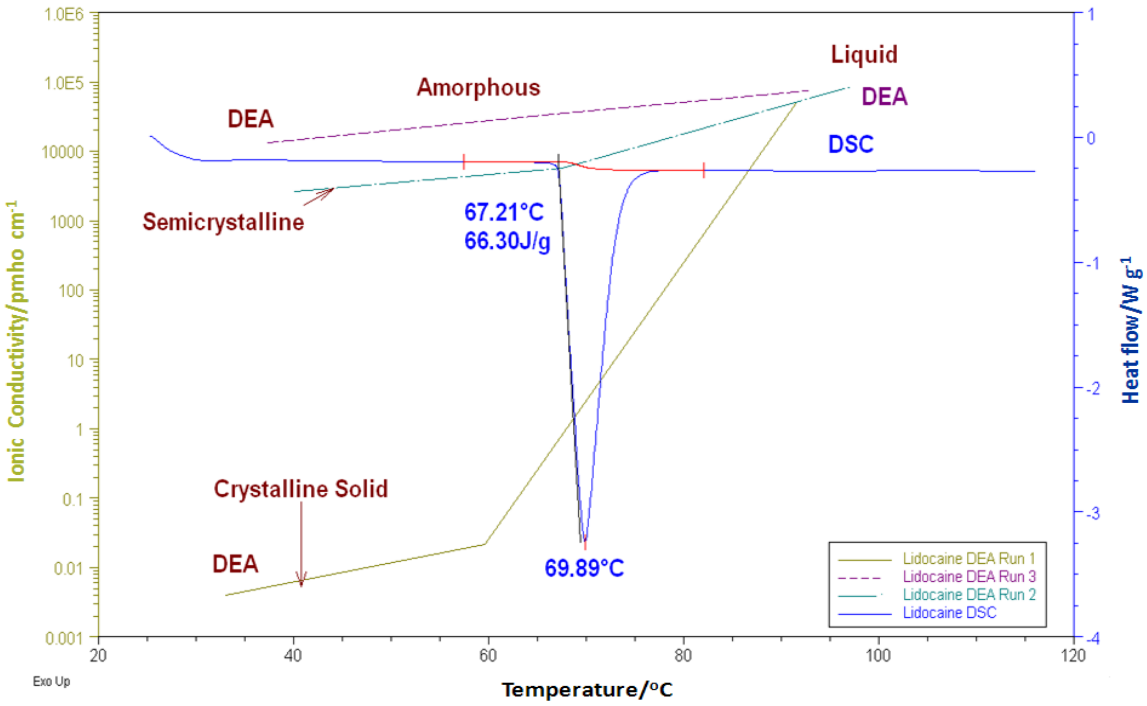

Figure 4.2. DEA Surface Analysis of Lidocaine at 0.5Hz (1st, 2nd & 3rd Runs); DSC Tm 69.89° C

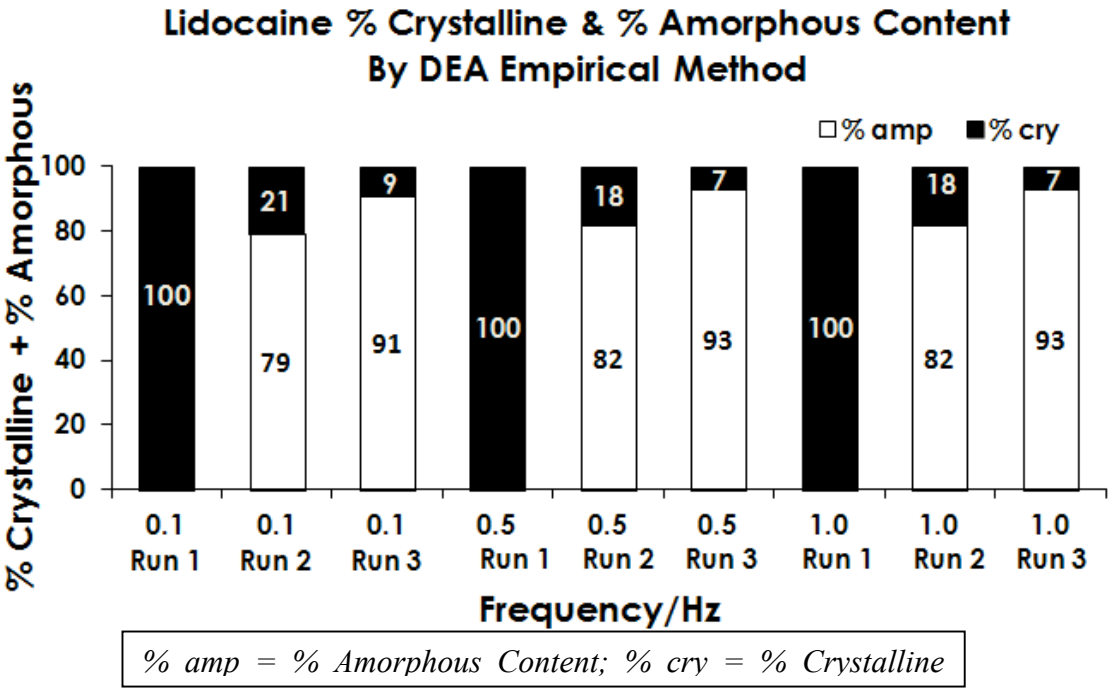

Figure 4. 3. Determination of % Crystalline and % Amorphous content vs. Frequency/Hz for Lidocaine at 0.1, 0.5 & 1.0 Hz (Run1 to Run3) by the DEA Empirical method

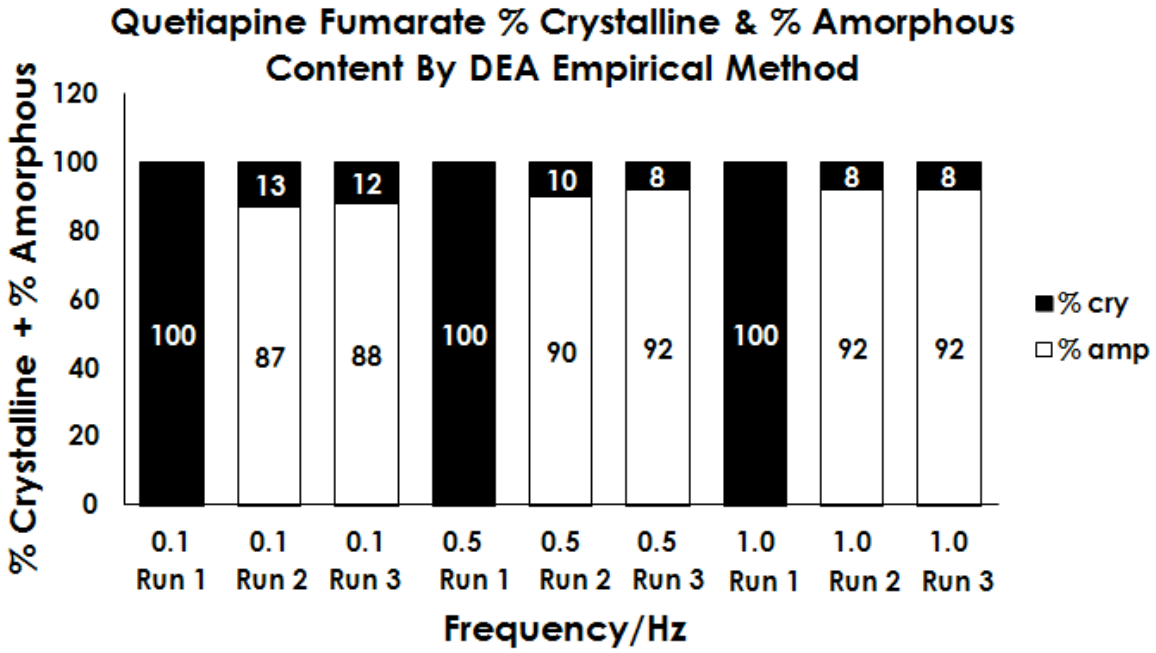

% amp = % Amorphous Content; % cry = % Crystalline Content

Figure 4.4. Determination of % Crystalline and % Amorphous content vs. Frequency/Hz for Quetiapine Fumarate at 0.1, 0.5 & 1.0Hz (Run 1 to Run 3) by the DEA Empirical method

Table 1

Quantification of Crystalline and Amorphous Content in various Pharmaceutical APIs by DEA Empirical method

Drug	Average content of 2nd and 3rd DEA Runs at 0.1,0.5 and 1.0 Hz	
	% Crystalline Content	% Amorphous Content
Sulfapyridine	9	81
Quetiapine Fumarate	10	90
Lidocaine	13	87
Procainamide HCl	19	81
Lidocaine HCl	24	76
Indomethacin	26	74
Acetophenetidin	78	22

Our second method to determine crystalline and amorphous content through the measurement of DEA activation energies was tested with several model pharmaceutical APIs. Results for Lidocaine and Acetophenetidin are discussed as follows. Analysis of the Lidocaine by the proposed DEA empirical method yields a supportive interpretation of the activation energy method, i.e. determination of the % crystalline and amorphous content in a drug. Other APIs successfully tested by the activation energy method are Sulfapyridine, Quetiapine Fumarate (Seroquel®), Procainamide HCl, Lidocaine HCl and Indomethacin.

A plot of the DEA Log Ionic conductivity (pS cm^{-1}) vs. Temperature (^{o}C) for crystalline Lidocaine is summarized in Figure 4.5. For the first run, we observed a slow

rise in ionic conductivity till 60° C, (10^{-2} pS cm^{-1}) followed by a very rapid increase (10^{5} pS cm^{-1}) from 60° C to 90° C. The DSC-DEA curve overlay maps out the melting transition that occurs at 67° C. The second run cycling after the initial heat curve produced a ionic conductivity response that was enhanced due to the formation of the amorphous phase in Lidocaine, was observed from the temperature range of 40-70° C. The slope of the first curve was steep and decreased significantly in the second and third run. The slope change tracked the decreasing activation energy with each heat cycle. The ionic conductivity increases proportionally with the enhanced amorphous content. A curve fit of the log ionic conductivity vs. the reciprocal temperature in Kelvin produces a linear curve with a correlation coefficient of R^2= 0.999 and a varying activation energy, for Lidocaine (Run 3) the Ea is 27 J mol^{-1} (see Figure 4.6.) for details. Table 2 summarized the Lidocaine data in triplicate for the DEA Activation Energy method and the determination of the % crystalline and amorphous content produced by a heat cycle at three frequencies, 0.1, 0.5 and 1.0 Hz (all frequencies are associated with occurrences at the sensor surface). The 2nd and 3rd runs produced an amorphous content of 93% at 0.1 Hz, 94% at 0.5 Hz and 1.0 Hz, (see Table 2).

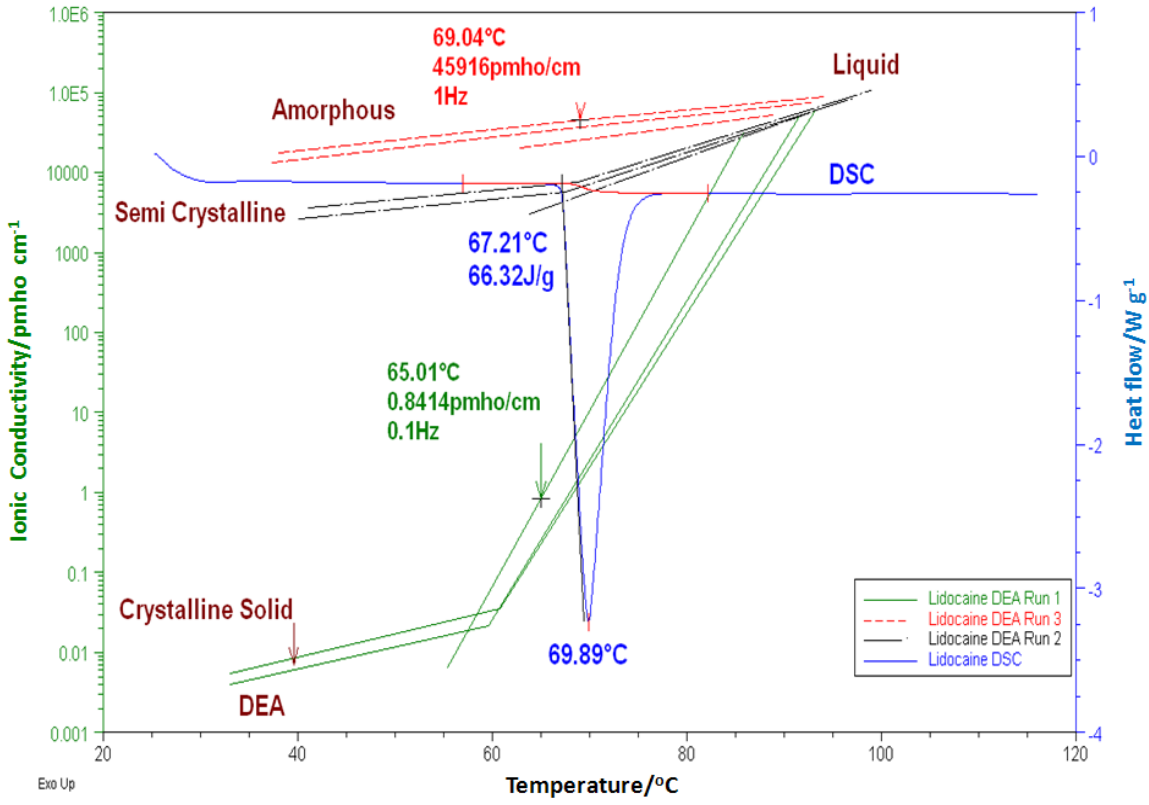

Figure 4.5. Lidocaine DEA and DSC curve overlay and comparing ionic conductivity in crystalline and amorphous samples by activation energy method at 0.1 Hz to 1.0 Hz (Run1, Run 2 & Run 3); Tm= 69.89^{o} C

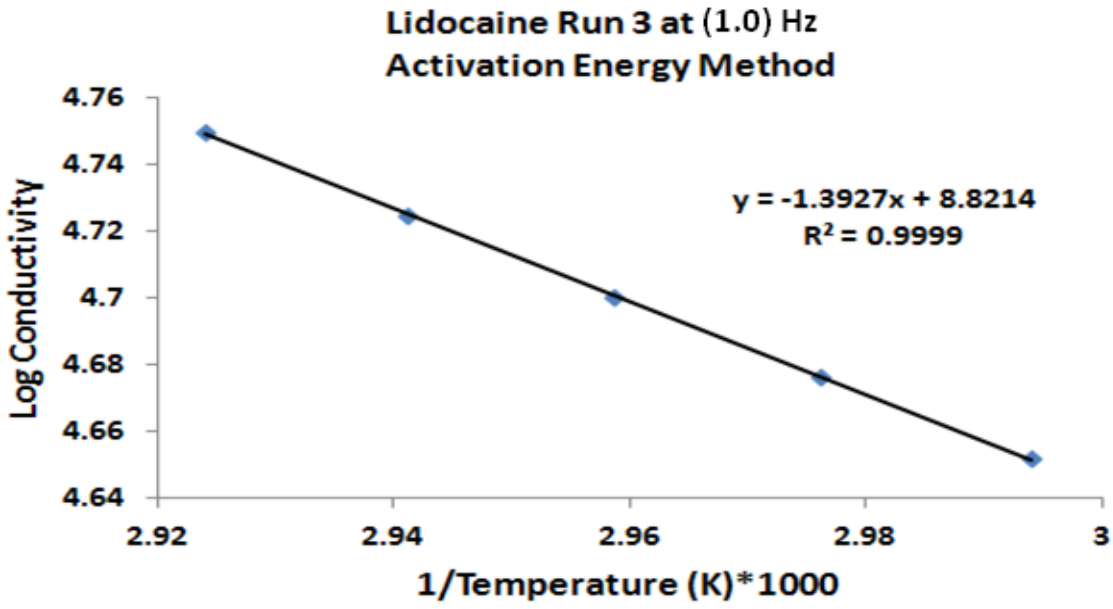

Figure 4.6. Log conductivity (k) vs. 1/T (Kelvin) x 1000 for Lidocaine (Run 3, 0.1Hz); Ea = 27 J mol^{-1}

Table 2

Lidocaine DEA Activation Energy (J mol^{-1}), % Crystalline and % Amorphous Content for 1^{st}, 2^{nd} and 3^{rd} Runs at 0.1, 0.5 and 1.0 Hz frequencies

Frequency/ Hz	Run	Ea/J mol^{-1}	% Crystalline Content	% Amorphous Content
0.1	1	480	100	0
0.1	2	35	7	93
0.1	3	35	7	93
0.5	1	435	100	0
0.5	2	30	7	93
0.5	3	29	6	94
1	1	419	100	0
1	2	29	7	93
1	3	27	6	94

Evaluation of Acetophenetidin by the proposed DEA method for amorphous-crystalline content was an outlier in this protocol, since this drug recrystallizes significantly while the other 6 drugs did not recrystallize to a noticeable extent. The activation energy for Acetophenetidin described in (Figure 4.7. and 4.8.) yielded a high value of 1240 J mol^{-1} at low ionic conductivities. It is our interpretation that this drug continues to recrystallize and therefore the method to quantify the concentration ratio of crystalline to amorphous varies. The 2^{nd} and 3^{rd} run produced varying values for the % amorphous and % crystalline content with frequency. The content was frequency

dependent for this drug but none of the other drugs evaluated. The 2nd and 3rd runs produced an amorphous content of 25, 49 % for 0.1 Hz, 58, 70% for 0.5 Hz and 46, 69% for 1.0 Hz, respectively.

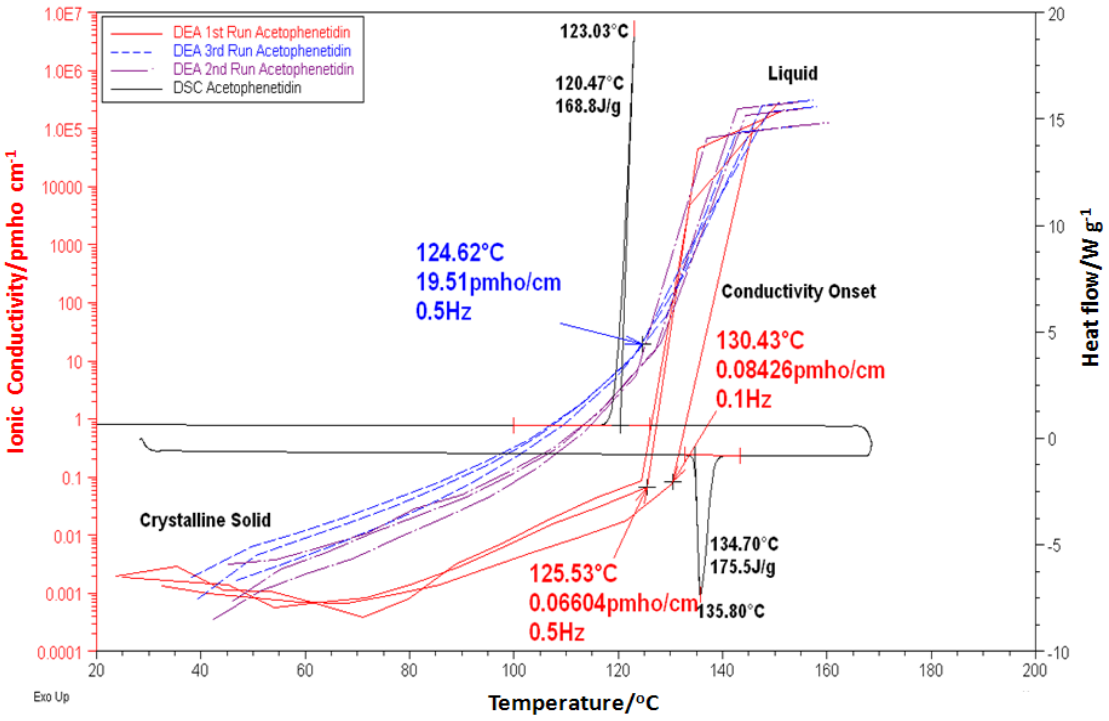

Figure 4.7. Acetophenetidin DEA and DSC curve overlay and comparing Ionic conductivity in crystalline and amorphous samples by activation energy method at 0.1 Hz to 1.0 Hz (Run1, Run 2 & Run 3); T_m= 135.80°C

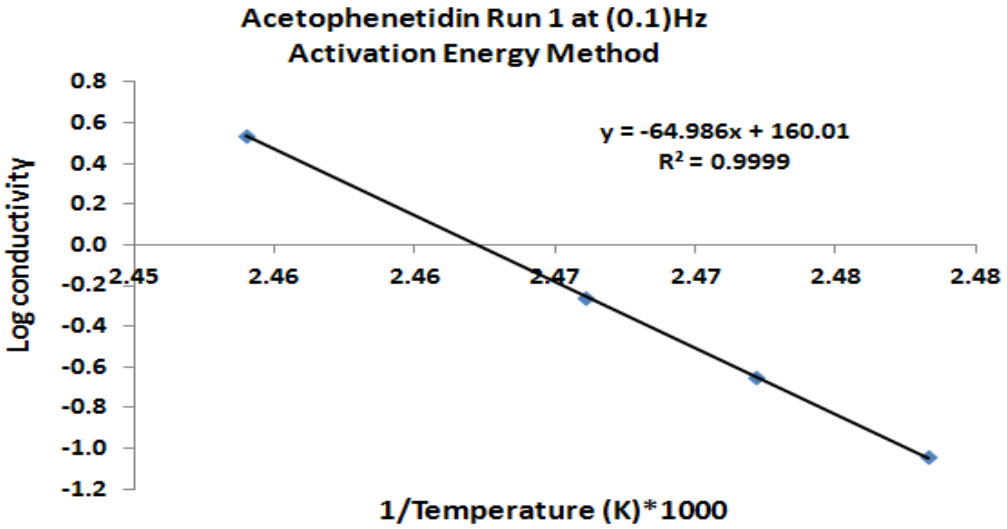

Figure 4.8. Log conductivity (k) vs. 1/T (Kelvin)*1000 for Acetophenetidin (Run 1, 0.1Hz); Ea = 1244 J mol^{-1}

Quantification of the amorphous and crystalline content of the drugs studied by the DEA Activation Energy Method is summarized in Table 3. A correlation was established between the Empirical method & Activation Energy method resulting in the correlation coefficient of R^2= 0.925 for the overall average % amorphous content of all the drugs studied (See Figure 4.9.).

Table 3

Quantification of Crystalline and Amorphous drug content of various pharmaceutical APIs by the DEA Activation Energy Method

Drug	Average content of 2nd and 3rd DEA Runs at 0.1,0.5 and 1.0 Hz	
	% Crystalline Content	% Amorphous Content
Lidocaine	7	93
Sulfa pyridine	9	81
Quetiapine Fumarate	11	89
Procainamide HCl	19	81
Lidocaine HCl	22	78
Indomethacin	24	76
Acetophenetidin	47	53

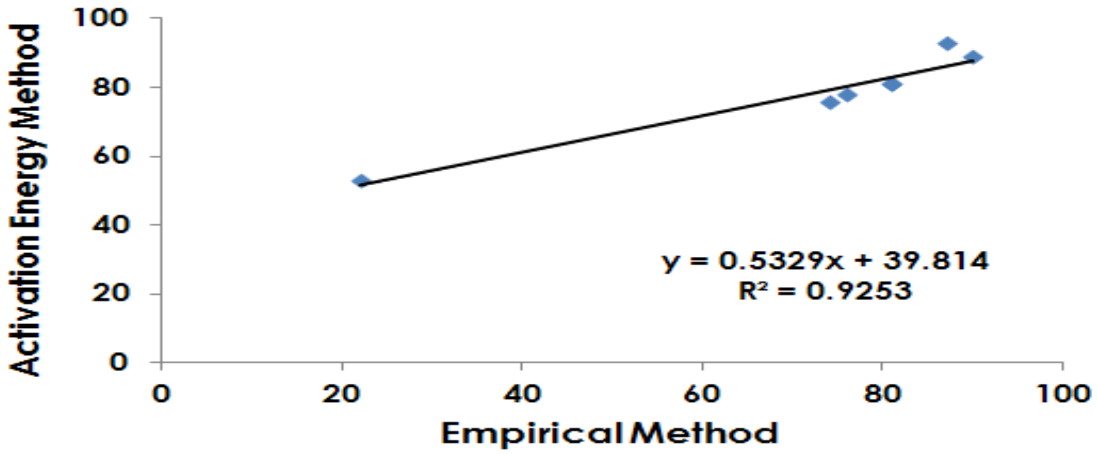

Figure 4.9. A correlation graph of Empirical Method versus Activation Energy Method (Ea) for the overall average % amorphous content of all the drugs studied

Semi-qualitative evaluation of the amorphous and crystalline states by macro-photomicrography clearly denotes the two phases, (see Figure 4.10.) for Sulfapyridine at 2.4X magnification. See Figure 4.11. for amorphous melt of Lidocaine HCL after 3rd run. All Pharmaceutical solids used in this study were characterized by this method. This material characterization technique aids the development of the DEA methods for identifying amorphous and crystalline character of the drug.

Figure 4.10. Macro photograph of DEA electrodes with sulfa pyridine in Crystalline Powder form (Right), and amorphous form (left) at 2.4 X magnification

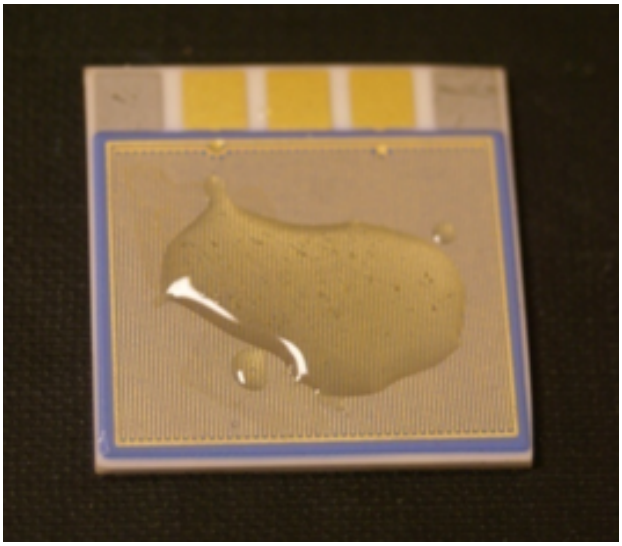

Figure 4.11. Macro photograph of DEA electrode with amorphous melt of Lidocaine HCl after 3rd Run

4.5 Conclusions

The most prominent conclusion is that we now have quantitative methods for determining the crystalline and amorphous content of pharmaceutical solids by dielectric analysis. We are basing this conclusion on the facts that the APIs distributed by pharmaceutical companies are ≥ 99.99% pure crystalline solids. Once the crystalline state is completely lost during melting the material becomes 100% amorphous.

Our studies reveal that 6 out of the 7 drugs evaluated showed this behavior of complete amorphous formation. In the case of Acetophenetidin, it recrystallized rapidly while the others remained predominantly amorphous. The crystalline and amorphous content of the drugs as determined by the empirical method was frequency independent. The frequencies studied relate to surface analysis at 0.1 - 1.0 Hz. The crystalline and amorphous content of the drugs as determined by the activation energy method was frequency dependent for one drug, i.e. Acetophenetidin. Therefore, Acetophenetidin was an outlier for these methods. DEA for the first run of the APIs is 100% crystalline with lower ionic conductivity and high activation energy, e.g., Acetophenetidin 1,200 -1,800

$Jmol^{-1}$. The second and third run of this drug showed repeatable variations with higher ionic conductivity and lower activation energy observed from 470 to 930 J mol^{-1}. The other drugs investigated yielded a stable activation energy e.g. for Lidocaine crystalline form it was 480 J mol^{-1} initially and for the amorphous form it was 27 J mol^{-1} at 1.0 Hz.

A comparison of overall average amorphous content by the Empirical method had a linear relationship with the Activation Energy method with a correlation coefficient of R^2 = 0.925. The correlation coefficient for overall average crystalline content was R^2= 0.94. After calibrating the DEA instrument, examining a 10 mg sample with a heating and cooling profile plus interpretation time will lead to a definitive amorphous content in one hour. Marco-photomicrography aids the DEA interpretation as an opaque solid material as crystalline solid against the transparent amorphous material. These methods determine the % amorphicity and % crystallinity and are significant contributions to the analytical science of pharmaceuticals.

4.6 References

1. Riga A, Judovits L. Materials characterization by dynamic and modulated thermal analytical techniques. West Conshohocken: ASTM. Special technical publication; 2011.
2. Yu L. Amorphous pharmaceutical solids: preparation, characterization and stabilization. Adv Drug Deliv Rev. 2001; 48:27 – 42.
6. 3.Jójárt-Laczkovich O, Szabó-Révész P. Amorphization of a crystalline active pharmaceutical ingredient and thermo analytical measurements on this glassy form. J. Therm Anal Calorim. 2009; Doi: 10.1007/s10973-009-0530-5.

3. Cui Y. A material science perspective of pharmaceutical solids. Int J Pharm. 2007; 339:3 –18.

4. Hancock BC. Disordered drug delivery: Destiny, dynamics and the Deborah number. J Pharm Pharmacol. 2002; 54:737 – 746.

5. B.C. Hancock, G. Zografi. Characteristic and significance of the amorphous state in pharmaceutical systems, J. Pharm. Sci. 1997; 86 1–12.

6. J. Keré, S. Sréié, Thermal analysis of glassy pharmaceuticals, Thermochim. Acta 248.1995; 81– 95.

7. Angell CA. The old problems of glass and the glass transition, and the many new twists. ProcNatlAcad Sci USA. 1995; 92:6675–6682.

8. Byrn S, Pfeiffer R, Ganey M, Hoi berg C, Poochkian G. Pharmaceutical solids: A strategic approach to regulatory consideration. Pharm Res. 1995; 12:945–954.

9. Vippagunta Sr, Brittain HG, Grant DJW. Crystalline solids. Adv Drug Deliver Rev. 2001; 48:3–26.

10. Venkatesh GM, Barnett ME, Fordjour CO, Galop M. Detection of low levels of the amorphous phase in the crystalline materials by thermally stimulated current spectrometry. Pharm. Res. 2001; 18:98–103.

11. Shah B, Kaumanu VK, Bansal AK. Analytical Techniques for Quantification of Amorphous/Crystalline Phases in Pharmaceutical Solids. J. Pharm. Sci. 2006; 95:1641-1665.

12. MinnaLappalainen, MaaritKarppinen. Techniques of differential scanning Calorimetry for quantification of low contents of amorphous phases. J. Therm Anal and Calorim. 2010; 102: 171 – 180.

13. Hancock BC, Parks M. What is the true solubility advantage for amorphous pharmaceuticals? Pharm Res. 2000; 17:397–403.

14. Singhal D, Curatolo W. Drug polymorphism and dosage form design: a practical perspective. Adv Drug Deliver Rev. 2004; 56: 335–47.

15. Schmitt EA, Law D, Zhang GGZ. Nucleation and Crystallization Kinetics of Hydrated Amorphous lactose above the Glass Transition Temperature. J. Pharm. Sci. 1999; 88:291–6.

16. Hancock BC, Shamblin SL, Zografi G. Molecular mobility of amorphous pharmaceutical solids below their glass transition temperature. Pharm Res. 1995; 12:799–806.

17. Seyer JJ, Luner PE, Kemper MS. Application of diffuse reflectance near infrared spectroscopy for the determination of crystallinity. J. Pharm. Sci. 2000; 89:1305–1316.

18. Hendrickson BA. Characterization of calcium fenoprofen 1. Powder dissolution rate and degree of crystallinity. Int J Pharm. 1990; 60:243–252.

19. Duddu SP, Sokoloski TD. Dielectric analysis in the characterization of amorphous pharmaceutical solids. 1. Molecular mobility in poly (vinylpyrrolidine) – water systems in the glassy state. J. Pharm. Sci. 1995; 84:773– 6.

20. Gustafson C, Lennholm H, Iversen T, Nystrom C. Comparison of solid state NMR and Isothermal Microcalorimetry in the assessment of the amorphous component of lactose. Int. J. Pharm. 1998; 174:243–252.

21. Taylor LS, Zografi G. The quantitative analysis of crystallinity using FT– Raman spectroscopy. Pharm. Res. 1998; 15:755–761.

22. Black BD, Lovering EG. Estimation of the degree of crystallinity in digoxin by x ray and Infrared methods. J. Pharm. Sci. 1997; 29:684–87.

23. Riga Alan T, Alexander Kenneth S. Electrical Conductivity Analysis/Dielectric Analysis Differentiates Physical-Chemical Properties of Drugs and Excipients. Am Pharm Rev. 2005; 8(6): 45-51.

24. Thakur SS, Maheswaram MPK, Mantheni DR, Kaza L, Perera I, Ball BW, Moran J, Riga AT. Solid – state mechanical properties of crystalline drugs and excipients: New data substantiate discovered dielectric viscoelastic characteristics. J Therm Anal and Calorim. 2011. Doi 10.1007/s10973-011-18559-0.

25. Mantheni DR, Maheswaram MPK, Sobhi HF, Perera NI, Riga AT, Ellen Matthews M, Alexander K. Solid state studies of drugs and chemicals by dielectric and calorimetric analysis. J of Therm Anal and Calorim. 2011. Doi 10.1007/s10973-011-1423-y.

26. Sharma M, Yashonath S. 2008. Correlation between conductivity and diffusivity and activation energy in amorphous solids. J. Chem. Phys: 129,144103.

27. Matthews, M.E., Atkinson, I., Presswala, L., Najjar, O., Gerhardstein, N., Wei, R., Rye, E. & Riga, A.T. Dielectric classification of *D* -and *L* -amino acids by thermal and analytical methods. J Therm Anal and Calorim. 2008; 93:281-7.

28. Presswala L, Matthews ME, Atkinson I, Najjar O, Gerhardstein N, Moran J, Wei R, Riga AT. The discovery of bound and unbound waters in crystalline amino acids revealed by thermal analysis. J Therm Anal and Calorim. 2008;93:295-300.

29. Matthews ME, Riga AT. Effects of thermal history on solid state and melting behavior of amino acids. J of Therm Anal and Calorim. 2009;96(3): 673- 6.

CHAPTER V

PHYSICAL AND CHEMICAL CHARACTERIZATION OF HYDROCHLORIDE SALTS OF DRUG SUBSTANCES BY DIELECTRIC AND CALORIMETRIC ANALYSIS

5.1 Introduction

The critical factors for drug development of pharmaceutical formulations are the solid-state properties of drug candidates. These solid-state properties are crucial in selecting the appropriate salt form of a drug molecule as more than 50% of all the drugs molecules used in the medicinal therapy are administered as organic salts [1-6]. For large-scale production of the pharmaceutical formulations these salts of drug substances must be suitable and technically feasible and its solid-state properties maintained batch wise as well as over time. Changing salts in the middle of a development program may require repeating most of the studies performed initially, i.e., biological, toxicological, formulation, and physical and chemical stability.

However, selection of a nonoptimal salt may lead to increased developmental and production costs, even product failure. Appropriate salt selection during the drug development process can significantly reduce time to market and will avoid these

problems and facilitate downstream development activities [2]. Salts are mainly used to alter the physical, chemical, biological, and economical properties of a drug substance. Salts with advantageous properties are usually patentable as new chemical entities. A major reason for choosing a salt form is based on a needed change in the solubility of a drug substance. Substances containing free acid and base groups have poor aqueous solubility.

However, with the saltification (i.e., salt formation) of these acid and base groups one can improve solubility, leading to greater bioavailability. The chloride, hydrogen sulfate, phosphate, sodium, and potassium salts exhibit significantly higher solubility and dissolution rates than the parent drug. In addition, salts usually exhibit a higher melting point and improved chemical stability compared to the parent drug (free acid or base), leading to greater stability and easier processing [4]. A choice of salts can also expand the formulation options for a material. For example Lidocaine, a compound limited to parenteral and topical formulations can be expanded to oral administration by changing it to a salt form (e.g. Lidocaine hydrochloride) with acceptable physical properties [7]. The different salts are different entities with altered behavior in the solid-sate and also in the liquid state. These properties have to be studied taking into account thermodynamic, surface, packing, mechanical and kinetic factors.

The most pertinent solid-state properties may affect the melting, heat capacity, crystallinity and/ or amorphicity, conductivity, bioavailability, pharmaceutical processing, toxicity, therapeutic efficacy, quality, solid-state reactions, reactivity, and stability of the drugs [8-14]. The International Conference on Harmonization (ICH) requires proper investigations and analytical methods for drug substances and drug

products following a decision tree (ICH) Q6A [15]. A number of analytical techniques are commonly used for characterization of the salt of the drug substance: They are thermal analysis, microcalorimetry and combined techniques, X-ray diffraction, solubility and stability studies.

Salt formation involves proton transfer from the acid and base entity. Theoretically, any substance or compound that exhibits acidic or basic characteristics can form salts. The major consideration is the relative acidity and/ or basicity of the chemical species involved. When using basic excipients in a formulation the relative acid/base strength of the resulting salt and its tendency to disproportionate should be considered. A common salt choice for basic drug substances approved by FDA is the hydrochloride (most encountered anion is chloride), mainly because of its availability and highly polar nature. However, due to the common ion effect, reports have shown that hydrochloride salts do not always increase the solubility of poorly soluble basic drugs [16-19].

Thermoanalytical methods have been used in the pharmaceutical area for 35 years. They are employed for quality control, preformulation, drug-excipient interactions and purity studies of raw materials and pharmaceutical products [20-24]. Thermal analysis techniques mainly (DSC, DEA and TG) play an important role in the detection of unexpected phase transitions and for the comparison of the suitability of the salt candidate prepared from the salt selection [25]. The observance of the thermal phase transitions by DSC is insufficient to fully characterize the behavior of a substance on heating. The formation of hydrates and solvates can be investigated using Thermogravimetry (TG). Other information, such as crystallinity and/ or amorphicity,

conductivity, solid-state reactions, reactivity, physical and chemical stability of drug salts can be obtained from dielectric analysis [26-29].

The pharmaceutical industry relies mainly on solid salts; primarily crystalline forms for the delivery of the APIs because they are thermally stable, there are easy to handle, and they are pure. In contrast, amorphous drug formulations are rarely found. Salts in the crystalline form tend to melt and decompose, while salts in the amorphous form have a glass transition (Tg) and no defined melt. However, crystalline solid forms have low solubility and low bioavailability, compared with an amorphous form. Amorphous forms have enhanced molecular mobility (poorer physical and chemical stability) as compared to their crystalline counterparts, owing to their thermodynamic (higher free energy) and kinetic properties (higher molecular represented by the molecular relaxation time constant) [30]. The molecular mobility is usually expressed as the polarization time, τ (Tau). The key factor responsible for their physical instability is because of their greater molecular mobility. Several studies have recognized the role of molecular mobility in time dependent recrystallization, chemical degradation, and structural collapse of amorphous systems.

The observed molecular mobility is related to chemical reactivity of amorphous pharmaceuticals [31-35]. These changes in the pharmaceuticals, may adversely lead to altercations in the physicochemical properties and the bioavailability of the molecule during storage. Therefore, an acceptable shelf life of amorphous compounds and their formulations is of critical importance and this can be determined by reducing the molecular mobility. However, a reduction in molecular motions does not necessarily result in increased storage stability, because physical characteristics like: dielectric,

mechanical and thermal properties may also vary with time and temperature on storage [36]. For these reasons, a constant screening for new drug forms including salts is ongoing and also because of financial interests caused by legal ramifications [37]. Several different techniques i.e., differential scanning Calorimetry (DSC), dielectric analysis, isothermal microcalorimetry, mechanical analysis, and solid-state NMR spectroscopy have been applied to study the relaxation or polarization phenomena in the amorphous pharmaceutical systems.

The primary aim of this study is to investigate the thermal and electrical behavior of pharmaceutical hydrochloride salts including the Lidocaine drug (non-salt) using DEA and DSC techniques. This analysis provides a perspective on the use of the data from these techniques for predicting the quality, stability and behavior of pharmaceutical salts. This study is also aimed at providing a comprehensive characterization of ionic conductivity and molecular mobility (related to tan delta in DEA) properties in pharmaceutical salts i.e., crystalline and amorphous forms through the measurement of the characteristic activation energies and polarization times.

5.2 Dielectric Analysis (DEA)

Riga et al. in 2005 published the first study of the physical-chemical properties of drugs including drug salts and excipients by dielectric analysis [26]. DEA has come into play in the pharmaceutical field because of its unique measurements, the electrical properties of the drugs (APIs) or to determine their amorphous and crystalline content. DEA measures the ability of dipoles and ions present in a material to align with an application of a time dependent alternating electric field as a function of time, temperature, and frequency [26 & 29]. The increase in molecular motion associated with

the glass transition allows the dipoles or ions in an amorphous material to more freely align with the electric field and dissipate energy. DEA measures two fundamental characteristics of a material, in our study, of crystalline and amorphous drug salts. First, the capacitive nature (permittivity; ε′) of the drug salts allows these materials to store electric charge. Second, the electrical conductivity (loss factor; ε″) characteristic represents the ability of the drug salt to transfer electrical charge or energy to move ions.

DEA of pharmaceutical drugs, amino acids, organic chemicals, and carbohydrates reveals a strong linear conductivity increase prior to the melt, peaking at the melt, associated with the dielectric solid-state and viscoelastic properties of the material [26 & 38]. This DEA technique is a perfect complement to the other different techniques of thermal analysis by identifying the phase transitions from the electrical properties of materials as a function of time, temperature, and wide range of frequency (e.g. 0.1 Hz to 100,000 Hz) [39]. The wide frequency range allows measurement of subtle transitions as well as multiple-mechanistic transitions that are sensitive to the frequency of measurement. Matthews et al. characterized and distinguished the unique dipole characteristics of chiral molecules, specifically 20 L-amino acids and 9 D-amino acids by employing DEA as an analytical technique. This technique has the capability to explore the rheology and molecular mobility of the amino acids 20 to 30 °C below the melting temperature established by DSC [40].

Specific and novel protocols to quantify the crystalline and amorphous content of various pharmaceutical drugs by dielectric and calorimetric analysis were developed by Maheswaram et al. It was observed that the ionic conductivity of a crystalline drug is typically less than 10^{-1} pS cm^{-1} at room temperature and a melted drug, an amorphous

form, has a conductivity of greater than 10^5 pS cm^{-1}. Further, the melted drug salts had an ionic conductivity of $>10^5$ pS cm^{-1} [29]. The drug salts showed a 10-fold increase in ionic conductivity, e.g., Lidocaine hydrochloride conductivity was 10^6 pS cm^{-1} and Lidocaine (non-salt) 10^5 pS cm^{-1}. The higher ionic conductivity is an important attribute of a drug salt.

Examination of drug salts by DEA also discovered a strong linear electrical conductivity prior to the pre-melt temperature through to the melt. Activation energies ($E_{a,}$ J mol^{-1}) of each drug salt can be calculated from the slope of Arrhenius plots of the log conductivity, Ea (k) versus reciprocal temperature in Kelvin [40]. This energy is associated with the energy for charging ions in polar materials or relates to the formation of charge transfer complexes prior to the melt in the solid state. Second activation energy, Ea (τ, Tau) can be calculated via Arrhenius plots of log tan delta peak frequencies vs. reciprocal temperature in Kelvin. This Ea (τ) is related to the activation energy for the relative rate of change of the ordered charging process, molecular or charge mobility. Therefore we can estimate the minimum energy attributed to charging of ions or creating charge transfer complexes. Plus, the second Ea (τ) estimates the energy associated with molecular mobility.

The polarization or the response time of the charged ion or ions can be measured from a Debye plot, where the inverted peak value is corrected with a constant and describes the time for the ions to be polarized for transport in the field. Therefore, DEA can be a widely used thermal analytical method that measures polarization response of various materials (e.g. drugs, chemicals, carbohydrates, proteins, electro rheological fluids etc.) in an AC electric field at isothermal temperatures or by scanning temperature

techniques [38-44]. The response times were calculated from a Debye plot of tan delta ($\varepsilon''/\varepsilon'$) vs. log frequency. The response time is directly related to the polarization time, which is inversely related to the critical peak frequency in the Debye plot [38]. The polarization time is calculated by using the following equation:

T (Tau) = $1/2\pi$fc x 1000 (MS) [see references 38, 45]

τ (Tau) = Polarization time (millisecond)

fc = Tan delta critical peak frequency (Hz)

These analyses demonstrate efforts to correlate the polarization (relaxation) properties to the molecular structure and behavior of the material [46].

5.3 Differential Scanning Calorimetry (DSC)

DSC is frequently used to measure the physical properties of Active Pharmaceutical Ingredients (APIs), and Excipients. This includes melting and vaporization temperatures, phase transitions, glass transition, stability, quality and purity studies of raw materials and pharmaceutical products. The quality of these pharmaceutical materials is based on the melting temperature and peak melting temperature, a range of 2 to 3 °C, i.e. melting peak temperature (Tmp) minus the melting temperature (Tm). The heat of fusion of a drug or drug salt is a criterion for drug crystalline/amorphous content and its purity. The heat of fusion is usually much greater for the salt that melts and decomposes vs. the one that only melts. The DSC curve for the former is typically broader at its half maximum, e.g. during decomposition the value is 17-20 °C and for a pure stable salt the half maximum is 3-5 °C. The DSC decomposition temperature of the drug salt as an exothermic or endothermic process is a key indicator that the drug is unstable. The apparent heat of fusion for a pure drug is <300 J/g while the

drug salt melting and followed by decomposition, probably endothermically, is 400-500 J/g. The DSC curve profile is also spiked detected as a second endothermic peak along with the melting the first endotherm.

Careful analysis of the DSC amorphous phase can reveal molecular mobility of the pharmaceutical that can be related to its performance. Amorphous materials have varying properties from their crystalline counterparts. Differences in the amorphous forms can be related to their kinetic solubility, storage stability as well as their mechanical characteristics [47]. These physical amorphous forms lead to unique physical chemical attributes and functionalities.

5. 4 Experimental

5.4.1 Materials. The following drug salts were studied by DSC & DEA. Procainamide hydrochloride (T_m, 169 °C), Lidocaine (T_m, 68 °C) and Lidocaine hydrochloride (T_m, 74–79 °C) were obtained from Sigma-Aldrich (St. Louis, Mo.). Fluoxetine hydrochloride (T_m, 156-158 °C) was obtained from Eli Lilly. Hydralazine hydrochloride (Tm, 273 °C) was obtained from Alfa Aesar; Quinapril hydrochloride was obtained from Toronto Research Chemicals Inc. (T_m, 120-130 °C).

5.4.2 Uses. Fluoxetine hydrochloride (Figure 5.1.) is an antidepressant of the selective serotonin reuptake inhibitor class. The multiple aromatic rings that are in conjugation with the highly electronegative fluorine atoms promote its structural stability. Hydralazine hydrochloride (Figure 5.2.) is a smooth muscle relaxant and is an antihypertensive. Its potential stability is based on the ring structures but the terminal amine is vulnerable and is less stable. Quinapril hydrochloride [48] (Figure 5.3.) is an angiotensin-converting enzyme inhibitor (ACE inhibitor) used in the treatment of

hypertension and congestive heart failure. Procainamide hydrochloride (Figure 5.4.) is an anti-arrhythmic agent used for the treatment of cardiac arrhythmias. Lidocaine hydrochloride (Figure 5.5.) is a local analgesic used quite frequently in dentistry and as antiarrhythmic drug. Its stability can be based on the ring conjugation with the carbonyl.

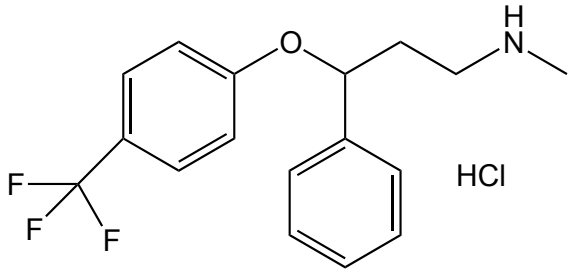

Figure 5.1. Skeletal structure of Fluoxetine hydrochloride

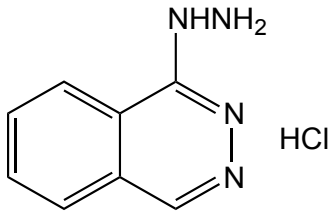

Figure 5.2. Skeletal structure of Hydralazine hydrochloride

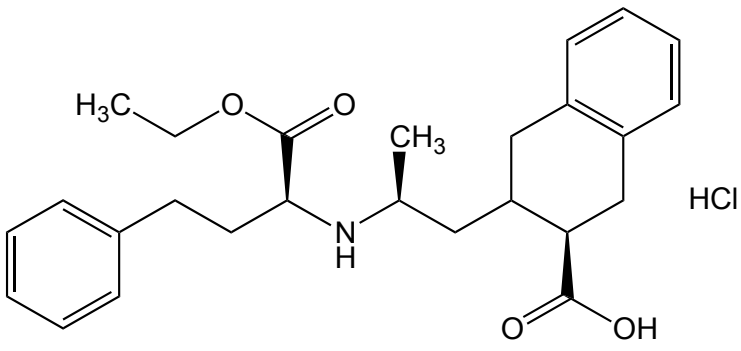

Figure 5.3. Skeletal structure of Quinapril hydrochloride

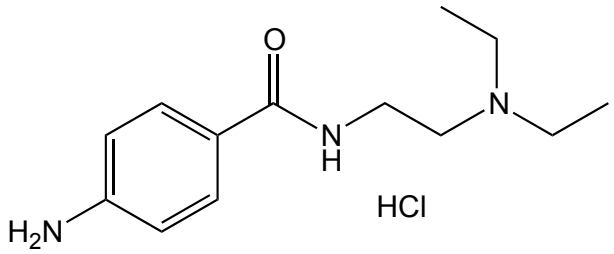

Figure 5.4. Skeletal structure of Procainamide hydrochloride

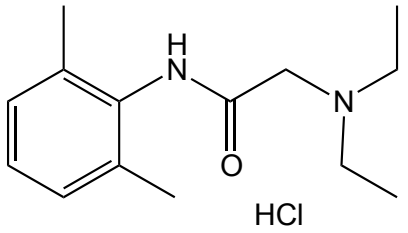

Figure 5.5. Skeletal structure of Lidocaine hydrochloride

5.5 Instrumentation

5.5.1 Differential scanning calorimetry (DSC). A TAI 2920 DSC was used to characterize melting, solid-liquid phase transitions, glass transition temperature (Tg) of pharmaceutical hydrochloride salts. Approximately 8-10 mg of sample was mass out and placed in sealed aluminum crimped pan (SFI pans) with a pinhole. An empty SFI aluminum pan was used as a reference. A heating rate of 10 °C min^{-1} was applied to all samples. A purge gas of nitrogen was flowed at a rate of 60 mL min^{-1} during heating and cooling cycles. The temperature range was typically from room temperature to 25 to 30 °C above the melting temperature (T_m) for the salts under study; the glass transition was also evaluated and then cooled to room temperature. DSC equipment was preliminarily calibrated with standard reference of indium (T_m, 156.6 °C). The purity determination

was accomplished with an E698 protocol an ASTM Method. Heat flow (W g^{-1}) values vs. time and temperature were generated using Universal Analysis 2000 (TA Thermal Advantage) software.

5.5.2 Dielectric analysis (DEA). A TAI 2970 DEA was used to determine the electrical ionic conductivity and Tan delta (ε″/ε′) for each drug salt studied. Approximately 20 mg of sample was placed on a single surface gold ceramic interdigitated electrode (entire electrode was covered). The sample were linearly heated at a rate of 10 °C min^{-1} in a purged inert nitrogen gas flow at rate of 60 mL min^{-1} from room temperature to 25-30 °C above the melting temperature of the salts studied. The samples were heated, using the above heating protocol, and air cooled for sequential runs. The DEA sensors were calibrated by the TA instrument software, which was initially calibrated by a 9-step fixture supplied by TAI. The ionic conductivity (pS cm^{-1}) and tan delta measurements were recorded at a controlled interval frequencies ranging from 0.10 to 10,000 Hz for all the temperatures. These DEA curves were generated using the Universal Analysis 2000 software (TA Thermal Advantage software).

5.6 Results and Discussion

5.6.1 Dielectric analysis: Ionic Conductivity (pS cm^{-1}). DEA profiles of the drug salts studied show that the initial ionic conductivity for a crystalline drug is 10^{-2} pS cm^{-1}. The ionic conductivity of the amorphous form (liquid) of a non-salt drug (e.g. Lidocaine) is 10^{5} pS cm^{-1}. The drug salt in the amorphous form will have an ionic conductivity of 10^{6}-10^{8} pS cm^{-1} in the melt. Therefore, the liquid drug salts can be modified by electrochemical synthesis in the melt state based on their enhanced ionic conductivity.

The DEA profile of Fluoxetine.HCl shows the changes in electrical behavior associated with solid-solid and solid-liquid transitions. The DEA curve shows a sharp linear increase in ionic conductivity leading up to the melt (DSC 157-161^{o}C) in the first run and an increase in ionic conductivity with temperature in the second and third runs. The ionic conductivity of the Fluoxetine HCl for the crystalline solid at 0.5 Hz (DEA 1st run) was 2.18 x 10^{-3} pS cm^{-1} at 54.34 ^{o} C and at 0.5 Hz it was 55.15 pS cm^{-1} at 140.60^{o} C.

In the melt region for DEA run 1 at 0.5 Hz it was 1.12 x 10^{7} pS cm^{-1} at 164.99^{o} C and at 10,000 Hz it was 5.30 x 10^{7} pS cm^{-1}. For the DEA 2nd run the ionic conductivity at 10,000 Hz was 1.06 x 10^{8} in the melt (164.99^{o} C) and at 0.5 Hz, 139.94^{o} C it was 4.2 x 10^{5}. For the 3rd run at 10,000 Hz, 164.81^{o} C the ionic conductivity was 1.07 x10^{8} pS cm^{-1} and at 0.5 Hz, 139.79^{o} C it was 5.13 x 10^{6} pS cm^{-1} (See Figure 5.6.). The DSC curve for Fluoxetine HCl reveals a sharp Tm at 157.45^{o} C and a heat of fusion of 130 J.g^{-1} (See Figure 5.7.). On the cooling cycle it doesn't recrystallize and therefore it indicates the formation of an amorphous material.

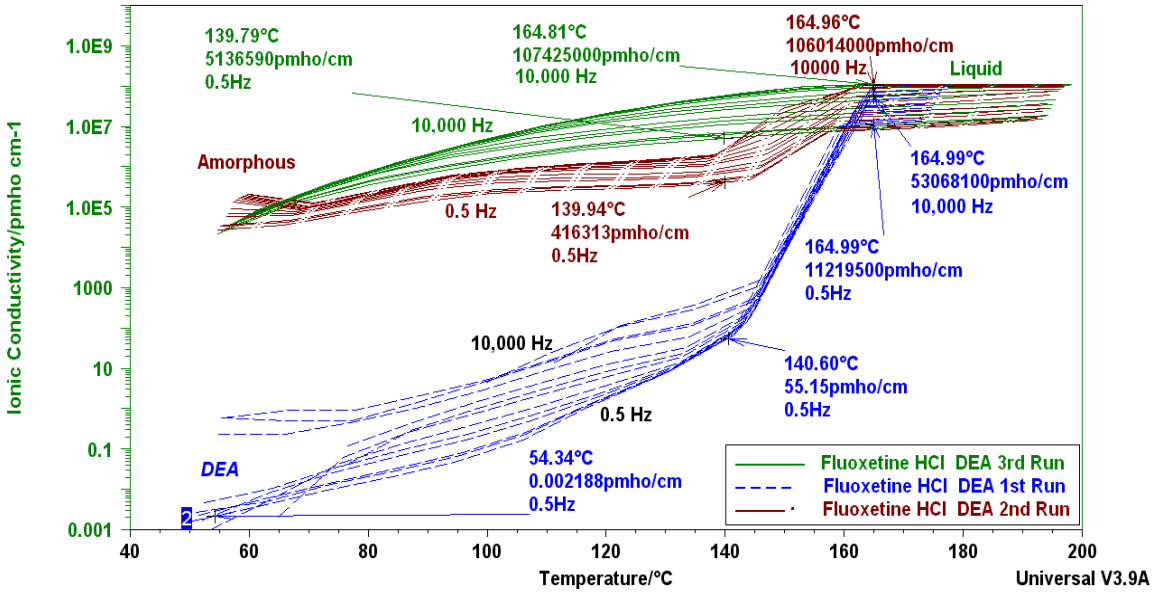

Figure 5.6. Log ionic conductivity versus Temperature profile, frequency range of 0.50 Hz – 10,000 Hz, of Fluoxetine.HCl; Overlay of DEA 1st, 2nd and 3rd runs

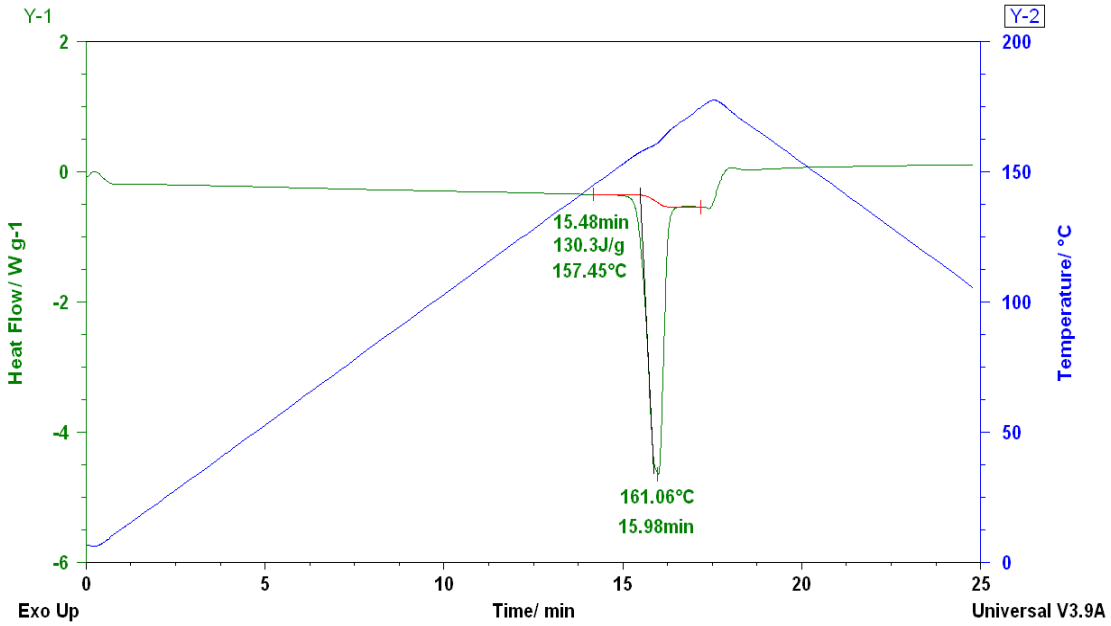

Figure 5.7. Fluoxetine.HCl DSC curve showing Tm = 157.45° C, Heat of fusion (130 J g^{-1}) for the first endothermic peak

The DSC and DEA profiles of Procainamide.HCl are compiled in Figure 5.8. The DSC profile yielded the Tm = 166.63 °C and Tmp (peak melting temperature) = 169.61 ° C plus the heat of fusion = 104.50 J g^{-1}. The DEA ionic conductivity results are as follows: 1st run, 59.80 °C, 0.50 Hz, 4.69 x 10^{-2} pS cm^{-1}; 152.18 °C, 0.50 Hz, 1.55 x 10^{3} pS cm^{-1}; 169.56 °C, 0.50 Hz, 6.63 x 10^{5} pS cm^{-1}. For the 2nd run, at 59.77 °C, 0.50 Hz, 6.44 x 10^{3} pS cm^{-1}; 152.18° C, 0.50 Hz, 3.36 x 10^{6} pS cm^{-1}; 169.53° C, 0.50 Hz, 1.01 x 10^{8} pS cm^{-1}. Consequently, from the crystalline solid (run 1) to the amorphous liquid (run 2) at 0.50Hz and 152 °C the ionic conductivity increased by 2200 times and at 169 °C it increased by 150 times. There is statistical significant difference in ionic conductivity from crystalline to amorphous form of the drug salt. Therefore, the first runs of Fluoxetine.HCl and Procainamide.HCl are more stable and are of higher quality than the higher conducting amorphous second and third runs.

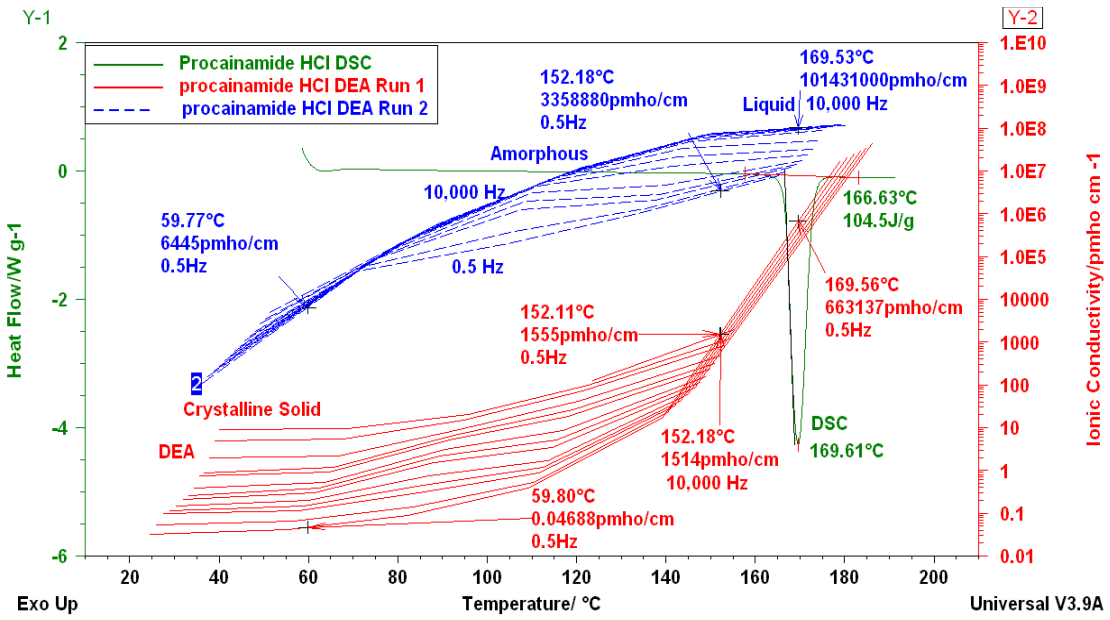

Figure 5.8. Overlay of DSC and DEA (1st, 2nd and 3rd runs) profile of Procainamide HCl showing DEA log ionic conductivity versus temperature profile, frequency range of 0.50 Hz to 10,000 Hz and DSC profile Tm = 166.6; Tmp = 169.6° C, Heat of fusion = 104.5 Jg^{-1}

The higher ionic conductivity is an important attribute of a drug salt. The DEA ionic conductivity of Lidocaine (non-salt) is 10^5 pS cm^{-1} and Lidocaine. HCl is 10^6 pS cm^{-1} for the amorphous form of the drug salt (2^{nd} run). Clearly the ionic salt (HCl) is contributing to the measured higher conductivity, a ten-fold increase. A quality drug salt attribute is that the 1^{st} DEA run ionic conductivity is low at room temperature (10^{-2} pS cm^{-1}). As the salt is heated and approaching the melt, in the pre-melt temperature range the conductivity increases from ca.10^{-1} to 10^6 pS cm^{-1}. Next, in the melt of the drug salt the conductivity is >10^6 to 10^8 pS cm^{-1}. Further, the DSC profile yields a curve where the endothermic melt is a smooth narrow peak with half maxima of 3-5 °C. A drug salt that melts and decomposes has a half maxima of >15 °C., e.g. Hydralazine.HCl. Its apparent heat of transition, fusion and endothermic decomposition was 300 - 400 J g^{-1}. This supports the DEA interpretation of first run (crystalline solid; 10^4 pS cm^{-1}) ionic conductivity decreased on the second run (10^3 pS cm^{-1}) atypically.

5.6.2 Activation Energies (J m^{-1}). It has been observed that some chemicals, amino acids and carbohydrates form charge transfer complexes prior to the melt in the solid state [29, 40]. A study of the electrical behavior of the drug salts, as determined for the amino acids and sugars, yielded repeatable activation energy values which can be correlated with real world solid-state properties, e.g. stability and/or quality. Activation energies ($E_{a,}$ J mol^{-1}) of each drug salt either as related to the conductivity (k) or to the tan delta (e"/e') peak frequencies (τ) can be calculated from the slope of Arrhenius plots of the log conductivity, Ea (k) or Ea (τ) versus 1/ temperature (K) x 1000. Therefore we can estimate the minimum energy attributed to charging of ions or creating charge transfer complexes and the energy associated with molecular or charge mobility.

The Activation energies Ea (k) (J m^{-1}) for the drug salts were evaluated at 0.50 Hz and at a temperature range of 20 ^{o}C to 30 ^{o}C below the DSC peak melting temperature employing an Arrhenius plot (See Table 1). The Ea (k) for Fluoxetine HCl (See Figure 5.9.), Procainamide HCl (See Figure 5.10.), and Quinapril HCl (See Figure 5.11.) were calculated from the DEA plots of Ionic conductivity (pS cm^{-1}) vs. temperature. DEA 1st run (Crystalline Solid); DEA 2nd run (Amorphous), and 3rd run (Amorphous) Ea (k) values for all the drug salts studied are summarized in Table 1.

Table 1

Activation Energies Ea (k) of Drug Salts

Drug Salts	Activation Energies: Ea (k) J m^{-1}		
	DEA 1st Run	DEA 2nd Run	DEA 3rd Run
	Crystalline	Amorphous	Amorphous
Procainamide.HCl	501	81	83
Fluoxetine.HCl	956	227	35
Lidocaine.HCl	340	33	31
Quinapril. HCl	380	176	134

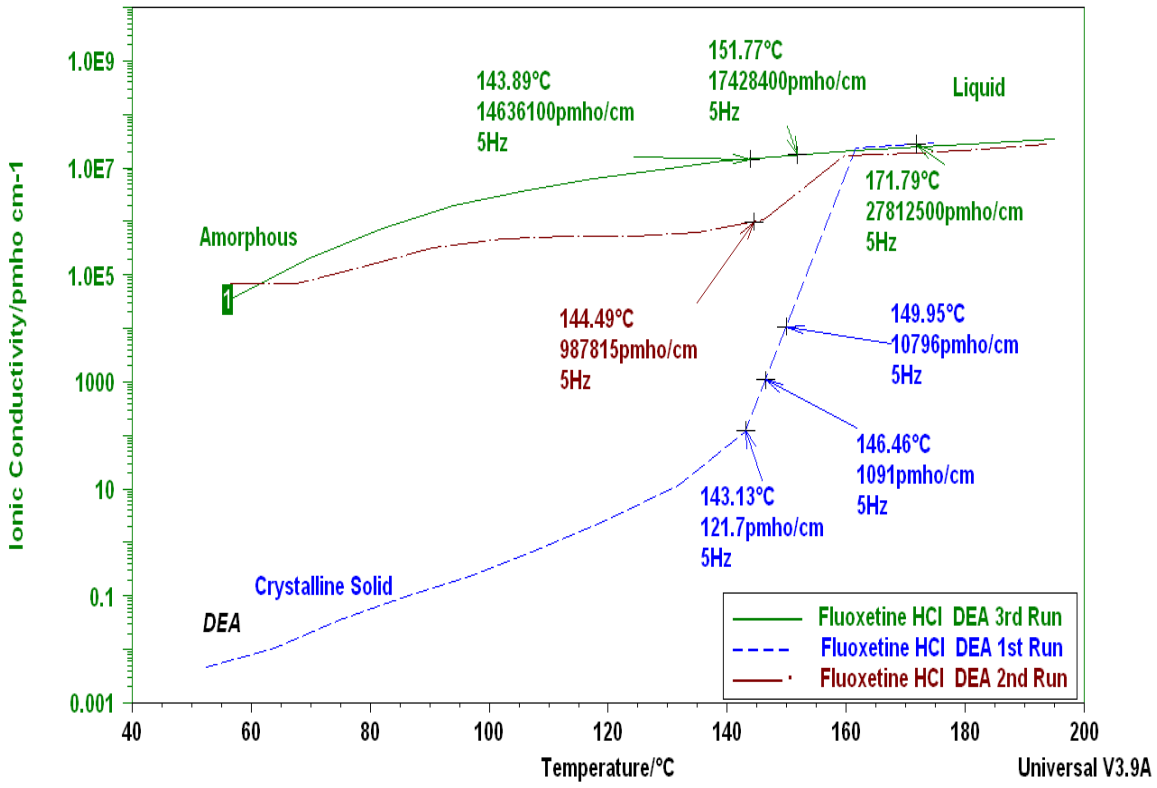

Figure 5.9. Overlay of DEA (1st, 2nd and 3rd runs) log ionic conductivity versus temperature profile of Fluoxetine HCl at 0.50 Hz

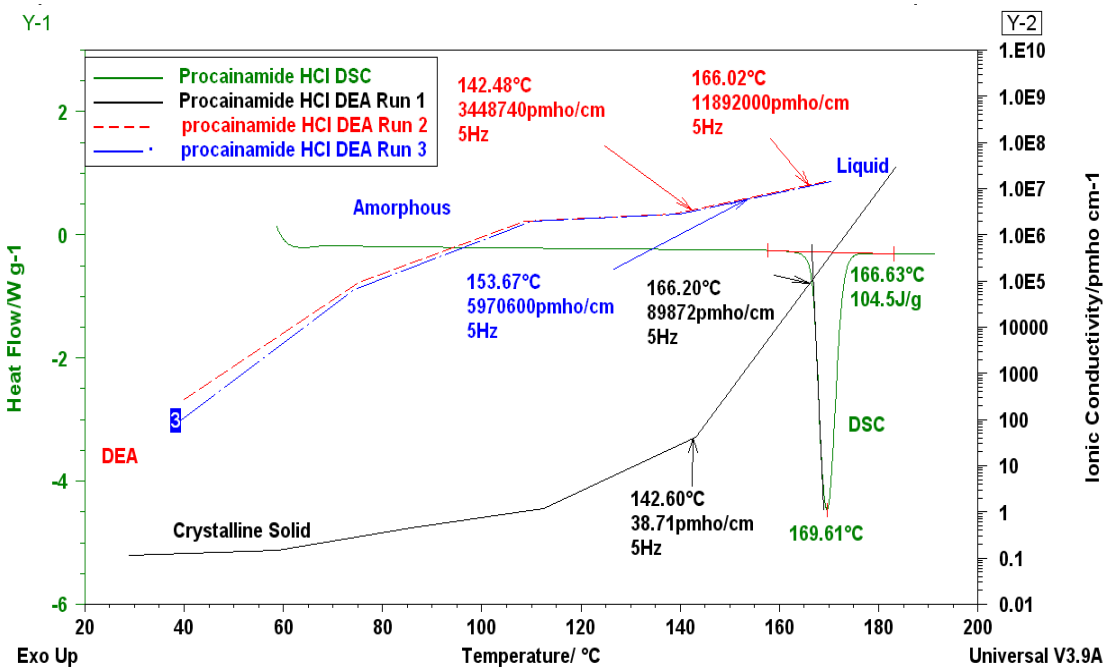

Figure 5.10. Overlay of DSC and DEA (1st, 2nd and 3rd runs) profile of Procainamide HCl showing DEA log ionic conductivity versus temperature profile at 0.50 Hz and DSC profile Tm = 166.6; Tmp = 169.6° C, Heat of fusion = 104.50 J g^{-1}

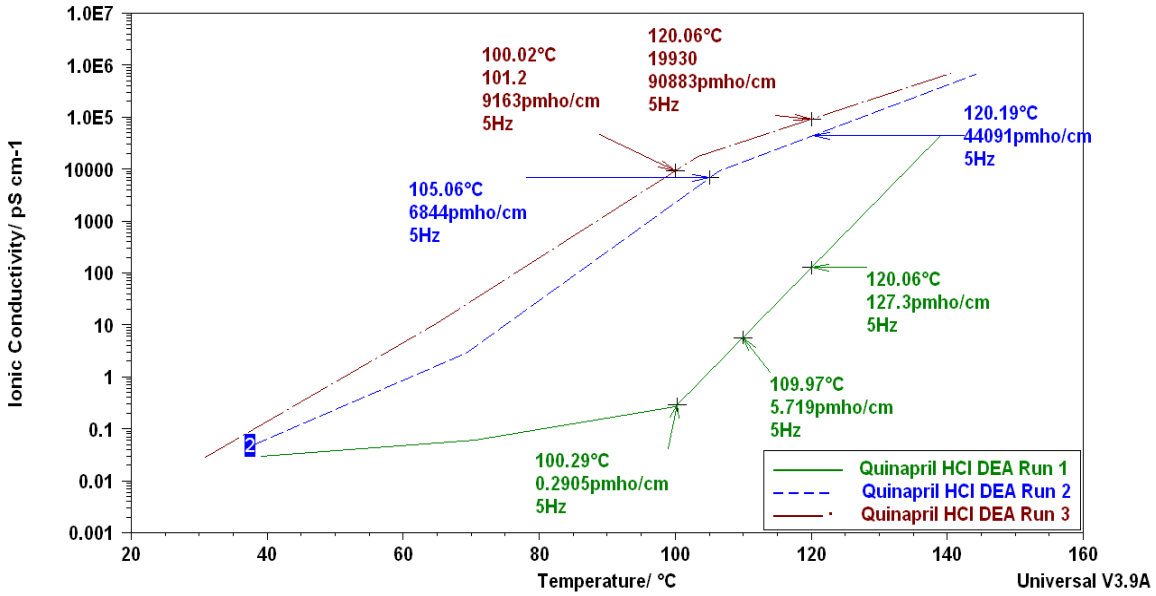

Figure 5.11. Overlay of DEA (1st, 2nd and 3rd runs) log ionic conductivity versus temperature profile of Quinapril HCl at 0.50 Hz

The Ea (k) for the 4 crystalline drug salts studied (DEA 1st run) was 340-956 Jm^{-1}. The Ea (k) for the 2nd and 3rd runs of Procainamide.HCl (501 J m^{-1}) and Lidocaine.HCl

(340 J m^{-1}) decreased from a higher value to a constant lower value of 82 and 32 J m^{-1}, respectively. Fluoxetine.HCl and Quinapril.HCl decreased by 85% and 24% of the 1st run Ea (k) value, respectively. A curve fit of the log conductivity vs. 1/T (K) x 1000 produced a linear curve with a correlation coefficient of R^2 = 0.996 or greater for all the drug salts (see Figure 5.12. for Fluoxetine.HCl Arrhenius plots). The Ea (k) is used to rank crystallinity/amorphicity in pharmaceutical solids [29], that is, a high Ea (k) value is crystalline material and low Ea (k) value is amorphous material. An Ea (k) value of <140 J m^{-1} suggests that the material is amorphous.

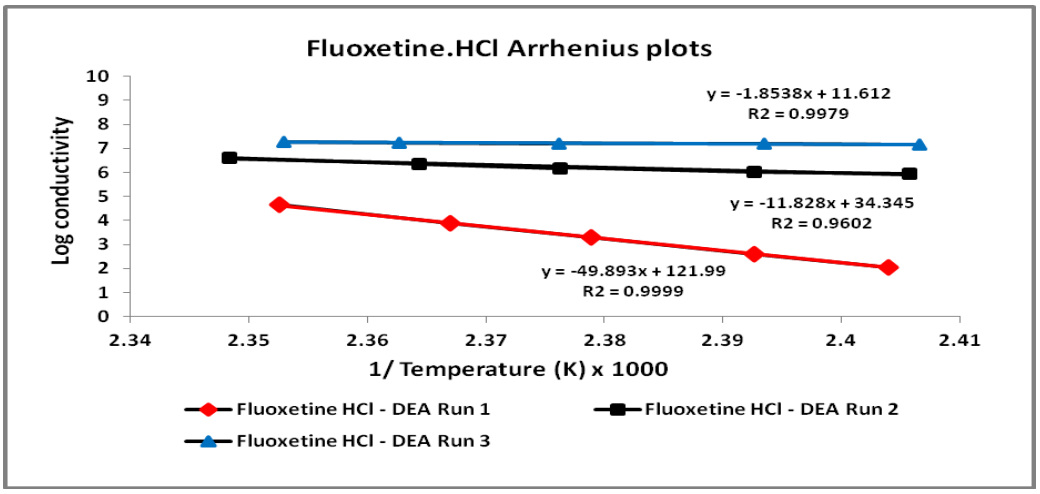

Figure 5.12. Arrhenius plots of Fluoxetine.HCl (1st, 2nd, 3rd runs; 0.5Hz); Ea = 956, 227, 35 J m^{-1} respectively

5.6.3 Tan delta. The Activation energies Ea (τ) for the drug salts were evaluated as a function of frequency and temperature. An Arrhenius plot was used to determine the Ea (τ) for each drug salt i.e. crystalline or amorphous material. The log tan delta peak frequencies (Hz) vs. reciprocal temperature in Kelvin x 1000 for the drug salts studied is summarized in Table 2. Tan delta curves for all the drug salts revealed a weak spectrum in the first run of the crystalline solid (Figure 5.13.). The second and the third runs

revealed strong spectra (See Figure 5.14. and 5.15. respectively). The resulting Ea (τ) only yields values after the 2nd and 3rd DEA scanning runs, as the material is amorphous. The Ea (τ) from run 2 to run 3 was constant for Procainamide.HCL at 84 J m^{-1} (See Figure 5.16.), Fluoxetine.HCl at 78 J m^{-1} and Quinapril.HCl at 25 J m^{-1}. The constant Ea (τ) values in the amorphous phase indicate the presence of a stable material. For Lidocaine.HCl, the Ea (τ) varied from the 2nd run (148 J m^{-1}) to the 3rd run ending in (20 J m^{-1}). This can be interpreted that there is some variability in this salt possibly related to the hydroscopic nature of this compound. The water aggregating on the salt can cause the variation in its solid – liquid state properties. This analysis scheme can be developed to predict storage stability or shelf life with a detailed experimental analysis based on the Ea (τ).

Table 2

Activation Energies Ea (τ) of Drug Salts

Drug Salts	Activation Energies : Ea (τ) J m^{-1}		
	DEA 1st Run	DEA 2nd Run	DEA 3rd Run
	Crystalline	Amorphous	Amorphous
Procainamide.HCl	Not Observed	84	85
Fluoxetine.HCl	Not Observed	78	79
Lidocaine.HCl	Not Observed	148	20
Quinapril.HCl	Not Observed	25	25

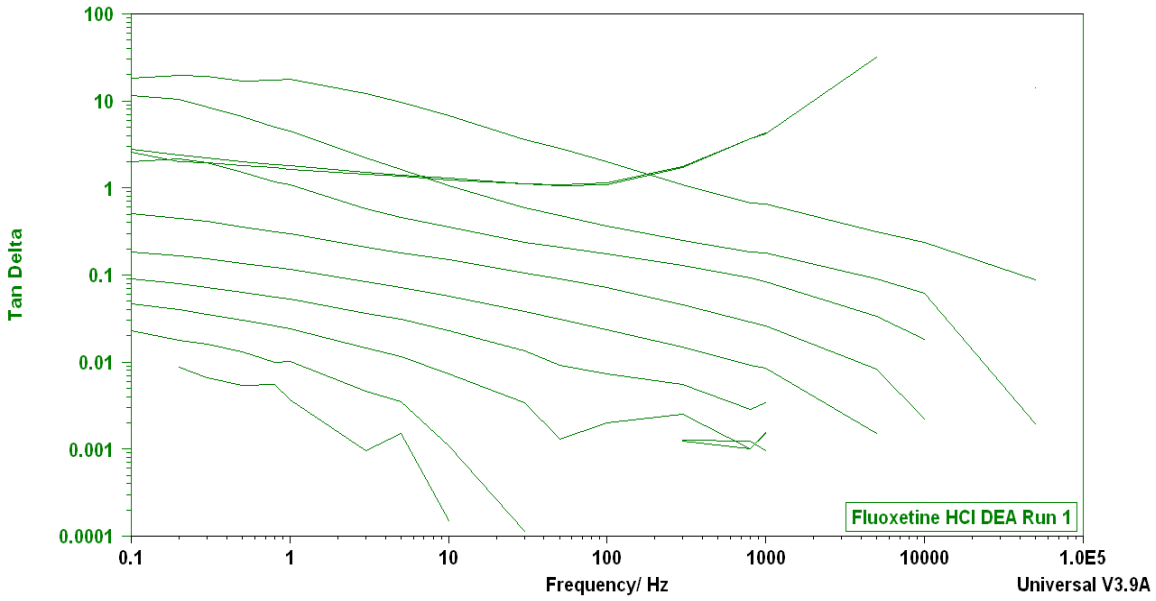

Figure 5.13. Tan Delta versus log frequency profile of Fluoxetine.HCl (DEA 1st run)

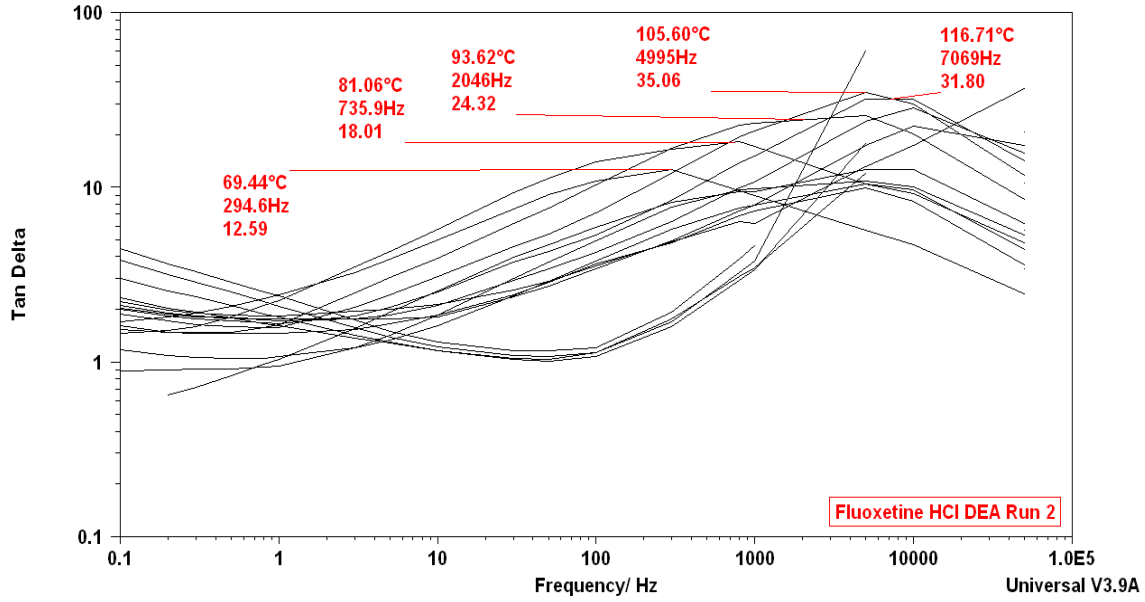

Figure 5.14. Tan Delta versus log frequency profile of Fluoxetine.HCl (DEA 2nd run)

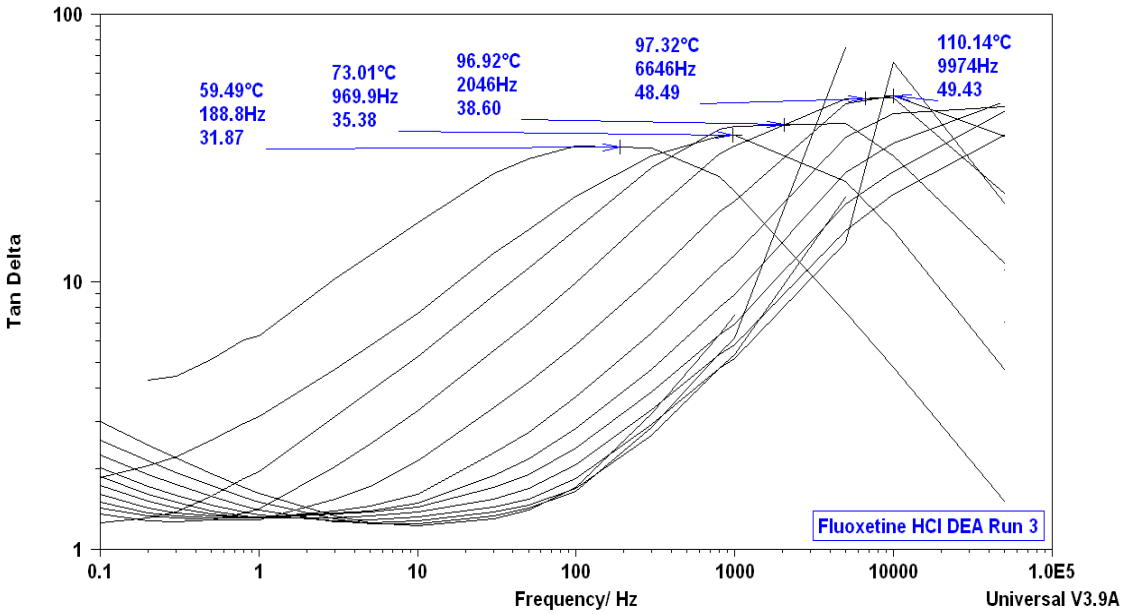

Figure 5.15. Tan Delta versus log frequency profile of Fluoxetine.HCl (DEA 3rd run)

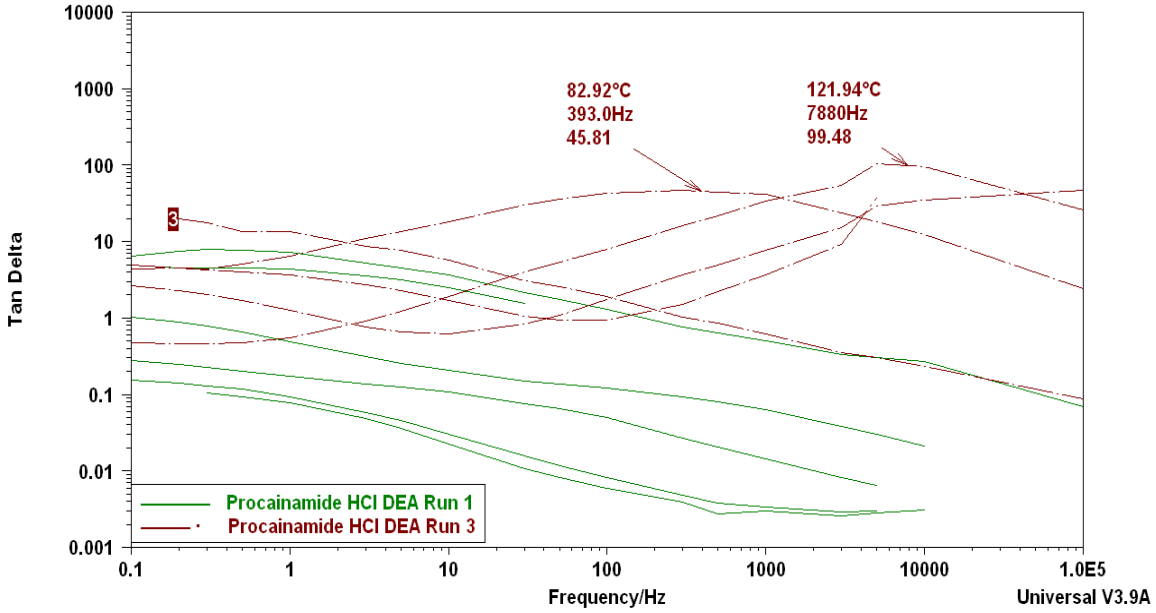

Figure 5.16. Overlay of Tan Delta versus log frequency profile of Procainamide.HCl (DEA 1st and 3rd runs)

5.6.4 Polarization times (ms). The polarization times for these drug salts were calculated from a Debye plot of tan delta (ε″/ ε′) vs. log frequency. These analyses demonstrate efforts to correlate the polarization (relaxation) properties to the molecular

structure and physical as well as electrical behavior. The polarization or response time to the AC electrical field produces a peak value where the loss factor is equal to the permittivity ($\varepsilon'' = \varepsilon'$) and the molecular mobility is enhanced. This enhanced molecular mobility behavior of the amorphous materials is thought to be the cause of their significant tendency towards crystallization, structural collapse, and chemical degradation. Studying the polarization times and the accompanying activation energy Ea (τ) gives us the opportunity to determine the effect of environment on the molecular mobility of the drug salts. We can also predict the storage stability or desirable shelf life of crystalline/amorphous pharmaceutical systems.

The polarization time for Fluoxetine.HCl DEA 1st run (crystalline solid) was 690 milliseconds. For Lidocaine.HCl and Procainamide.HCl the τ was 530 milliseconds indicating longer polarization times reflecting a stable material. The 2^{nd} and 3^{rd} DEA runs of the amorphous form of the drug salts exhibited a distribution of polarization times due to the dynamically heterogeneous nature of the amorphous state. However, a crystalline Quinapril.HCl after the first DEA run produced a τ of 0.320 milliseconds, shorter times for a crystalline drug salt is indicative of enhanced molecular mobility behavior. This change suggests a structural collapse or chemical degradation as the crystalline material becomes amorphous.

5.7 Conclusions

In the development of the solid pharmaceutical forms, quality control, stability and behavior of the materials are important parameters to ensure the final product quality. This study aids in the selection and evaluating the drug salt candidates by DEA and DSC techniques. Salts with advantageous properties are typically patentable as new chemical

entities. The relative amount crystalline/amorphous content in pharmaceutical solids can be clearly identified by DEA activation energy, Ea (k) [29]. The higher conductivity of the salt promotes better solubility and bioavailability characteristics. Evaluation of drugs by DEA yields to a more conducting amorphous phase with the HCl salt e.g. Lidocaine.HCl (10^6 pS cm^{-1}) and Lidocaine (10^5 pS cm^{-1}). The DSC melting profile of the salt form of Lidocaine (i.e. Lidocaine.HCl) had a higher melting temperature or a more stable phase. The first DEA run of the drug salts are more stable and of higher quality than the higher conducting amorphous 2^{nd} and 3^{rd} runs. A combination of DEA and DSC profiles can identify a vulnerable drug salt through decomposition (e.g. Hydralazine.HCl).

The identification of the pre-melt and melt ionic conductivities and activation energies for the drug salts appears to be a pathway for establishing the experimental conditions that can be used to modify the quality, stability and performance of the final drug product. We can predict the minimum activation energy Ea (k) attributed to charging ions or creating charge transfer complexes and activation energy Ea (τ) associated with charge mobility. The DEA properties described here can be further developed to estimate the storage stability or shelf life of the drug salts by Ea (τ) and polarization times. Stable drug salts by DEA evaluation renders an Ea (τ) that is constant in the 2^{nd} to the 3^{rd} DEA runs. The approaching stability of the amorphous phase relates that the Ea (τ) remains constant, as observed for Lidocaine HCl.

5.8 Acknowledgments

I want to thank Barbara Bryant (Office of Sponsored Programs and Research) Cleveland State University for her steadfast support in securing funds for my PhD research through DDREAFP.

5.9 References

1. Stahl PH, Wermuth CG (Eds). Handbook of Pharmaceutical Salts, Properties, and Use, IUPAC, Wiley-VCH, Verlag Helvetica Chimica Acta, Zürich 2002.
2. Berge SM, Bighley LD, Monckhouse DC. J. Pharm. Sci., 66 (1977) 1.
3. Bighley LD, Berge SM, Monckhouse DC. Salt forms of drugs and absorption. Encyclopedia of Pharmaceutical Technology, (Eds: J. Swarbrick, J.C. Boylan) Vol.13, Marcel Dekker, New York 1996, p. 453.
4. Gould PL, Int. J. Pharm., 33 (1986) 201.
5. Wells JI, Pharmaceutical Preformulation, Ellis Horwood Series in Pharmaceutical Technology, Chi Chester 1988.
6. Bastin RJ, Bowker MJ, Slater BJ, Organic Proc. Res. & Dev., 4 (2000) 427.
7. Koehler HM, Hefferren JJ. Mineral salts of lidocaine. J. Pharm. Sci., 53(9): 1126, 1964.
8. Haleblian J, J. Pharm. Sci., 64 (1975) 1269.
9. Giron D, Labo-Pharma, Probl. Techn., 307 (1981) 151.
10. Byrn SR, Solid State Chemistry of Drugs, Academic Press 1982.
11. Giron D, Thermochim. Acta, 248 (1995) 1.
12. Brittain HG, “Polymorphism in Pharmaceutical Solids”, Ed., Marcel Dekker 1999.

13. Giron D, S. T. P. Pharma, 4 (1988) 330.

14. Walkling WD, Sisco WR, Newton MP, Fegely BY, Plampin HN, Chrzanowski FA, Acta Pharm. Technol., 32 (1986) 10.

15. International Conference on Harmonization (ICH), Guideline Specification Q6A 1999.

16. Byrn S, Pfeiffer R, Ganey M, Hoiberg C, Poochikan G. Pharmaceutical solids: A stratergic Approach to Regulatory Considerations. Pharm. Res., 12(7): 945, 1995.

17. Agharkar S, Lindenbaum S, Higuchi T. Enhancement of solubility of drug salts by hydrophilic counter ions: Properties of Organic Salts of an Antimalarial Drug. J. Pharm. Sci., 65 (5): 747, 1976.

18. S. Miyazaki, M. Oshiba, T. Nadai. Precaution on Use of Hydrochloride Salts in Pharmaceutical Formulation. J. Pharm. Sci., 70(6): 594, 1981.

19. Paulekuhn GS, Dressman JB, Saal C. Trends in active pharmaceutical ingredient salt selection based on analysis of the orange book database. J. Med. Chem. 2007; 50: 6665-72.

20. Balestrieri F, Magri AD, Magri AL, Marini D,cSacchini A, Thermochim. Acta, 285 (1996) 337.

21. Glass BD, Novak Cs, Brown ME. J. Therm. Anal. Cal., 77 (2204) 1013.

22. Ksiazczak A, Ksiazczak T, Zielenkiewicz T, J. Therm. Anal. Cal., 77 (2004) 233.

23. Mashru RC, Sutariya VB, Sankalia MG, Yagnakumar P, J. Therm. Anal. Cal., 82 (2005) 167.

24. Xu F, Sun LX, Tan ZC, Liang JG, Zhang T, J. Therm. Anal. Cal., 83 (2006) 187.

25. Giron D, J. Therm. Anal. Cal., Vol. 73 (2003) 441- 457.

26. Riga A, Alexander KS. Electrical conductivity analysis/dielectric analysis differentiates physical chemical properties of drugs and excipients. Am Pharm Rev. 2005;8(6): 45–51.

27. Mantheni DR, Maheswaram MPK, Sobhi HF, Perera IN, Riga AT, Ellen Matthews M, Alexander K. Solid state studies of drugs and chemicals by dielectric and calorimetric analysis. J Therm Anal Calorim, 2011. DOI: 10.1007/s10973-011-1423-y.

28. Yoerg L, Ellen Matthews M, Kaza L, Perera IN, Ball David W, Moran J, Riga AT. Thermally- induced dielectric relaxation spectra in three aldohexose monosaccharides. J. Therm. Anal. Calorim. (2012) 108: 19-24.

29. Maheswarm MPK, Mantheni D, Perera IN, Venumuddala H, Riga A, Kenneth A. Characterization of crystalline and amorphous content in pharmaceutical solids by dielectric thermal analysis. J. Therm. Anal. Calorim, 2011. DOI: 10.1007/s10973-011-2140-2.

30. Zhou D, Zhang GGZ, Law D, Grant DJW, Schmitt EA. Physical stability of amorphous pharmaceuticals: Importance of configurational thermodynamic quantities and molecular mobility. J. Pharm. Sci., 2002; 91: 1863-1872.

31. Aso Y, Yoshioka S, and Kjima S. Moleculcar mobility based estimation of the crystallization rates of amorphous nifedipine and phenobarbital in poly (vinylpyrrolidone) solid dispersions. J. Pharm. Sci., 93: 384- 391 (2004).

32. Andronis V, Yoshioka M, and Zografi G. Effects of sorbed water on the crystallization of indomethacin from the amorphous state. J. Pharm. Sci., 86: 346-351 (1997).

33. Guo YS, Bryn SR, and Zografi G. Physical characteristics and chemical degradation of amorphous quinapril hydrochloride. J. Pharm. Sci., 89: 128- 143 (2000).

34. Bryn SR, Xu W, and Newman AW. Chemical reactivity in the solid-state pharmaceuticals: formulation implications. Adv. Drug Deliv. Rev. 48: 115- 136 (2001).

35. Pikal MJ, Shah S. The collapse temperature in freeze- drying – dependence on measurement methodology and rate of water removal from the glassy phase. J. Phys. Chem. 62: 165- 186 (1990).

36. Gunwan L, Johari GP, Shankar RM. Structural relaxation of acetaminophen glass. Pharm Res. 23: 967- 979, (2006). DOI: 10. 1007/s11095-006-9898-0.

37. J. Stoimenovski, D.R. MacFarlane, K. Bica, R. Rogers. Crystalline vs. ionic liquid salt forms of active pharmaceutical ingredients: A position paper. Pharmaceutical Research, Vol. 27, No. 4, April 2010. DOI: 10.1007/s11095-009-0030-0.

38. Riga A, Cahoon J, Pialet JW. Characterization of electrorheological processes by dielectric thermal analysis. In: Riga AT, Judovits L, editors. Materials characterization by dynamic and modulated thermal analytical techniques, ASTM STP 1402. West Conshohocken, PA: American Society for testing Materials; p 139 – 56, 2001.

39. Brown ME. Principles and practice. Handbook of thermal analysis and Calorimetry, Vol. 1. Amsterdam: Elsevier; 1998.

40. Matthews ME, Atkinson I, Lubaina Presswala, Najjar O, Nadine Gerhardstein, Wei R, Elizabeth Rye, Riga AT. Dielectric classification of D and L amino acids

by thermal analytical methods. J Therm Anal Calorim. 2008; 93:281–7.

41. L. Nunez-Regueira, S. Gomez-Barreiro and C. A. Gracia-Fernandez, "Study of the Influence of Isomerism on the Curing Properties of the Epoxy System DGEBA (n = 0)/1,2 DCH by DEA and MDSC," J. Therm Calorim, Vol. 82, No. 3, 2005, pp. 797-801. Doi: 10.1007/s10973-005-0966-1.

42. C. M. Kinart, W.J. Kinart, D. Checinska-Majak and A. Bald, "Densities and Relative Permittivities for Mixtures of 2-Methoxyethanol with DEA and TEA, at Various Temperatures," J. Therm Calorim, Vol. 75, No. 1, 2004, pp. 347-354. Doi: 10.1023/B: JTAN.0000017355.26845.a4

43. N. Zanati, M. E. Mathews, N. I. Perera, J. J. Moran, J. A. Boutros, A. T. Riga and M. Bayachou, "Cholesterol Levels and Activity of Membrane Bound Proteins: Characterization by Thermal and Electrochemical Methods," J. Therm Calorim., Vol. 96, No. 3, 2009, pp. 669-672. Doi: 10.1007/s10973-009-0032-5.

44. Shablakh M., Hill RM, Dissado LA. (1982) J. Chem. Soc., Farad. Trans. 2 78 625.

45. Perera IN, Maheswaram MPK, Mantheni D, Riga AT, " Dielectric Analysis of Response time in Electro-rheological Fluids Developed for Medical Devices," American Journal of Analytical Chemistry, 2011, 2, 85-92.

46. Duncan Q. M. Craig, "Dielectric Analysis of Pharmaceutical Systems, Taylor and Francis Pub. Bristol Pa., 1995; 123-144.

47. Bruno CH, Shamblin SL, "Molecular Mobility of amorphous pharmaceuticals determined using differential scanning Calorimetry." Thermochim. Acta. 380 (2001) 95-107.

48. Xu W. August 1997. Investigations of solid-state stability of selected bioactive compounds. Ph.D. Thesis. West Lafayette, IN: Purdue University.

CHAPTER VI

DIELECTRIC PROPERTIES OF PHARMACEUTICAL SOLIDS REVEAL UNIQUE AMORPHOUS CHARACTERISTICS: VALIDATED BY THERMAL, MICROSCOPIC AND X-RAY METHODS

6.1 Introduction

Diffraction techniques are the most defined methods for detecting and quantifying the crystalline and amorphous content in any pharmaceutical system. For example, Powder X-ray Diffraction Analysis (PXRD) of APIs and excipients gives a good observation of the crystalline phase. The diffraction planes of the given sample delineate the interplanar distances that identify the crystalline character. The area under the diffraction peaks, either a key intense peak or series of peaks, can be related to the % crystallinity. The amorphous content in this analysis is then measured by difference from 100% crystalline. Alternately, the amorphous phase is only seen as broad diffuse XRD bands. The area under the amorphous bands has been correlated to the amorphicity, but with a great deal of specific requirements per XRD pattern. Although, these methods only "observe" the molecular order, and the disorder in the system is predicted by the absence of the order [1]. Complications and errors in interpretation arise due to complex

scattering patterns of the sample, weak diffraction peaks, preferred crystal orientation, and optimized particle size so as not to contribute to line intensity broadening, and finally instrumental errors. The main disadvantage in using this approach is that it cannot differentiate surface/ bulk amorphicity.

Additional analytical techniques used to characterize amorphous pharmaceutical solids with thermal energy as the basic principle are DSC, IMC, and SC. DSC is the most relevant and significant method that is used to characterize the melting behavior, purity, glass transitions, crystallization, polymorphism, solid-solid transitions and chemical reactions of the drug including the detection of the amorphous content [2, 3]. DSC is performed by heating the sample through its melting point with linear heating rate of 2.0 to 10 $^{o}C\ min^{-1}$. As T_g is the characteristic property of amorphous material, the DSC scan of an amorphous or blend of crystalline/ amorphous material shows a glass transition, with crystallization exothermic peak, and melting endothermic peak [1, 2, 4]. Amorphous content is quantified in a sample by preparing a calibration curve using 100% amorphous and crystalline standards and their blends, and with their respective heats of fusion (ΔHf) and crystallization [2].

Using, $\mathbf{X_C\ (\%) = (\Delta H/\Delta H_o)*100}$ [1, 2, 4]

Where, ΔHis the Heat of fusion of the sample and ΔH_o is that of the 100% crystalline standard. Also, amorphous content can be calculated without the calibration curve using the equation:

Amorphous content = ΔHf amorphous /ΔHf crystalline

Where, **ΔHf amorphous** is heat of fusion of amorphous portion and **ΔHf crystalline** is the heat of fusion for the pure crystalline material.

Although proven, DSC technique shows several drawbacks: that it cannot differentiate surface vs. bulk amorphicity; thermal changes in the sample during the scan or given time after the scan; crystallinity is measured during the melting process. The key parameter for identifying the amorphous phase is the glass transition temperature. However, the amorphous content is only qualitatively related to the Tg and not quantitatively proportional to it. In order to obtain reliable results several variables like sample size, sample pan used (open or closed), and the thermal contact resistance between the sample pan and the DSC cell has to be considered.

It is well known that DSC melt properties are correlated to the structure of the drug, which can be validated by a variety of structural tools like PXRD [2, 5] and Scanning Electron Microscopy (SEM) [2]. Morphological and thermodynamic transitions in drugs as well as their amorphous and crystalline content in the solid state have been initiated by thermal analytical techniques, which include Dielectric Analysis [3, 5].

The primary aim of this study is to achieve the amorphization of the APIs Clopidogrel hydrogen sulfate [6] and Quinapril.HCl [7] by solvent evaporation method. A further aim is to characterize the crystalline and amorphous content in these APIs by the DEA activation energy method. Finally, the dielectric science developed to understand the crystalline and amorphous components in pharmaceuticals would be validated by Calorimetry, X-ray diffraction and scanning electron microscopy.

6.2 Materials and Experimental Procedure

6.2.1 Materials. The following drugs were evaluated in this study: Lidocaine.HCl (T_m, 74°-79°C), Sulfapyridine (T_m, 192°C), Indomethacin (T_m, 155°C), Quetiapine

fumarate (Seroquel®) (T_m, 173°C), Procainamide.HCL (T_m, 169°C), Clopidogrel hydrogen sulfate (T_m, 177.4 °C), Quinapril.HCl (T_m, 120-130 °C).

6.2.2 Preparation of amorphous form of a drug

6.2.2.1Clopidogrel Hydrogen sulfate (CHS). Amorphous samples were made using ethanol. 100 mg of CHS was dissolved in sufficient amount of ethanol with magnetic stirrer for 5 min at room temperature [6]. The solvent was evaporated by two methods: with blown room temperature air or by vacuum. After drying, samples were pulverized in a porcelain mortar with a pestle. DEA, DSC, PXRD and SEM techniques were used to characterize the amorphous and crystalline forms of Clopidogrel hydrogen sulfate.

6.2.2.2 Quinapril.HCl (Q.HCl). Q.HCl was dissolved in a minimum amount of dichloromethane required to form a solution [7]. The solvent was removed initially using a rotary evaporator under vacuum at room 30^{o} C, and the residue was dried under vacuum for 24 hrs. DEA, DSC, PXRD and SEM techniques were used to characterize the amorphous and crystalline forms of Q.HCl.

6.2.3 Experimental procedure.

6.2.3.1 Differential scanning calorimetry. DSC studies were performed with a TAI 2920 DSC instrument with samples of approximately 5-10 mg weighed into non-hermetically sealed pans. The samples were heated from room temperature to 20 ^{o}C above the peak melting temperature at a heating rate of 10 ^{o}C/min. The instrument was calibrated with use of indium.

6.2.3.2 Dielectric analysis. A TAI 2970 DEA (TA Instrument) was used to determine the electrical conductivity for each drug studied. Sample of approximately 20

mg was placed on a single surface gold ceramic interdigitated sensor. The samples were ramped at a rate of 10 ^{o}C min-1 from room temperature to 20 ^{o}C above the melting temperature of the drug. The conductivity measurements were recorded at controlled interval frequencies ranging from 0.10 to 10,000 Hz for all temperatures.

6.2.3.3 X-ray powder diffraction (PXRD). XRD patterns were obtained using an X'Pert PRO MPD system (X-ray Diffractometer Phillips). Where the tube anode was Cu with Kα1= 1.5408 Å. The pattern was collected at a tube voltage of 45kV and a tube current of 35 mA in step can mode. Angle range: 10^{o} to 80^{o} 2Θ. The data were evaluated with origin software or JADE software. The powder diffraction files come from the International Center for Diffraction Data (ICDD).

6.2.3.4 Scanning electron microscopy. The surface morphology of various amorphous drug samples was investigated using an Amray 1830 scanning electron microscope. The dry powder was mounted onto metal stubs by applying silver paint onto the metal stubs. The drug sample was sprinkled on the silver paint and then it is dried. Then the samples are vacuum-coated with a platinum film using a gold sputter coater unit.

6.3 Results and Discussion

We tested the applicability of the novel activation energy method for quantifying crystalline and amorphous content with several other pharmaceutical solids including the amorphous forms of the API prepared by solvent evaporation methods e.g., Clopidogrel hydrogen sulfate and Quinapril.HCl. The DEA results obtained from the activation energy method for all the drugs studied were validated with other established methods, e.g., DSC, PXRD and SEM analysis.

6.3.1 DEA study. The comparison of four runs of Clopidogrel hydrogen sulfate by DEA and DSC are overlayed in Figure 6.1. The ionic conductivity in crystalline and amorphous samples as a function of temperature were used to calculate the activation energy from 0.1-10,000 Hz (first and second runs) [8, 9]; Clopidogrel HS pure amorphous sample DEA run overlays the DEA amorphous run 2; DSC Tm = 176.11^{o}C, Tmp = 179.42 ^{o}C, Heat of fusion = 81.33 J/g. Therefore, the DEA 2nd run was the same as the 1st run prepared out of the DEA i.e., the sample prepared with ethanol by solvent evaporation method, was amorphous. To confirm that the prepared sample was amorphous, a DSC analysis was performed (See Figure 6.2). The characteristic melting point disappeared completely from the DSC curve; a Tg [10] was observed. The resulting Tg was at 89 ^{o}C and the ΔCp at Tg was 0.256 J/g/C. The result confirms the presence of the amorphous form by DEA and DSC.

Figure 6.3. shows the DEA surface analysis profile for Clopidogrel hydrogen sulfate at 0.1 Hz.

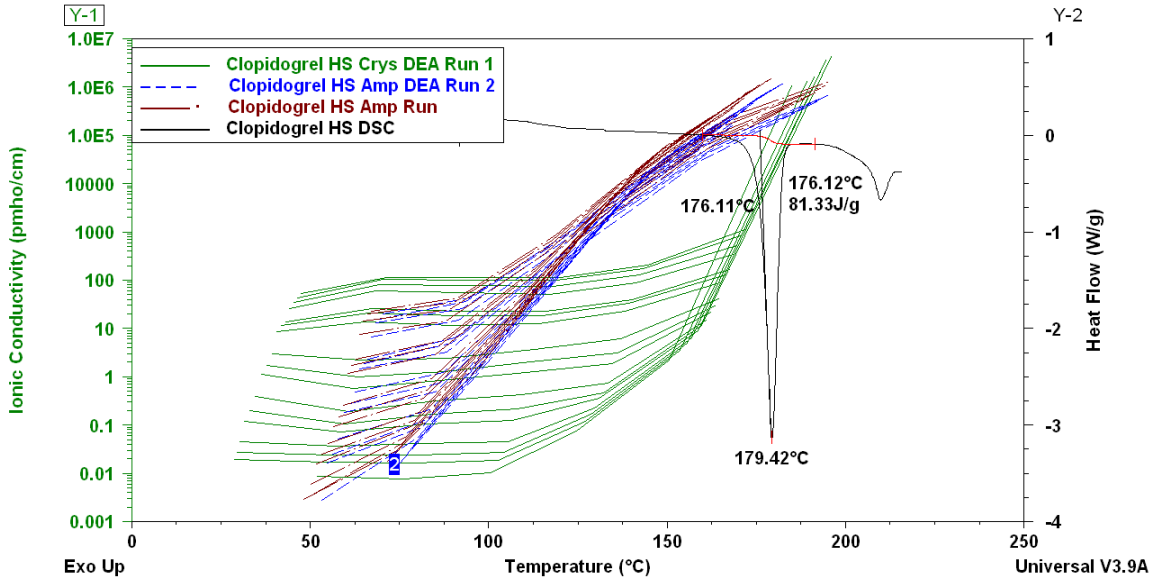

Figure 6.1. DEA and DSC curve overlay of Clopidogrel hydrogen sulfate. DEA 1st run Crystalline (Green) and 2nd run Amorphous (Blue); DEA 1st run pure amorphous form (Prepared (Brown)

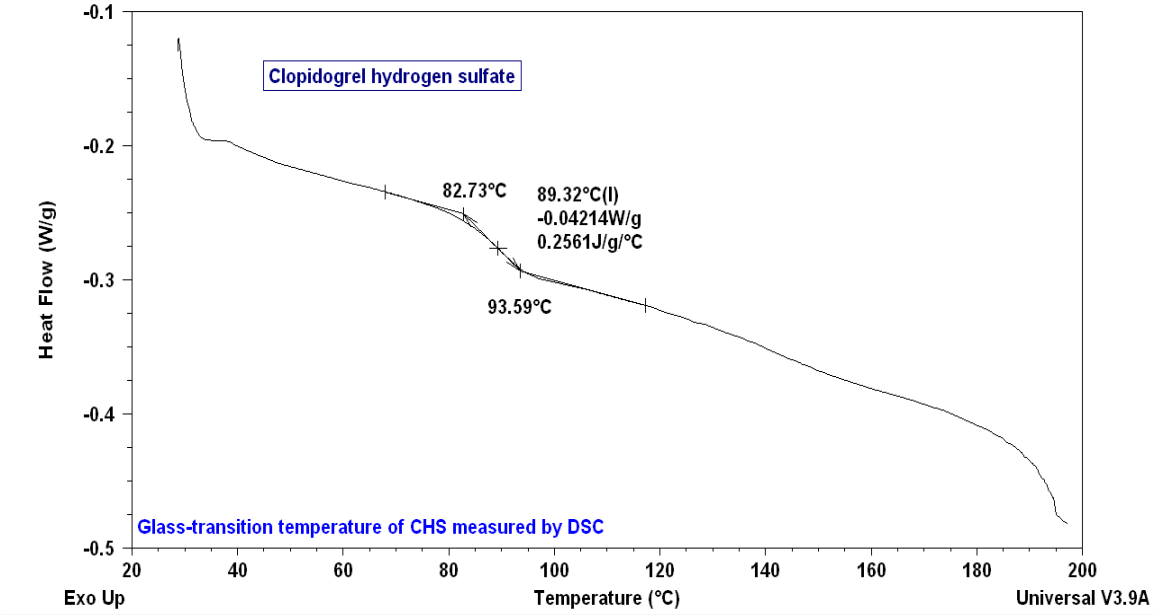

Figure 6.2. Glass transition temperature of Clopidogrel hydrogen sulfate measured by DSC; Tg = 89.32^{o} C

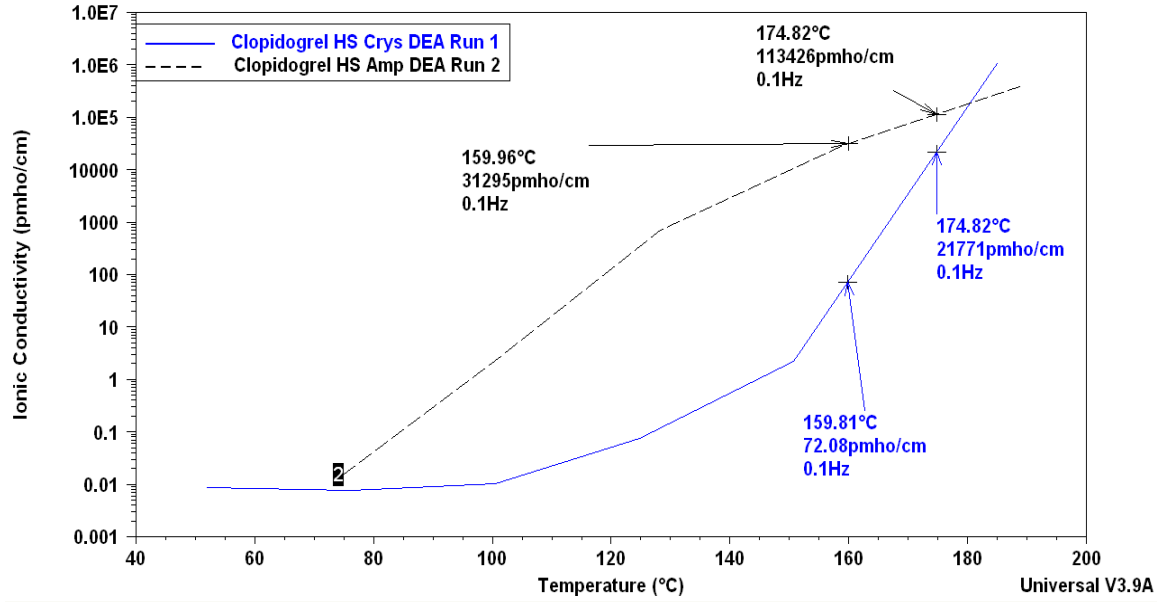

Figure 6.3. Clopidogrel hydrogen sulfate DEA curve overlay of crystalline and amorphous sample by activation energy method surface analysis at 0.1 Hz (first and second runs)

Table 1 identifies the activation energies for Clopidogrel hydrogen sulfate (Ea in J/mol) with the higher value for the crystalline form (DEA 1st run) and a significantly lower value for the amorphous form (DEA 2nd run). For the 2nd run at 0.1, 0.5, and 1.0 Hz the amorphous sample content was 76-78% (See Table 2).

Table 1

Clopidogrel hydrogen sulfate DEA activation energy (J/mol), % crystalline, and % amorphous content for first and second runs at 0.1, 0.5, and 1 Hz frequencies

Clopidogrel hydrogen sulfate	Frequency/ Hz	DEA Run	Ea/ $Jmol^{-1}$	% Crystalline content	% Amorphous content
Crystalline	0.1	1	622	100	0
Amorphous	0.1	2	138	22	78
Crystalline	0.5	1	576	100	0
Amorphous	0.5	2	136	24	76
Crystalline	1	1	576	100	0
Amorphous	1	2	138	24	76

Table 2 summarizes Clopidogrel hydrogen sulfate DEA activation energies for the pure crystalline form and the pure amorphous form, for Run1 at 0.1, 0.5 and 1.0 Hz.

Table 2

Clopidogrel hydrogen sulfate DEA activation energy (J/ mol), % Crystalline, and % amorphous content for first run crystalline sample and first run pure amorphous sample

Clopidogrel hydrogen sulfate	Freq/ Hz	Run	Ea/ J mol^{-1}	% Crystalline Content	% Amorphous Content
Crystalline	0.1	1	622	100	0
Amorphous (Pure)	0.1	1	138	22	78
Crystalline	0.5	1	576	100	0
Amorphous (Pure)	0.5	1	130	23	77
Crystalline	1	1	576	100	0
Amorphous (pure)	1	1	127	22	78

Quantification of crystalline and amorphous drug content of Clopidogrel hydrogen sulfate by DEA activation energy method is summarized in **Table 3.** The activation energies for the DEA amorphous form of the drug (2^{nd} run) correlate with activation energies for the pure amorphous form prepared with ethanol (1^{st} run). The average content of the DEA 1^{st} run for the pure amorphous form prepared with ethanol was 22% crystalline and 78% amorphous (0.1- 1.0 Hz). For the 2^{nd} run of DEA amorphous form the average content was 23% crystalline and 77% amorphous (0.1-1.0Hz).

Table 3

Quantification of crystalline and amorphous drug content of Clopidogrel hydrogen sulfate by DEA activation energy method

Drug	Average content of DEA first run (pure Amorphous Form) at 0.1, 0.5, and 1.0 Hz	
	% Crystalline content	% Amorphous content
Clopidogrel hydrogen sulfate	22	78

The summary table 4 describes the average value of the content, both % crystalline and amorphous, for the drugs studied by DEA activation energy method, at various frequencies for the 2nd and 3rd DEA runs.

Table 4

Quantification of crystalline and amorphous drug content of various pharmaceutical APIs by the DEA activation energy method

Drugs	Average content of second and third DEA runs at 0.1, 0.5, and 1.0 Hz	
	% Crystalline content	% Amorphous content
Clopidogrel hydrogen sulfate	23	77
Quinapril HCl	35	65
Quetiapine Fumarate	11	89
Lidocaine.HCl	22	78
Sulfapyridine	19	81

6.3.2 DSC study. A well-established tool for pharmaceutical analysis is DSC, which can examine the degree of fusion and crystallization of an API. The heat of fusion (J/g) associated with the first DSC examination of the crystalline API (run 1) is recorded. The thermal analysis curve represents a physical chemical property of the sample drug, i.e., melting. Cooling of the API sample after melting through the crystallization yields the temperature and heat of crystallization (J/g). This cooling DSC data is a measure of the amount of sample recrystallized.

The ratio of the heat of crystallization divided by the heat of fusion times 100 is the % crystalline and the difference is the % amorphous content. For example, Sulfapyridine melts at a 192 ^{o}C (run 1) and crystallized at 123 ^{o}C (run 2) in the DSC Cooling cycle. The measured heat of fusion was 174 J/g and heat of crystallization was 57 J/g, see Figure 6.4. Therefore the recrystallized sample contained 33% crystalline and 67% amorphous material. The % amorphous by DEA activation method is 81% and by this DSC heat-cool method is 67% amorphous. The other drugs analyzed by the DSC heating and cooling cycles are listed in the Table 5.

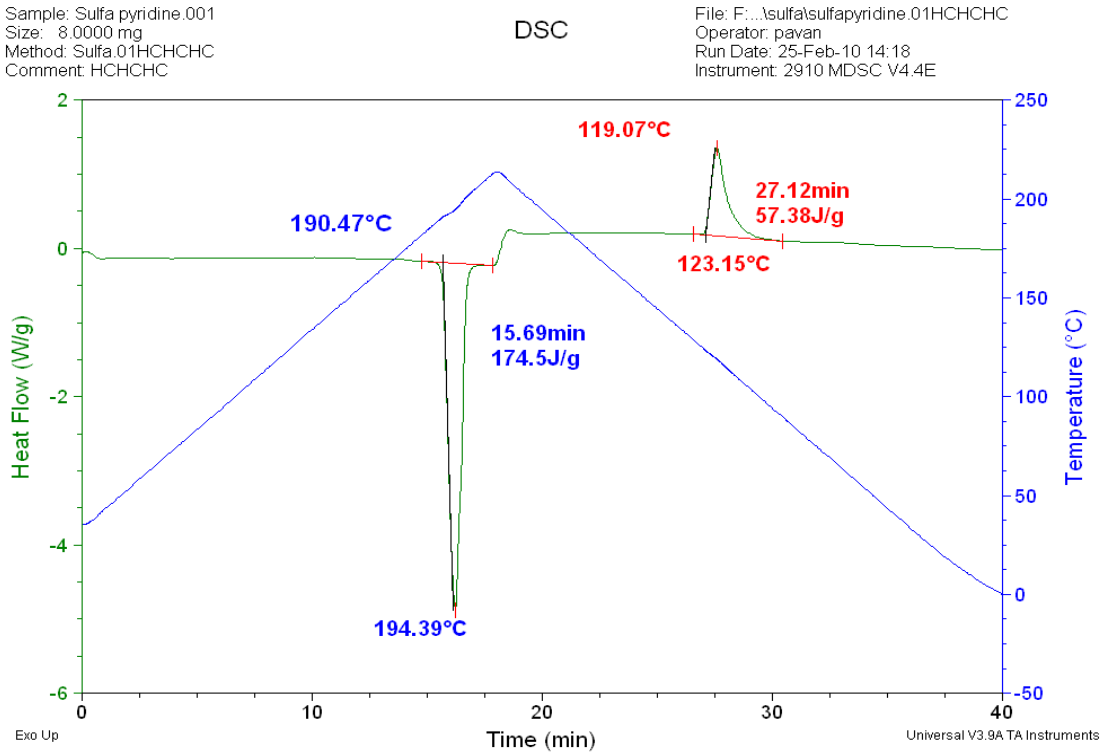

Figure 6.4. DSC curve of Sulfapyridine showing Heat-Cool cycle; Tm = 191oC, Tmp =194.39^{o} C, Heat of Fusion = 174 J/g; Heat of Crystallization = 57 J/g, Tmc=119^{o}C, Tmpc = 123^{o} C

6.3.2.1 Confirmation of amorphous form by DSC. Prepared amorphous sample i.e., Clopidogrel hydrogen sulfate amorphous was measured primarily by DSC. Characterization of amorphous form by DSC is quick and easy. The pure crystalline forms of both the drugs were tested at first by DSC (see Figure 6.1). The crystalline Clopidogrel hydrogen sulfate melted at 176.11^{o} C. The Heat of Fusion was 81.33 J/g. The samples prepared in ethanol, dried in vacuum were transformed to the amorphous form. The characteristic melting point disappeared completely from the DSC curves of the amorphous form. The glass transition temperature is a very important parameter for amorphous materials. Approximately for the all the amorphous materials the Tg is usually observed at 2/3 to 4/5 of Tm (in Kelvin) [6]. The melting point of crystalline

Clopidogrel hydrogen sulfate is 176.11^{o}C (449.11 K). Accordingly, the expected Tg for Clopidogrel hydrogen sulfate is the temperature interval of 26.4 - 86.2 ^{o}C.

The DSC curve reveals all the structural changes accompanied by enthalpy changes. The Tg is usually indicated by a step in the DSC curve. However, for the first heat cycle of Clopidogrel hydrogen sulfate Tg could not be detected. The Tg was observed or appeared in the 2nd heating curve of DSC (see Figure 6.2). The resulting Tg was at 89^{o} C and the ΔCp at Tg was 0.256 J/g/C.

Quinapril.HCl amorphous sample was prepared by solvent evaporation method. The solvent used to prepare the amorphous sample was dichloromethane. DSC was used to determine the physical properties i.e., the glass transition temperature. For the amorphous Quinapril.HCl the Tg was observed at 79 – 85 ^{o}C for the first and the second heating cycle respectively. The melting point of crystalline Quinapril.HCl was 104 ^{o}C and Heat of fusion = 25J/g. The other drugs analyzed by the DSC heating and cooling cycles are listed in the Table 5.

Table 5

Summary of DSC heat-cool method for all the drugs studied

Drugs	Tm ^{o}C	Heat of Fusion ΔHf (J/g)	Heat of crystallization ΔHc (J/g)	% Crystalline	% Amorphous	Comments
Lidocaine.HCl	79	201	Tg = 17^{o}C	-	-	Amorphous
Sulfapyridine	192	174	57, Tg = 61-62^{o}C	33	67	Semicrystalline &Amorphous (2^{nd} Heat Cycle)
Quetiapine Fumarate	173	124	Tg = 44-49^{o}C	-	-	Amorphous
Indomethacin	155	127	Tg = 42-47 ^{o}C	-	-	Amorphous
Quinapril.HCl	104	25	1^{st} run Tg = 79 ^{o}C & 2^{nd} run Tg = 85^{o}C	-	-	Amorphous
Clopidogrel hydrogen sulfate	179	81	2^{nd} Heating Tg = 89 ^{o}C	-	-	Amorphous
Procainamide.HCl	169	83	Tg = 47 ^{o}C	-	-	Amorphous

6.3.3 Powder x-ray diffraction (PXRD) analysis.

6.3.3.1 Methodology. X-ray Diffraction Analysis (XRD) is a structural tool to identify APIs based on their molecular structure. Each drug has its own unique crystal structure. If single crystal diffraction data is appropriately available the exact space group structure can be determined clearly distinguishing it from most other structures. The complex structure of pure drugs yields to an API crystal system probably an orthorhombic, monoclinic or triclinic system. Most drugs analyzed by Wide Angle XRD (WAXRD) can be viewed as multiple sharp intense peaks (half peak maxima typically 0.3^{o} 2Θ) delineating their highly crystallinity nature. Contrary to the multiple sharp peaks are the broad XRD bands (half maxima of 5-10^{o} 2Θ) typical of amorphous materials. Therefore, a sharp peak spectrum is a crystalline material and a broad diffuse peak spectrum is an amorphous material.

All drugs examined by PXRD were first evaluated by DEA and then sampled for PXRD.

6.3.3.2 Confirmation of Clopidogrel hydrogen sulfate and Quinapril.HCl amorphous form by PXRD. The Clopidogrel hydrogen sulfate (CHS) and Quinapril.HCl (Q.HCl) amorphous samples were tested by PXRD measurement. Diffractograms are can be seen in (Figure 6.5) and (Figure 6.6) respectively. The investigation supported the DSC results throughout for both Clopidogrel hydrogen sulfate and Quinapril.HCl. Figure 6.5 shows that the products prepared with ethanol for Clopidogrel hydrogen sulfate and dichloromethane for Quinapril.HCl (see Figure 6.6) were converted to the amorphous form, because the peaks disappeared from the diffractograms, and the spectra became smooth. The DSC and the PXRD results suggested that samples prepared by solvent

evaporation method for both the crystalline drugs i.e., CHS and Q.HCl were transformed to the amorphous form.

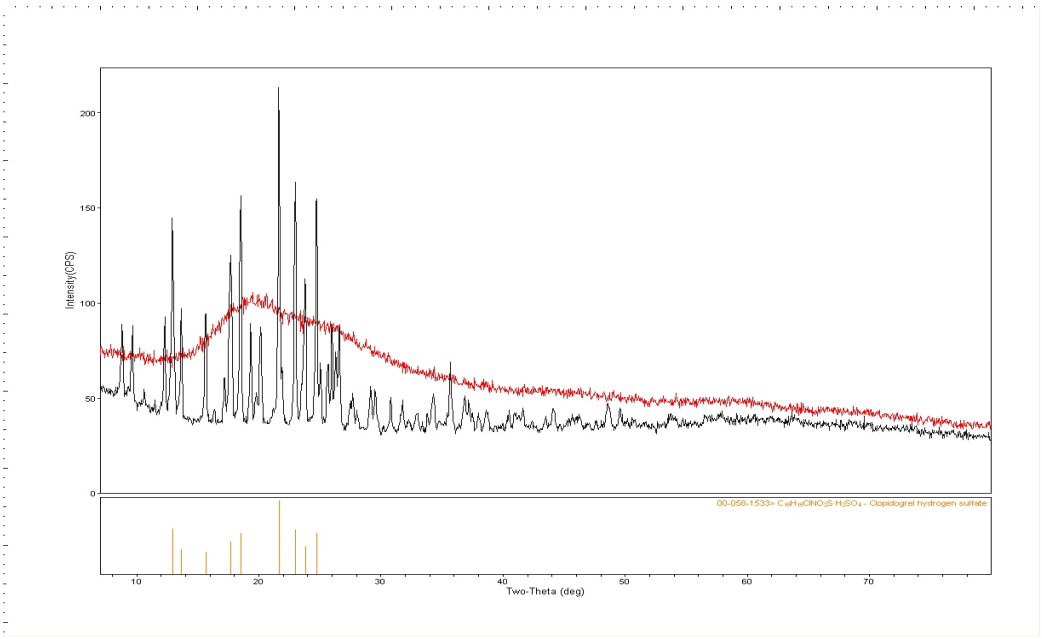

Figure 6.5. Clopidogrel hydrogen sulfate samples measured by PXRD. (A) Crystalline form, (B) Amorphous sample prepared with ethanol, dried under vacuum, (C) ICDD diffractogram of Clopidogrel hydrogen sulfate (bottom curve)

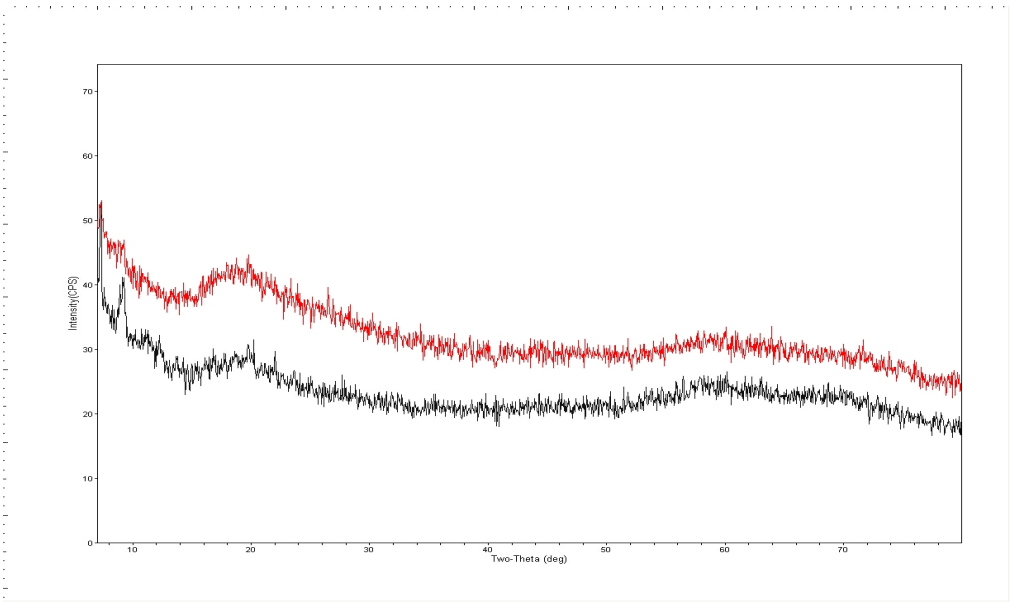

Figure 6.6. PXRD diffractograms of different batches of Quinapril.HCl amorphous forms. Amorphous samples prepared with dichloromethane, dried under vacuum

Indomethacin was initially crystalline and after either quench cooling or heating it in the DEA and cooling to room temperature became amorphous. This behavior was also observed in the diffractogram of the amorphous Indomethacin with broad diffuse XRD bands. The diffractograms of pure crystalline and amorphous forms of Indomethacin is shown in Figure 6.7. The indomethacin diffractogram shows that the sample that was heated in the DEA was amorphous, because the peaks disappeared from the diffractograms of the amorphous Indomethacin sample, and the spectra became smooth. Likewise, Lidocaine.HCl, Quetiapine fumarate, Sulfapyridine (Figure 6.8), Quinapril.HCl and Clopidogrel hydrogen sulfate all became totally amorphous after the DEA first run. Also, PXRD analysis aided the determination of the amorphous/crystalline form whether it was a surface vs. bulk identification by DEA activation energy method.

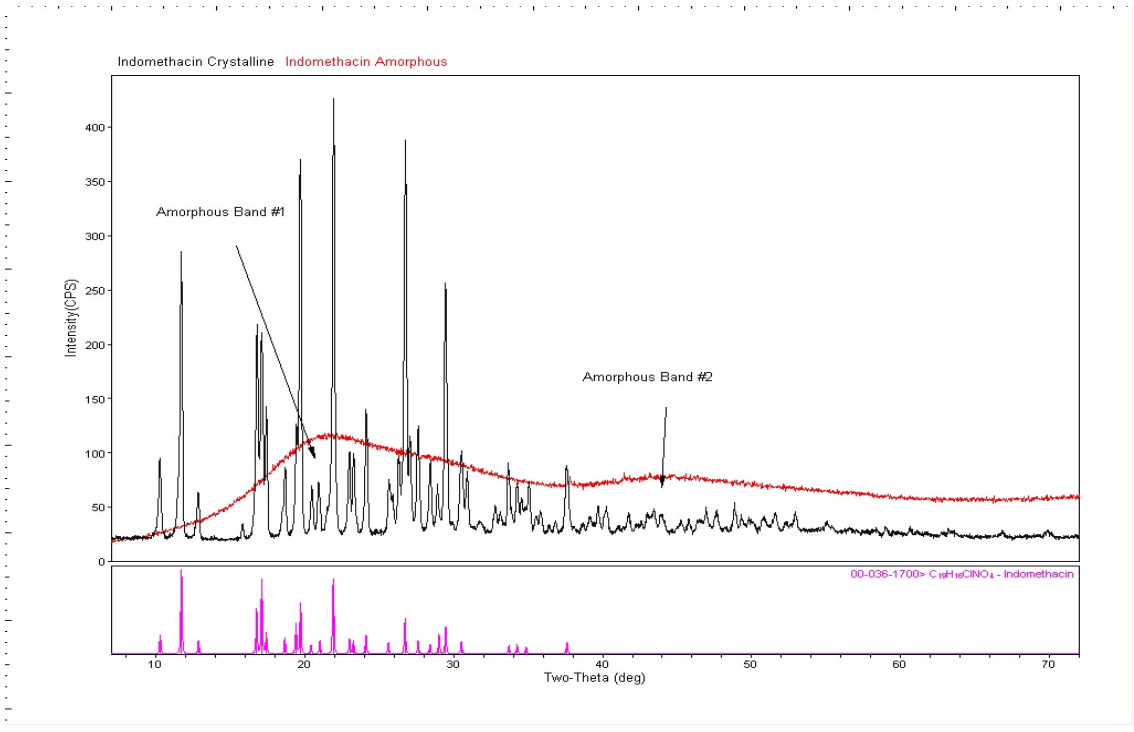

Figure 6.7. PXRD diffractograms of Indomethacin Crystalline and Amorphous forms. Amorphous sample analyzed on DEA, Bottom curve (ICDD)

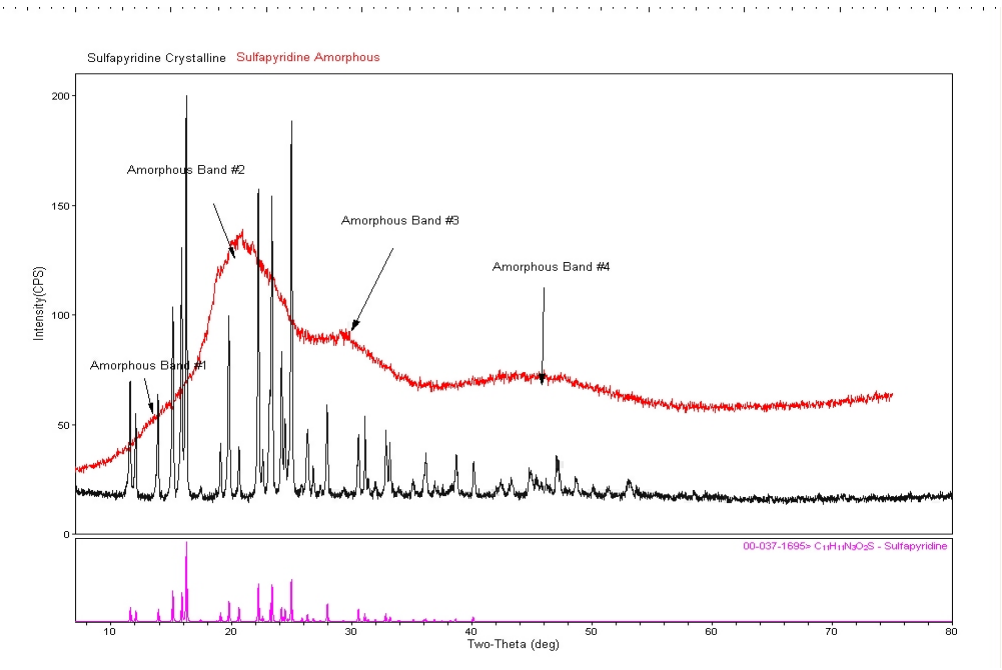

Figure 6. 8. PXRD of Sulfapyridine Crystalline Form and DEA amorphous form, bottom curve (ICDD)

The summary of all the drugs, their identity (ICDD), distribution of crystalline peaks and amorphous bands is elucidated in Table 6.

Table 6

Summary of all the drugs, their identity (ICDD), distribution of crystalline peaks and amorphous bands

PXRD Peak Values 2 Θ / Cu Kα Radiation									
Drugs	Identity ICDD	Crystalline Peaks				Amorphous Bands			
Lidocaine.HCl	Yes	10	12	15	16, 21, 25, 27	17	25	37	50
Sulfapyridine	Yes	11	12	15	16, 20, 22,23,24, 25, 28	16	21	28	45
Quetiapine Fumarate (Seroquel) ®	Yes	15	16	20	21, 22, 23, 25	16	22		45
Procainamide. HCl	Yes	16	17	19	21, 24, 26, 29, 30		28		46
Clopidogrel hydrogen sulfate	Yes	13	15	18	19, 21, 23, 24, 25	19	26	45	57
Quinapril.HCl (Accupril)®	Yes	8	12	14	18, 22, 23, 25	18			58
Indomethacin	Yes	11	17	20	22, 27, 29, 31		22	29	50

6.3.4 Scanning electron microscopy study.

6.3.4.1 Clopidogrel Hydrogen Sulfate. SEM photomicrographs obtained for a pure crystalline form of Clopidogrel Hydrogen Sulfate (CHS) and an amorphous form of CHS are shown in (Figure 6.9 and Figure 6.10) in selected magnifications. From the photomicrograph of pure drug CHS; it is clear that the drug was present as irregularly shaped beads and aggregate structures confirming the crystal nature of the material as seen by DEA, DSC, PXRD data analyses.

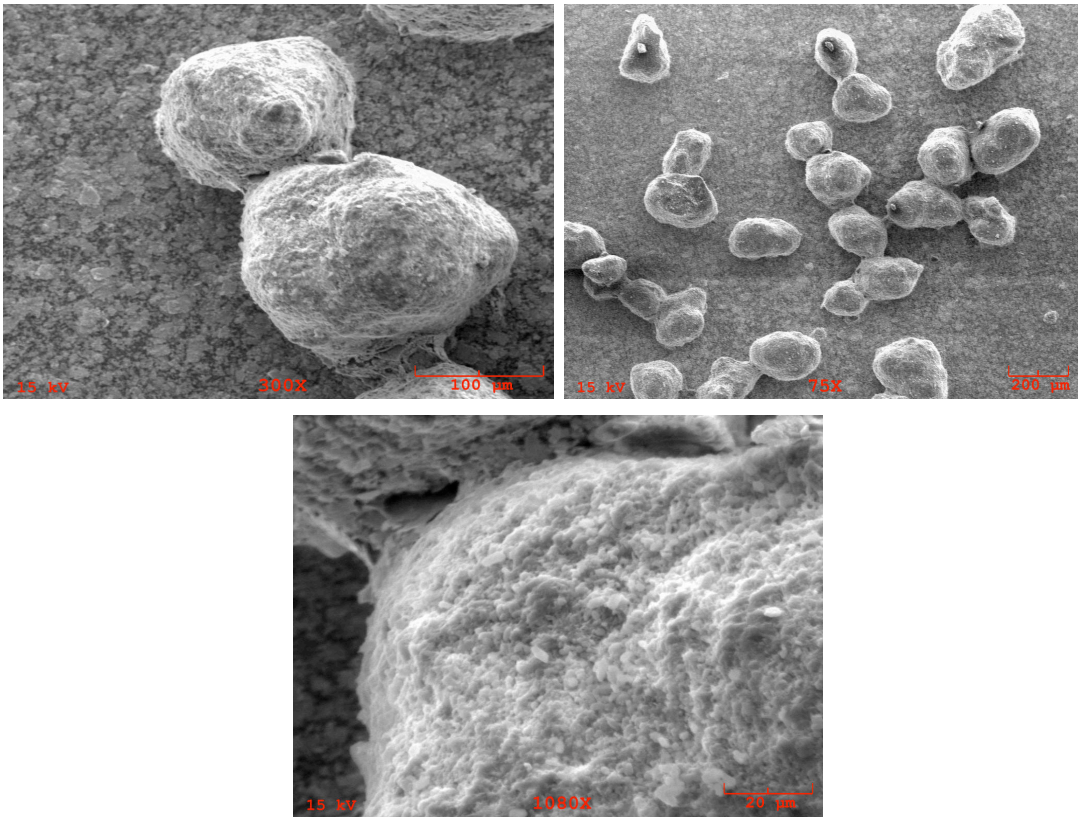

Figure 6.9. SEM photomicrographs of pure crystalline drug Clopidogrel Hydrogen Sulfate at (a) 75X (top left); (b) 300X (top right) and (c) 1080X (bottom); 15 KV

The CHS amorphous form by SEM was identified as a flexible soft structure and as layered plates or a round structure as soft scales (see Figure 6.10). The DSC and DEA

as well as PXRD analysis of the CHS amorphous material correlates with the SEM images.

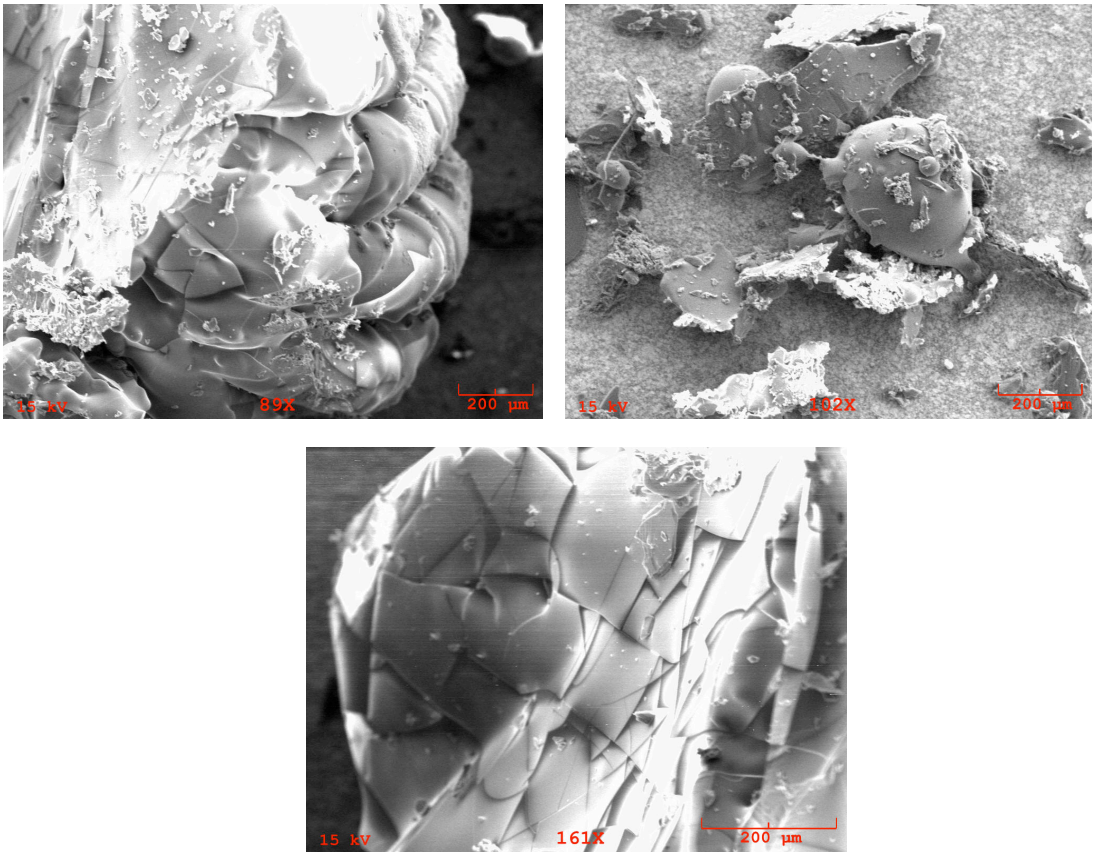

Figure 6.10. SEM photomicrographs of amorphous forms of Clopidogrel Hydrogen Sulfate at (a) 89X (top left); (b) 102X (top right) and (c) 161X (bottom); 15 KV

6.3.4.2 Quinapril.HCl . SEM photomicrographs obtained for pure crystalline forms of Quinapril.HCl (Q.HCl) and an amorphous form of Q.HCl are shown in (Figure 6.11 and Figure 6.12) in selected magnifications. From the photomicrographs of pure drug Q.HCl; it is clear that the drug was present as a rod-like structure (1260X), overlayed rods (200X) and an aggregate like structure at 100X. SEM photomicrographs of the amorphous forms of Quinapril.HCl are viewed in Figure 6.12. The droplet-like structures were apparently amorphous and underwent fluid flow.

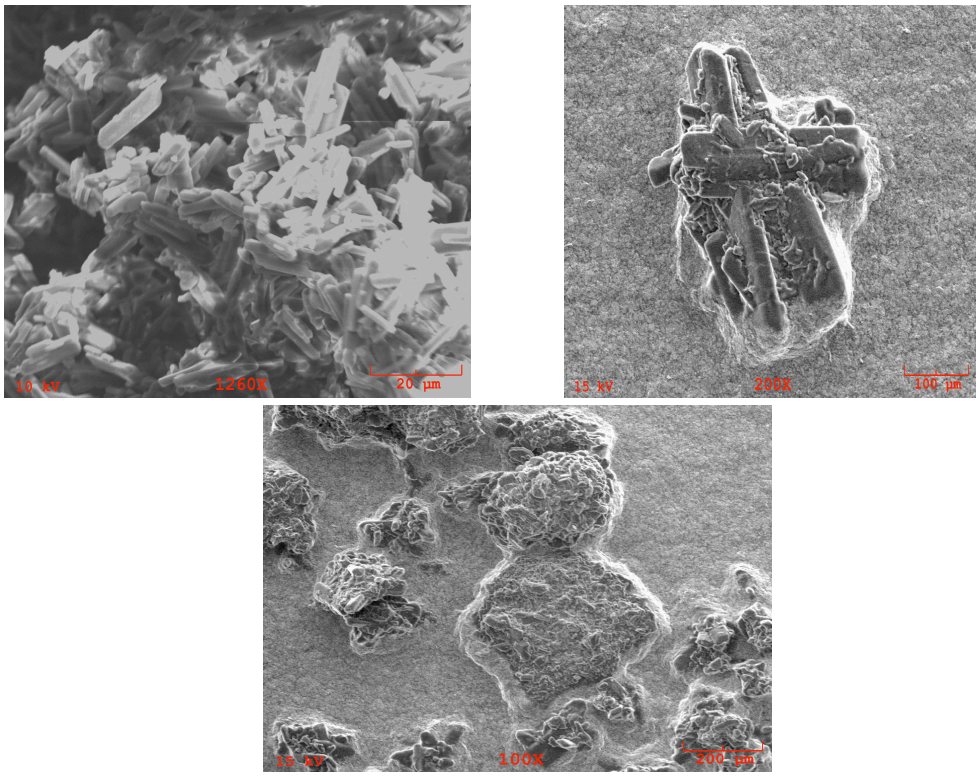

Figure 6.11. SEM photomicrographs of pure crystalline drug Quinapril.HCl at (a) 1260X (top left); (b) 200X (top right) and (c) 100X (bottom); 15 KV

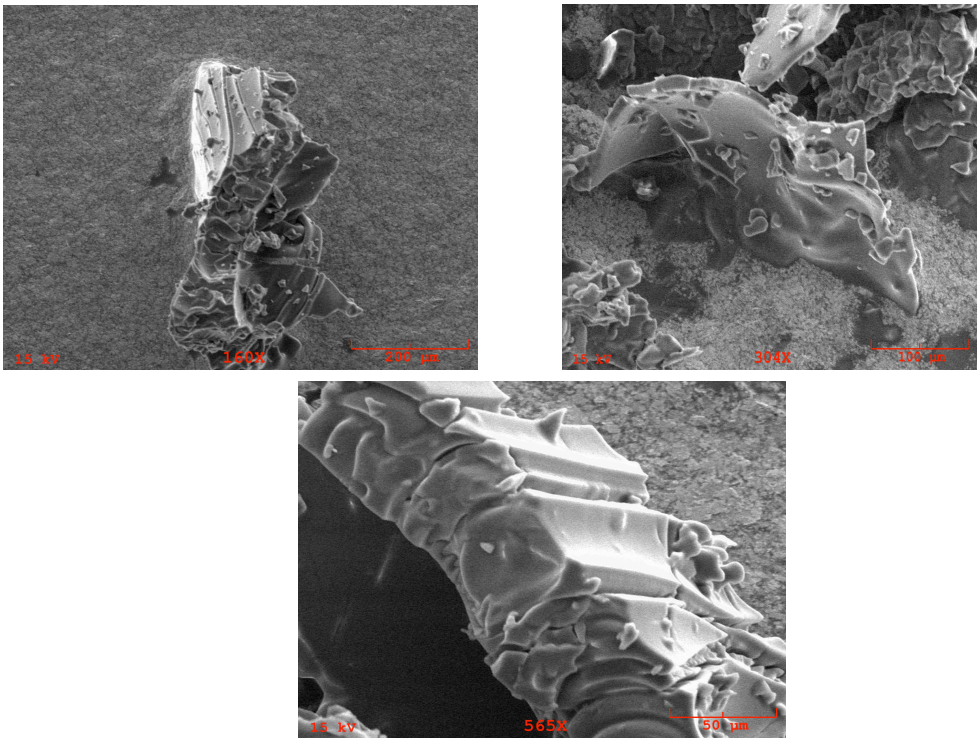

Figure 6.12. SEM photomicrographs of amorphous forms Quinapril.HCl at (a) 160X (top left); (b) 304X (top right) and (c) 565X (bottom); 15 KV

6.3.4.4 Quetiapine fumarate (Seroquel). SEM photomicrographs obtained for pure crystalline form of Quetiapine Fumarate (Seroquel) and an amorphous form of Quetiapine Fumarate (Seroquel) are shown in (Figure 6.13 and Figure 6.14) at selected magnifications. From the photomicrographs of pure crystalline drug we can clearly differentiate the amorphous form of the drug, where the structures are smooth, and no distinct edges as well as appeared to have smooth surfaces.

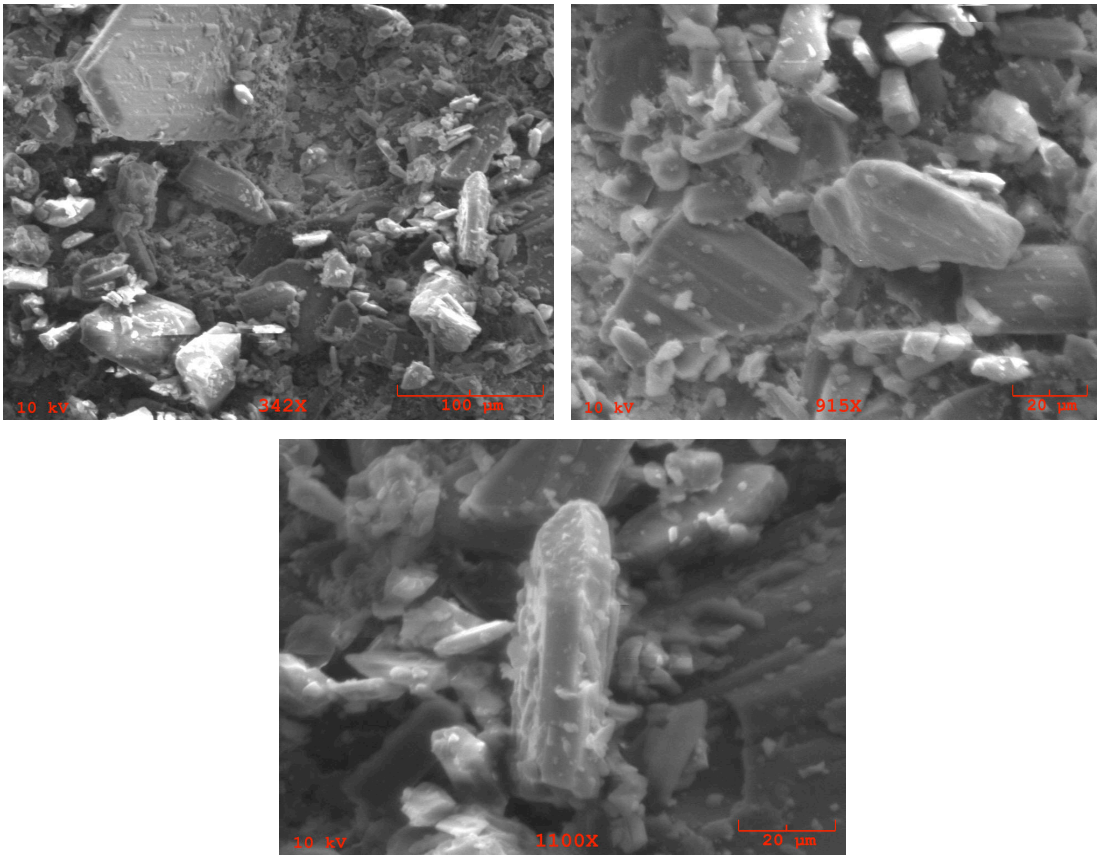

Figure 6.13. SEM photomicrographs of pure crystalline drug Quetiapine Fumarate (Seroquel) at (a) 342X (top left); (b) 915X (top right) and (c) 1100X (bottom); 10 KV

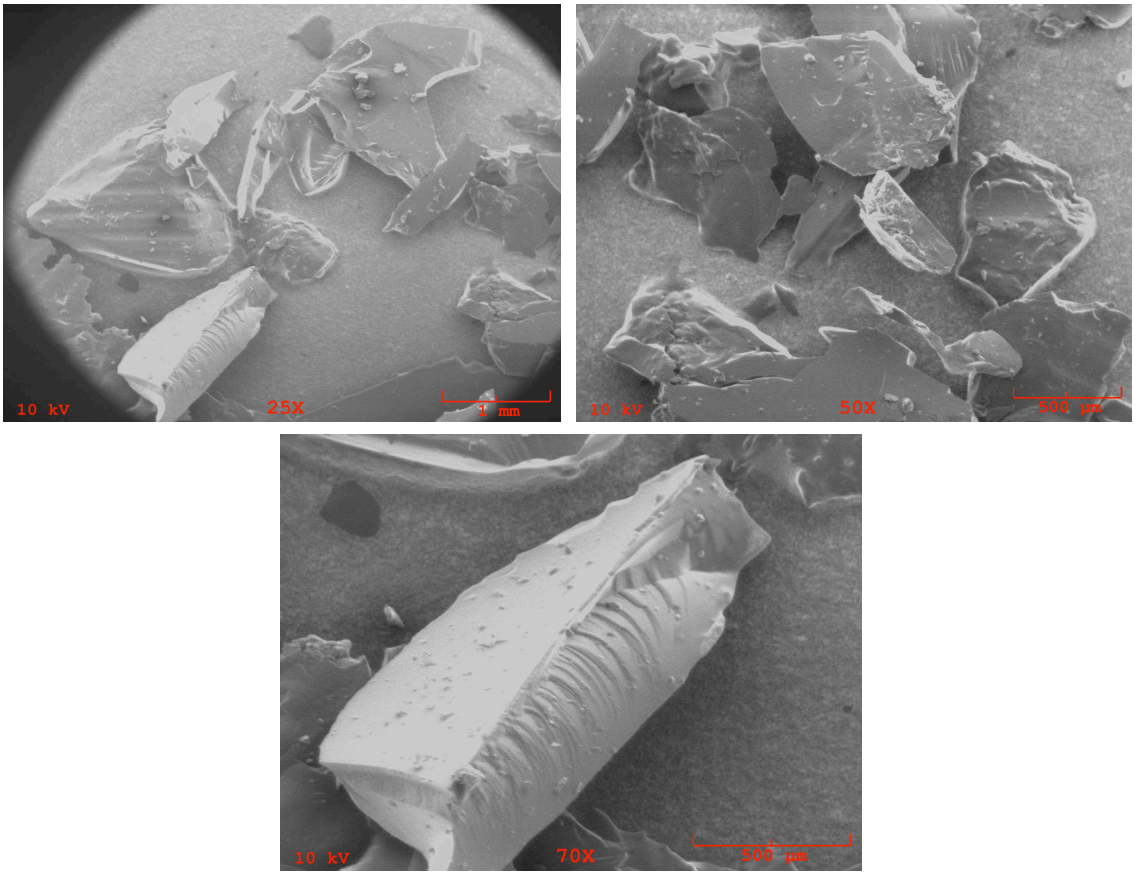

Figure 6.14. SEM photomicrographs of amorphous form Quetiapine Fumarate (Seroquel) at (a) 25X (top left); (b) 50X (top right) and (c) 70X (bottom); 10 KV

6.3.4.4 Sulfapyridine. SEM photomicrographs obtained for pure crystalline form of Sulfapyridine and an amorphous form of Sulfapyridine are shown in (Figure 6.15) in selected magnifications. From the photomicrograph of pure drug sulfapyridine it was present as triangular crystals and the amorphous form was a block of the material with surface fragments.

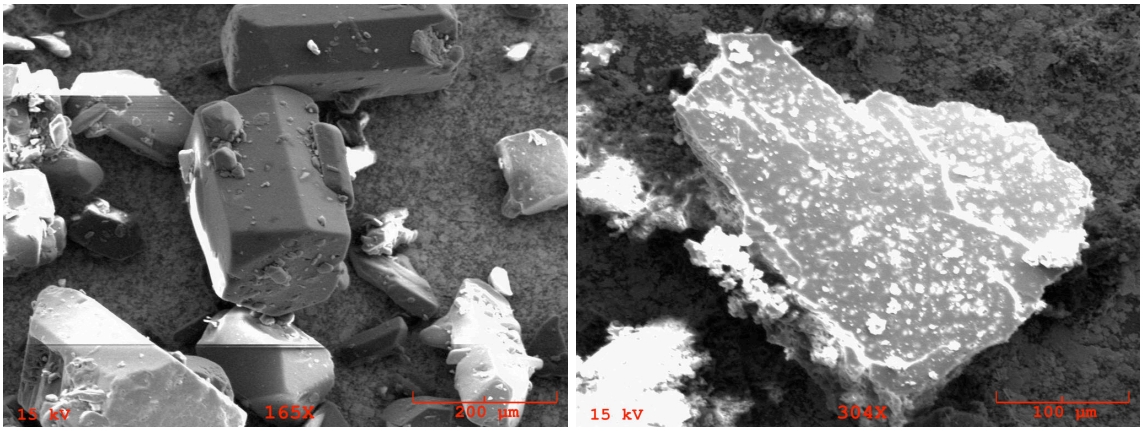

Figure 6.15. SEM photomicrographs of pure crystalline drug Sulfapyridine and amorphous drug Sulfapyridine (a) 165X (Left, Crystalline Solid); (b) 304X (Right, Amorphous); 15 KV

6.3.4.5. Lidocaine.HCl. SEM photomicrographs obtained for pure crystalline forms of Lidocaine.HCl are shown in (Figure 6.16) in selected magnifications. From the photomicrograph of pure drug Lidocaine.HCl it is clear that the drug had geometric shapes as plates and rods. The amorphous form of this drug was hygroscopic resulting in a rubbery sticky structure. This was not amenable for SEM analysis. This amorphous compound was analyzed by DEA.

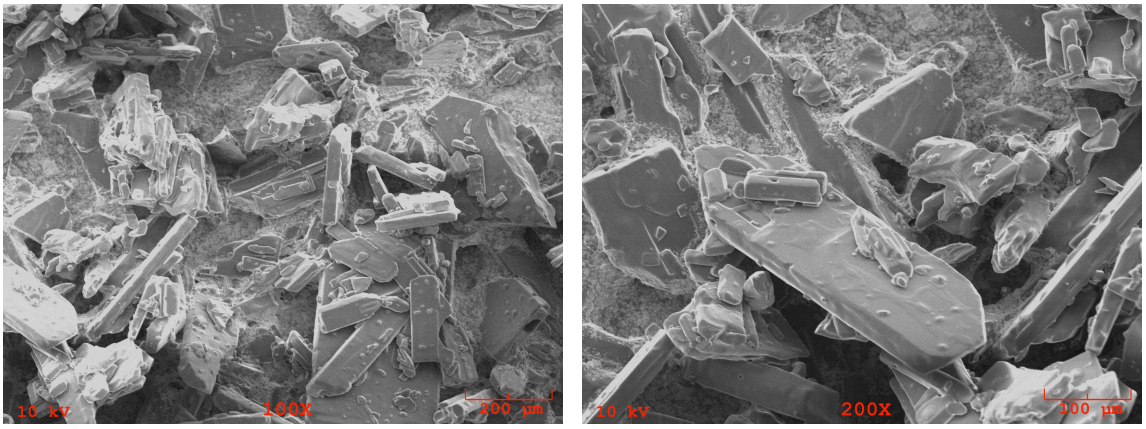

Figure 6.16. SEM photomicrographs of pure crystalline Lidocaine.HCl (a) 100X (Left); (b) 200X (Right); 10 KV

6.4 Conclusions

We were successful in establishing new DEA analytical methods to determine the crystalline and amorphous content of drugs. i.e., the two DEA methods, the activation energy method, as well as, the empirical method agreed with a correlation coefficient of 0.96. This protocol was additionally validated by DSC studies. DSC Analysis verified the presence of amorphous and crystalline material based on changes in the heat of fusion and the appearance of an amorphous Tg. PXRD succinctly separated the amorphous and crystalline materials based on the multiple sharp and narrow peaks for crystalline materials and exceptionally broad bands for the amorphous materials. SEM analysis revealed softening and rounding on edges of amorphous materials while not changing those images of crystalline structure.

6.5 References

1. B.C. Hancock, G. Zografi. 1997. Characteristic and significance of the amorphous state in pharmaceutical systems, J. Pharm. Sci. 86 1–12.
2. Birju Shah, Vasu Kumar Kaumanu, Arvind K. Bansal. 2006. Analytical Techniques for Quantification of Amorphous/Crystalline Phases in Pharmaceutical Solids. J. Pharm. Sci. 95:1641-1665.
3. Alan T. Riga, Kenneth S. Alexander. 2005. Electrical Conductivity Analysis/Dielectric Analysis Differentiates Physical-Chemical Properties of Drugs and Excipients. American Pharmaceutical Review.8, Issue 6, 45-50.
4. Hancock BC, Shamblin SL, Zografi G. 1995. Molecular mobility of amorphous pharmaceutical solids below their glass transition temperature. Pharm Res. 12:799–806.

5. Venkatesh GM, Barnett ME, Fordjour CO, Galop M. 2001. Detection of low levels of the amorphous phase in the crystalline materials by thermally stimulated current spectrometry. Pharm. Res. 18:98–103.

6. Orsolya Jójárt-Laczkovich. Piroska Szabó-Révész. 2009. Amorphization of a crystalline active pharmaceutical ingredient and thermo analytical measurements on this glassy form. J. Therm Anal Calorim. Doi: 10.1007/s10973-009-0530-5.

7. Guo YS, Bryn SR, and Zografi G. Physical characteristics and chemical degradation of amorphous quinapril hydrochloride. J. Pharm. Sci., 89: 128- 143 (2000).

8. Manju Sharma and S. Yashonath. 2008. Correlation between conductivity and diffusivity and activation energy in amorphous solids. J. Chem. Phys: 129,144103

9. Maheswarm MPK, Mantheni D, Perera IN, Venumuddala H, Riga A, Kenneth A. Characterization of crystalline and amorphous content in pharmaceutical solids by dielectric thermal analysis. J. Therm. Anal. Calorim, 2011. DOI: 10.1007/s10973-011-2140-2.

10. J. Keré, S. Sréié, Thermal analysis of glassy pharmaceuticals, Thermochim. Acta 248 (1995) 81–95.